



140  
853  
THS

THESIS  
2  
2008



This is to certify that the  
thesis entitled

UNIT CELL ANALYSIS OF COMPOSITE  
MICROSTRUCTURES

presented by

SHAWN KLANN

has been accepted towards fulfillment  
of the requirements for the

M.S. degree in Mechanical Engineering

A handwritten signature in cursive script, appearing to read "Dalvin Liu".

Major Professor's Signature

May 7, 2008

Date

**PLACE IN RETURN BOX** to remove this checkout from your record.  
**TO AVOID FINES** return on or before date due.  
**MAY BE RECALLED** with earlier due date if requested.

DATE DUE	DATE DUE	DATE DUE

**UNIT CELL ANALYSIS OF COMPOSITE MICROSTRUCTURES**

**By**

**Shawn Christopher Klann**

**A THESIS**

**Submitted to  
Michigan State University  
in partial fulfillment of the requirements  
for the degree of**

**MASTER OF SCIENCE**

**Department of Mechanical Engineering**

**2008**

## **ABSTRACT**

### **UNIT CELL ANALYSIS OF COMPOSITE MICROSTRUCTURES**

By

Shawn Christopher Klann

Composite materials are replacing traditional metals in many applications due to their superior stiffness and strength to weight ratios. However, one problem with composites is the tendency of successive layers in a structure to delaminate in the thickness direction. This problem has been addressed in many ways such as z-pinning, stitching, and woven fabrics that help to maintain the structural integrity of a composite. Fiber weaving does not introduce the high stress concentration present in the other two cases. A new type of composite, the Quasi-Three Dimensional (Q3D) weave, has shown great promise in combating delamination. Unlike the popular 2D Plain Weave, this weave holds successive layers together in order to increase the delamination resistance. There are no fibers aligned in the thickness direction but the tight weave creates a 3D network. An analytical technique is needed to predict the properties of the weave. This thesis presents an analytical method based on Classical Laminate Theory, using unit cell analysis, to predict the mechanical properties of weaving patterns. It is derived on the 2D Plain Weave and compared to other composite microstructures, such as laminates and the Q3D Weave. It was found that the Q3D weave has very similar properties to the 2D Plain Weave while having increased delamination resistance, by experimental tests. Several case studies involving the material and geometric parameters of the composite weave are also presented. The undulation zones in the weave are found to be the most critical for the weave properties.

## ACKNOWLEDGMENTS

I would like to thank my professor, Dr. Dahsin Liu, for both the financial support of my research and the directing of the research work. His insight allowed me to find suitable topics for research and complete this thesis in a timely manner. I would also like to thank Dr. Patrick Kwon and Dr. Alfred Loos for agreeing to serve on my thesis committee. Special thanks are required for Dr. Elias Shakour, Dr. Guojing Li, and Mr. Kirit Rosario for their assistance in the research work. Lastly, I would especially like to thank my parents, Dan and Vicki Klann, for their love and support through years.

## TABLE OF CONTENTS

LIST OF TABLES.....	v
LIST OF FIGURES.....	vi
NOMENCLATURE.....	vii
CHAPTER 1	
INTRODUCTION.....	1
1.1 Background.....	1
1.2 Statement of Problem.....	6
1.3 Organization of Thesis.....	7
CHAPTER 2	
ANALYTICAL METHOD.....	8
2.1 Model Derivation.....	8
2.1.1 Unit Cell Derivation.....	8
2.1.2 Undulation Model.....	17
2.1.3 Subregion Integration.....	21
2.1.4 Computer Code.....	24
2.2 Comparison with Published Articles.....	26
2.3 Summary.....	27
CHAPTER 3	
STUDY OF MICROSTRUCTURE GEOMETRY.....	28
3.1 Yarn Parameters.....	28
3.1.1 Fiber Volume Fraction.....	28
3.1.2 Yarn Thickness.....	30
3.2 Cell Parameters.....	33
3.2.1 Undulation Length.....	33
3.2.2 Weaving Angle.....	35
3.2.3 Cell Size.....	37
3.2.4 Undulation Angle Effects.....	39
3.3 Layer Parameters.....	42
3.3.1 Matrix Layer Thickness.....	42
3.3.2 Number of Layers (2D).....	43
3.3.3 Number of Layers (Q3D).....	45
3.4 Summary.....	47
CHAPTER 4	
COMPARISONS OF WEAVE PATTERNS.....	48
4.1 Weave Patterns.....	48
4.1.1 Laminate.....	48

4.1.2	Quasi-3D Weave.....	49
4.2	Comparisons.....	50
4.2.1	Moduli.....	50
4.2.2	Bending Stiffness.....	55
4.3	Summary.....	57
<b>CHAPTER 5</b>		
<b>CONCLUSIONS AND RECOMMENDATIONS.....</b>		<b>58</b>
5.1	Conclusions.....	58
5.2	Recommendations.....	59
<b>APPENDICES.....</b>		<b>60</b>
<b>Appendix A – Poisson Ratios of Case Studies.....</b>		<b>61</b>
A.1	Fiber Volume Fraction.....	61
A.2	Yarn Thickness.....	62
A.3	Undulation Length.....	62
A.4	Weaving Angle.....	63
A.5	Cell Size.....	63
A.6	Undulation Angle Effects.....	64
A.7	Matrix Layer Thickness.....	64
A.8	Number of Layers.....	65
A.9	Q3D Number of Layers.....	65
<b>Appendix B – Mathematica Code.....</b>		<b>66</b>
B.1	Laminate.....	66
B.2	2D Plain Weave.....	71
B.3	Q3D Weave.....	82
<b>REFERENCES.....</b>		<b>94</b>

## LIST OF TABLES

Table 1.	Composite Yarn Properties.....	18
Table 2.	Matrix Material Properties.....	18
Table 3.	Unit Cell Geometric Properties.....	18
Table 4.	Comparison of Undulation Models for 2D Plain Weave.....	19
Table 5.	Comparison of the Subregion Alignments.....	23
Table 6.	Comparison with Published Articles.....	26
Table 7.	Comparison of 3D and 2D Models.....	27
Table 8.	Undulation Angle Parameters.....	39
Table 9.	Composite Yarn Properties.....	51
Table 10.	Matrix Material Properties.....	51
Table 11.	Unit Cell Geometric Properties.....	52
Table 12.	Comparison of the Properties for Different Weaving Patterns.....	52

## LIST OF FIGURES

Figure 1. Quasi3D Weave (a) Projected View, (b) Fill Side View, and (c) Warp Side View.....	4
Figure 2. 2D Plain Weave (a) Projected View and (b) Side View.....	9
Figure 3. 2D Plain Weave Unit Cell (a) Projected View and (b) Side View.....	10
Figure 4. Region 1 of 2D Plain Weave Unit Cell.....	10
Figure 5. Weaving Angle for 2D Plain Weave.....	15
Figure 6. Undulation Angle of 2D Plain Weave.....	16
Figure 7. Side Views of (a) Sinusoidal Undulation, (b) Linear Undulation, (c) Vertical Undulation, (d) Horizontal Model, and (e) Mosaic Model.....	18
Figure 8. Undulation Angle of Linear Model.....	19
Figure 9. Subregion Alignment of (a) Parallel and (b) Series.....	21
Figure 10. Series-Parallel Undulation Alignments with (a) Horizontal Slices and (b) Vertical Slices.....	22
Figure 11. Flow Chart for Unit Cell Computer Code.....	25
Figure 12. Effective Moduli for Varying Yarn Fiber Volume Fraction.....	29
Figure 13. Yarn Fiber Volume Fraction for Varying Yarn Fiber Volume Fraction.....	30
Figure 14. 2D Plain Weave Side View.....	31
Figure 15. Effective Moduli for Varying Yarn Thickness.....	32
Figure 16. Effective Moduli for Varying Undulation Length.....	34
Figure 17. Top View of the Weaving Angle.....	35
Figure 18. Effective Moduli for Varying Weaving Angle.....	36
Figure 19. Top View of Unit Cell Size.....	37
Figure 20. Effective Moduli for Varying Cell Size.....	38

Figure 21. Parameters Affected by the Undulation Angle.....	39
Figure 22. Geometric Changes for Varying Undulation Angles.....	40
Figure 23. Effective Cell Moduli for Varying Undulation Angles.....	41
Figure 24. Side View of Matrix Layers in 2D Plain Weave Structure.....	42
Figure 25. Effective Moduli for Varying Matrix Layer Thickness.....	43
Figure 26. Projected View of Multiple 2D Unit Cells with Matrix Layers.....	44
Figure 27. Effective Moduli for Varying Number of Layers.....	45
Figure 28. Projected View of Q3D Unit Cell with 5 Layers.....	46
Figure 29. Effective Moduli for Varying Number of Q3D Layers.....	46
Figure 30. 0/90 Laminate Unit Cell (a) Projected View and (b) Side View.....	48
Figure 31. Quasi3D Weave Unit Cell (a) Projected View and (b) Side View.....	49
Figure 32. Edge Replication of the (a) Laminate, (b) 2D Plain Weave, and (c) Q3D Weave.....	51
Figure 33. Comparison of Weave Pattern Young's Moduli for Varying Weave Angle...54	54
Figure 34. Comparison of Weave Pattern Shear Moduli for Varying Weave Angle.....54	54
Figure 35. Comparison of Weave Pattern Poisson's Ratios for Varying Weave Angle...55	55
Figure 36. Bending Stiffness for Varying Weave Angle.....56	56
Figure 37. Poisson Ratios for Varying Yarn Fiber Volume Fraction.....61	61
Figure 38. Poisson Ratios for Varying Yarn Thickness.....62	62
Figure 39. Poisson Ratios for Varying Undulation Length.....62	62
Figure 40. Poisson Ratios for Varying Weaving Angle.....63	63
Figure 41. Poisson Ratios for Varying Cell Size.....63	63
Figure 42. Poisson Ratios for Varying Undulation Angles.....64	64
Figure 43. Poisson Ratios for Varying Matrix Layer Thickness.....64	64

Figure 44. Poisson Ratios for Varying Number of Layers.....65

Figure 45. Poisson Ratios for Varying Number of Q3D Layers.....65

## NOMENCLATURE

$A_{effective}$	= effective extensional stiffness matrix for unit cell
$A_{mk}$	= extensional stiffness matrix for an individual constituent
$\tilde{A}_{mk}$	= extensional stiffness matrix for region integrated over its area
$a$	= unit cell length
$a_u$	= undulation length
$a_0$	= non-undulating length
$a^*$	= length of specified square area
$B_{mk}$	= coupling matrix
$C_A$	= area of the unit cell
$C_{mk}$	= stress-strain relation of an individual constituent
$D_{mk}$	= bending stiffness matrix
$E_x$	= Young's modulus in the x direction
$E_y$	= Young's modulus in the y direction
$E_z$	= Young's modulus in the z direction
$G_{xy}$	= in-plane shear modulus
$G_{xz}, G_{yz}$	= out-of-plane shear moduli
$h$	= thickness of the composite yarn
$i$	= number of subregions per region
$l$	= directional cosine matrix
$M$	= resultant moment
$N$	= resultant force
$n$	= number of plies
$p$	= number of regions per unit cell
$Q3D$	= quasi3D weave
$T$	= transformation matrix
$t_m$	= thickness of matrix layer
$v_f$	= fiber volume fraction
$z$	= z coordinates of the composite constituents
$\varepsilon$	= strain
$\eta$	= Lekhnitskii coefficients
$\theta$	= undulation angle
$\mu$	= Chentsov coefficients
$v_f$	= fiber volume fraction
$\nu_{xy}$	= in-plane Poisson ratio
$\nu_{xz}, \nu_{yz}$	= out-of-plane Poisson ratios
$\sigma$	= stress
$\varphi$	= weaving angle

## **CHAPTER 1 – INTRODUCTION**

### **1.1 Background**

Composite materials have become increasingly popular over the last several decades. This is in large part due to their adaptability to meet the requirements of a specific design. Composites have been proven to have extremely high strength and stiffness to weight ratios, as compared to conventional metals. This, coupled with the fact that they may be manufactured to any shape has contributed to their increased usage.

Composite materials are usually anisotropic materials consisting of two constituents, reinforcing fibers and a bonding matrix. The strength of the material comes from the fibers, while the addition of matrix allows the desired shape to be achieved and transfers the mechanical loading among the fibers. The fibers bundles, known as yarns, may be stacked in unidirectional plies or woven together in any number of patterns. This is known as the composite microstructure. The fibers may be oriented in various directions. This feature allows the designer to orient the yarn fibers in the directions that require stiff and strong properties. Consequently, this makes analysis of composite materials much more complex.

The ability to align the fibers in any direction gives composites excellent in-plane properties. However, they are vulnerable to out-of-plane loading. Impact, bending, and fatigue loadings have the potential to cause delamination of the composite. This is the separating or debonding of successive layers. This occurs due to the weak matrix bonding between layers. Delamination causes a large reduction in the composites strength, especially compressive. Many different methods have been used to remedy this

problem. The three most popular methods are stitching, z-pinning, and fiber weaving. Stitching involves the tying of all the layers together with very high strength fibers. Stitching the layers together can cause damage of the fibers and induce resin rich and stress concentration areas that become weak points in the material. Z-pinning is the use of rods that are inserted through the thickness of the composite structure that help to tie the layers together for specific loadings, especially bending. However, Mouritz [1] has shown through finite element analysis that the introduction of the pins has been shown to moderately reduce the in-plane moduli of the composite. Also the creation of holes leads to stress concentrations throughout the part.

Fiber weaving, where the yarns are interlaced with each other, has been effective in keeping the layers together to maintain the integrity of the structure. Once again, these weaves require more complex analysis in the determination of the composite properties. Kim and Sham [2] studied impact and delamination properties in woven fabrics and unidirectional plies. Crack propagation, damage area, fracture toughness, and max load were analyzed by experimentally impacting specimen. They found the woven fabrics to have superior out-of-plane loading properties. The woven fabrics were found to hold their structural integrity after impact better than for laminated plies, as well as increase delamination resistance. Atas and Liu [3] experimentally explored the effect of weaving angles on two-dimensionally woven composite samples for out-of-plane loading. Special attention was paid to peak force, contact duration, maximum deflection, and absorbed energy of the impacted specimens. They found that small angles differences between yarns improved the impact properties of the samples. This was attributed to a decreased bending stiffness in the plies.

The most common weave pattern is the 2D Plain Weave. Two-dimensional weaves interlace the yarns together for only one layer. However, the layers are only held together by the weak bonding matrix, as with the unidirectional laminates. 2D weaves have been used to derive most of the available analytical models. This is due to the simplicity of the weave to model and the popularity of this weave in industry. Three-dimensional fabrics are increasing in popularity. The interlocking of successive layers creates a 3D structure and helps prevent delamination of the composite. Companies such as 3TEX [4] offers 3D weave and braids for combating delamination.

A new class of composite weaves, the so-called Quasi-Three Dimensional (Q3D) Weave [5], as seen in Figure 1(a) was introduced to combat delamination. The green portions represent the fill yarns while the white areas are the warp yarns. The weaving of the fill and warp yarns together forms the basis of the composite structure. In the figure, the yarns have been infused with resin to give it a rigid structure. The gray areas in the figure are regions of pure matrix. There are actually no fibers aligned in the thickness direction in the Q3D Weave, but the tight weave creates a solid, 3D structure. It was designed to avoid large undulation angles that weaken the in-plane stiffness properties and created the high stress concentration. As seen in Figures 1(b) and (c), each layer is woven into the layers above and below. Counting from the bottom, the first fill (green) yarn is woven into the third ply. Each odd numbered ply follows the same pattern. The third will be woven into the fifth, and so forth. The warp (white) yarns follow the same trend. The even numbered plies are woven into each other. The only difference is the top and bottom layers that are unable to be woven into the layers above or below, respectively, as there is none.

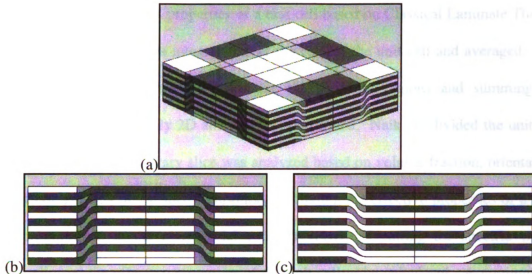


**Figure 1.** Quasi3D Weave (a) Projected View, (b) Fill Side View, and

(c) Warp Side View

In a composite weave, the yarns are woven in a particular pattern. The anisotropic behavior of these materials means that the properties are changing periodically with the weave. Therefore, the stress-strain equation may not be used with the assumption of constant elastic properties. This significantly increases the complexity of the problem. However, the periodicity of the weave allows for an assumption to be made. Within the weave, there is a repeatable unit called the unit cell. Finding the average values of the properties for the unit cell and using those values would allow the equations for constant elastic properties to be used. The averaged values are known as effective properties. Effective properties provide accurate averages so that classical methods may be used. Analysis of the unit cell will give a good understanding of the properties of the composite material upon which it is based. Optimization of cell structure and hence the composite material may then follow.

There are many methods based on the unit cell that have been used to find the effective elastic properties of weaves. Raju and Wang [6] derived a method for

determining the mechanical properties of a unit cell based on Classical Laminate Theory. The constitutive matrix was integrated over the area of the unit cell and averaged. The constitutive matrix was found by dividing the cell into regions and summing the components. However, only 2D analysis was performed. Naik [7] divided the unit cell into many slices. An arbitrary slice was analyzed based on volume fraction, orientation, and the components of the slice. Formulas for finding the effective properties of a slice were programmed in the commercial code *TEXCAD*. Inputting the specific weave pattern allowed the effective properties of the unit cell to be calculated. A minimum of 12 slices would cause the value of the properties to converge. Naik and Ganesh [8] used a small unit cell composed of a warp tow, a fill tow, and resin pockets. The cell was then idealized as a cell with the constituents composed of flat layers one on top of the other. Laminate Theory was then applied to find the overall properties. Scida et al. [9] divided the unit cell into infinitesimal slices. The averaged constitutive matrix for each slice was calculated using Classical Laminate Theory based on the volume fractions of the components. The slices were then added up to find the overall matrix of the unit cell. Hur and Kapania [10] divided the unit cell into many slices and integrated the strain energy density function over the volume of the slices. The constitutive relation was found from the results and summed over all the slices. Hsieh and Tuan [11] evaluated particle reinforced composites on the basis of parallel and series alignment of the particles with the matrix phase. They realized that the alignment at the interfaces of constituents had a significant impact on the properties. This defined an upper and lower bound for the range of the properties.

Computational methods have also been used to analyze the unit cell. Whitcomb [12] used finite element analysis to find the effective properties of the unit cell. The cell was modeled and had loads applied in the three primary directions. From the computer generated displacements, strains were determined. The effective properties could then be found through energy equations. Foye [13] used inhomogeneous elements to analyze subregions of the unit cell. This required personal calculation of the subregions properties for each subregion. Loads were then applied and the effective properties were calculated, as a result of the displacements.

## **1.2 Statement of Problem**

The complexity of composite analysis requires the use of an accurate model for calculating the properties of various composite patterns. Confidence in the model requires analytical studies that are comparable to accepted, published results. The 2D Plain Weave unit cell has been used in the development of most unit cell models. This is the most fundamental weave and will allow for comparison with other previously constructed models. The model will need to be adaptable to analyze various weaving patterns, including the Q3D Weave. Evaluation of property dependence and composite response on geometric constraints is important for designing superior weaving patterns. This includes studying weaving angle, undulation size, unit cell size, and other variable geometric constraints. This will require a computer code that will allow material and geometric properties to be input for quick calculation of the desired unit cell properties and trends to be found. The primary goal of this thesis is to (1) create a model and code for evaluating the properties of composite materials, (2) justify the code with other

published results, and (3) evaluate the properties of the Q3D weave. Complex geometry requires computational investigation to sort out the effects due to individual parameters. Throughout the study, perfect bonding between constituents is assumed.

### **1.3 Organization of Thesis**

The approach taken in this paper is analytical. Chapter 1 is the introduction. Chapter 2 will outline the analytical approach used in the model and the theory behind the model. Justification of the model by comparison with published data of similar problems is also included. Multiple case studies of composite unit cells are examined in Chapter 3. This involves property dependence on geometric and material constraints. Chapter 4 compares the properties of various weaving patterns. Finally, Chapter 5 presents the conclusions of the study and recommendations for future research.

## CHAPTER 2 – ANALYTICAL METHOD

### 2.1 Model Derivation

#### 2.1.1 Unit Cell Derivation

The analytical approach used in the model is based on Classical Laminate Theory [14]. It follows a similar approach to that of Raju and Wang [6]. However, there are several modifications made to the model both for simplification and greater accuracy. These include three dimensional analysis, undulation modeling, and subregion integration (parallel and series alignments). All of these modifications will be explained throughout the chapter. Three dimensional analysis is used because the weaving patterns create a three dimensional structure. It is important to know all of the properties of the structure.

One layer of the 2D (two-dimensional) Plain Weave is shown graphically in Figure 2. This is the most fundamental composite weave. The unit cell of the 2D Plain Weave is outlined in Figure 2(a). This is the subset of the weave that is repeated throughout the whole structure. As before, the green and white areas represent the fill and warp composite regions, respectively. These regions are called yarns and are fiber bundles that have been mixed with matrix. The gray areas represent pure matrix zones. Figure 2(b) shows the side view of the weave.

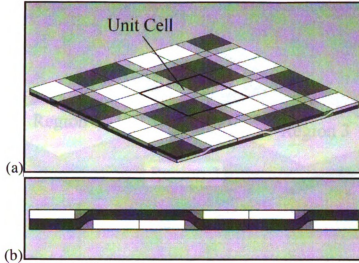


**Figure 2.** 2D Plain Weave (a) Projected View and (b) Side View

Classical Laminate Theory is based on plies that are stacked on top of each other. Only thickness is taken into account in the analysis. Therefore, regions must be identified that allow this analysis to be conducted. In order to achieve this, the cell is divided up into the four regions shown in Figure 3(a). The details of the three geometric dimensions  $a$ ,  $a_u$ , and  $h$ , representing cell length, undulation length, and yarn thickness, respectively, are shown in Figure 3(b). These values are measured after the structure has been manufactured. The length,  $a_0$ , is defined as the difference between the cell length ( $a$ ) and the undulation length ( $a_u$ ).

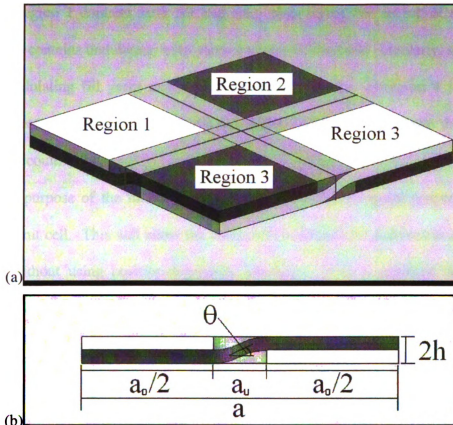


**Figure 3.** 2D Plain Weave Unit Cell (a) Projected View and (b) Side View

Each of the regions has a fill component (green), a warp component (white), matrix channels (gray), and a matrix pocket (gray). The regions can then be further broken down into four subregions as Figure 4 displays.

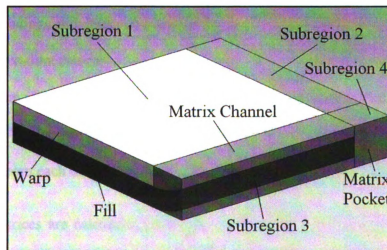


**Figure 4.** Region 1 of 2D Plain Weave Unit Cell

Subregion 1 contains both fill and warp plies laying flat on top of each other. Subregion 2 contains undulating warp yarns and matrix channels. Similarly, subregion 3 contains undulating fill yarns and matrix channels. Finally, subregion 4 is a matrix pocket. These regions of pure resin are unavoidable results of the weave that must be taken into account.

The purpose of the model is to find the effective mechanical properties of the composite unit cell. This will allow the composite weaves to be analyzed as anisotropic materials without using position-dependent functions. This is achieved through the constitutive relation, the relation between forces ( $N$ ) and bending moments ( $M$ ) to strain ( $\epsilon$ ) and curvature ( $\kappa$ ). The constitutive relation is shown in the following equation.

$$\begin{Bmatrix} N \\ M \end{Bmatrix} = \begin{bmatrix} A & B \\ B & D \end{bmatrix} \cdot \begin{Bmatrix} \epsilon \\ \kappa \end{Bmatrix} \quad (1)$$

The **A**, extensional stiffness, matrix is of particular interest in this study as it relates in-plane loading to in-plane straining. From this equation, the mechanical properties of the unit cell may be calculated. The **D**, bending stiffness, matrix relates out-of-plane loading to out-of-plane curving while the **B**, coupling stiffness, matrix couples the in-plane and out-of-plane loadings and deformations together.

For three-dimensional analysis, all matrices are of size 6x6. They represent the properties of the material in all three directions. Each of the constituents of the unit cell has matrices. The constituents are the fill and warp yarns, as well as the matrix. The contributions from each of the subregions must be integrated over the volume of the cell.

All matrices are calculated from the stiffness matrix, **C**, and geometry. The **C** matrix is associated with the material properties, such as Young's modulus ( $E$ ), shear

modulus ( $G$ ), and Poisson's ratios ( $\nu$ ). It also holds the relationship between stress and strain as shown in Equation (2).

$$\{\sigma\} = [C]\{\varepsilon\} \quad (2)$$

The stiffness matrix for orthotropic materials is seen in Equation (3)

$$C = \begin{bmatrix} \frac{E_x(\nu_{yz}\nu_{zy} - 1)}{\beta} & -\frac{E_x(\nu_{yz}\nu_{zx} + \nu_{yx})}{\beta} & -\frac{E_x(\nu_{yx}\nu_{zy} + \nu_{zx})}{\beta} & 0 & 0 & 0 \\ -\frac{E_x(\nu_{xz}\nu_{zy} + \nu_{xy})}{\beta} & \frac{E_x(\nu_{xz}\nu_{zx} - 1)}{\beta} & -\frac{E_x(\nu_{xy}\nu_{zx} + \nu_{zy})}{\beta} & 0 & 0 & 0 \\ -\frac{E_x(\nu_{xy}\nu_{yz} + \nu_{xz})}{\beta} & -\frac{E_x(\nu_{xz}\nu_{yx} + \nu_{yz})}{\beta} & \frac{E_x(\nu_{xy}\nu_{yx} - 1)}{\beta} & 0 & 0 & 0 \\ 0 & 0 & 0 & G_{yz} & 0 & 0 \\ 0 & 0 & 0 & 0 & G_{xz} & 0 \\ 0 & 0 & 0 & 0 & 0 & G_{xy} \end{bmatrix} \quad (3)$$

where

$$\beta = \nu_{xy}(\nu_{yx} + \nu_{yz}\nu_{zx}) + \nu_{yz}\nu_{zy} + \nu_{xz}(\nu_{zx} + \nu_{yx}\nu_{zy}) - 1 \quad (4)$$

The properties substituted in Equation (3) are those of a unidirectional composites, since the warp and fill yarns are prepared with unidirectional yarns. However, the  $C$  matrix for the matrix channels and pockets are based on pure matrix properties. The properties of the yarns are determined by the fiber properties ( $E_f$ ), matrix properties ( $E_m$ ), and fiber volume fraction ( $\nu_f$ ). Depending on which property is being determined, one of the following equations is used, where  $E_C$  represents the property of the composite. Properties along the fiber direction use Equation (5). All other properties use Equation (6).

$$E_C = E_f \nu_f + E_m (1 - \nu_f) \quad (5)$$

$$\frac{1}{E_c} = \frac{\nu_f}{E_f} + \frac{(1 - \nu_f)}{E_m} \quad (6)$$

The extensional stiffness matrix of each subregion,  $A_{mk}$ , is simply the integration of transformed stiffness matrices through the thickness. The differing material properties between successive plies causes the integration to take the form of Equation (7), where  $n$  is the number of plies.

$$A_{mk} = \sum_{j=1}^n \bar{C}_{mk} \cdot \Delta z \quad (7)$$

Once the  $\mathbf{A}$  matrix for each subregion is found, it is integrated over its area. The four subregions are then summed for the integrated regional matrices. The tilde represents that the  $\mathbf{A}$  matrix has been integrated over the region area,  $R_A$ .

$$\tilde{A}_{mk} = \sum_{i=1}^4 \int_{R_A} A_{mk} dA \quad (8)$$

The summation integer,  $i$ , ranges from 1 to 4 due to the four subregions in each region. The integration is dependent on the geometric parameters of the unit cell. These include the undulation length ( $a_u$ ), unit cell length ( $a$ ), and yarn thickness ( $h$ ). The effective extensional stiffness matrix,  $A_{eff}$ , is then the summation of the regional matrices divided by the cell area,  $C_A$ , of the unit cell.

$$A_{eff} = \frac{\sum_{p=1}^4 \tilde{A}_{mk}}{C_A} \quad (9)$$

The summation integer,  $p$ , ranges from 1 to 4 due to the four regions in the unit cell. The  $\mathbf{A}$  matrix holds the relation between the force and strain for the unit cell. The effective elastic constants can then be found through the inverse  $\mathbf{A}$  matrix.

$$\mathbf{a} = \mathbf{A}_{eff}^{-1} \quad (10)$$

From the inverted  $\mathbf{A}_{eff}$  matrix,  $\mathbf{a}$ , the properties are easily calculated. The elastic constants are calculated as shown.

$$E_x = \frac{1}{a_{11}t} \quad E_y = \frac{1}{a_{22}t} \quad E_z = \frac{1}{a_{33}t} \quad (11)$$

The shear moduli are calculated similarly.

$$G_{xy} = \frac{1}{a_{66}t} \quad G_{xz} = \frac{1}{a_{55}t} \quad G_{yz} = \frac{1}{a_{44}t} \quad (12)$$

The Poisson's ratios are calculated as follows:

$$\nu_{xy} = -\frac{a_{21}}{a_{11}} \quad \nu_{xz} = -\frac{a_{13}}{a_{11}} \quad \nu_{yz} = -\frac{a_{23}}{a_{22}} \quad (13)$$

The Lekhnitskii coefficients, which relate shear stress to normal strain or shear strain to normal stress, are calculated using Equation (14).

$$\begin{aligned} \eta_{xx,yz} &= a_{41}a_{11} & \eta_{xx,xz} &= a_{51}a_{11} & \eta_{xx,xy} &= a_{61}a_{11} \\ \eta_{yy,yz} &= a_{42}a_{22} & \eta_{yy,xz} &= a_{52}a_{22} & \eta_{yy,xy} &= a_{62}a_{22} \\ \eta_{zz,yz} &= a_{43}a_{33} & \eta_{zz,xz} &= a_{53}a_{33} & \eta_{zz,xy} &= a_{63}a_{33} \end{aligned} \quad (14)$$

Chentsov's coefficients, which relate shear stress in one plane to shear strain in another plane, are determined from Equation (15).

$$\mu_{yz,xz} = a_{54}a_{44} \quad \mu_{yz,xy} = a_{64}a_{44} \quad \mu_{xz,xy} = a_{65}a_{55} \quad (15)$$

Now that the overall procedure has been layed out, there are several additional calculations that need to be made. One possibility in the weave is that the fill and warp yarns are not orthogonal to each other. There is a weave angle,  $\varphi$ , which is the angle

between the yarns. This is displayed in Figure 5, below. The lines represent the direction of the fibers in the yarns.

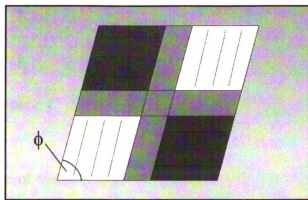


Figure 5. Weaving Angle for 2D Plain Weave

This weave angle must be accounted for in the determination of the transformed,  $C'$ , matrix for each subregion. If there is indeed a non-orthogonal weave angle, the fibers in the warp yarns are now aligned in a different direction and the tensorial transformation must be used to find the transformed matrix,  $C'$ , for the new direction. This is shown in Equation (16).

$$C' = TCT^T \quad (16)$$

$T$  is the tensorial transformation matrix and is composed of directional cosines. The directional cosines are the cosines of the angles between the original coordinate system and the new coordinate system that is aligned with the fibers in the warp yarns. The directional cosine matrix is shown below.

$$l = \begin{bmatrix} \cos(\phi) & \cos(\phi + 90^\circ) & \cos(90^\circ) \\ \cos(90^\circ - \phi) & \cos(\phi) & \cos(90^\circ) \\ \cos(90^\circ) & \cos(90^\circ) & \cos(0^\circ) \end{bmatrix} \quad (17)$$

The transformation matrix is then composed from the directional cosines as shown in Equation (18).

$$T = \begin{bmatrix} l_{11}^2 & l_{21}^2 & l_{31}^2 & 2l_{21}l_{31} & 2l_{31}l_{11} & 2l_{21}l_{11} \\ l_{12}^2 & l_{22}^2 & l_{32}^2 & 2l_{22}l_{32} & 2l_{12}l_{32} & 2l_{12}l_{22} \\ l_{13}^2 & l_{23}^2 & l_{33}^2 & 2l_{23}l_{33} & 2l_{13}l_{33} & 2l_{13}l_{23} \\ l_{12}l_{13} & l_{22}l_{23} & l_{32}l_{33} & l_{22}l_{33} + l_{32}l_{23} & l_{12}l_{33} + l_{32}l_{13} & l_{12}l_{23} + l_{22}l_{13} \\ l_{11}l_{13} & l_{21}l_{23} & l_{31}l_{33} & l_{21}l_{33} + l_{31}l_{23} & l_{11}l_{33} + l_{31}l_{13} & l_{11}l_{23} + l_{21}l_{13} \\ l_{11}l_{12} & l_{21}l_{22} & l_{31}l_{32} & l_{21}l_{32} + l_{31}l_{22} & l_{11}l_{32} + l_{31}l_{12} & l_{11}l_{22} + l_{21}l_{12} \end{bmatrix} \quad (18)$$

The transformed C matrix, C', is then used in place of the original C matrix for the warp yarn portions.

The same type of transformation is used for the undulation portion of the yarns.

The undulation angle,  $\theta$ , is displayed in Figure 6.

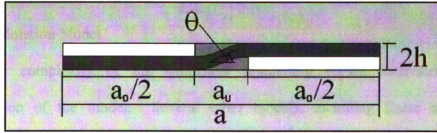


Figure 6. Undulation Angle of 2D Plain Weave

The curved nature of the yarn undulation causes the angle,  $\theta$ , to vary with position. The height of the undulation of a fill yarn in the  $x$  direction is given by a piecewise function.

The following sinusoidal function is just an approximation of the height.

$$h(x) = \begin{cases} 0 & -a/2 \leq x \leq -a_u/2 \\ \left(1 + \sin \frac{\pi x}{a_u}\right) \cdot \frac{h}{2} & -a_u/2 \leq x \leq a_u/2 \\ h & a_u/2 \leq x \leq a/2 \end{cases} \quad (19)$$

The undulation angle is found by taking the derivative of Equation (19)

$$\tan(\theta) = \frac{dh(x)}{dx} = \frac{\pi \cdot h}{2 \cdot a_u} \cos \frac{\pi x}{a_u} \quad (20)$$

As the curved yarn is a function of position, the integration of the regions over the cell area must be done numerically. The directional cosines to be used in the transformation matrix for the undulating regions are shown below.

$$l = \begin{bmatrix} \cos(\theta) & \cos(90^\circ) & \cos(\theta - 90^\circ) \\ \cos(90^\circ) & \cos(0^\circ) & \cos(90^\circ) \\ \cos(\theta + 90^\circ) & \cos(90^\circ) & \cos(\theta) \end{bmatrix} \quad (21)$$

These directional cosines are then used in the transformation matrix for the undulating subregions.

### 2.1.2 Undulation Model

The complexity of the sinusoidal undulating region motivated potential simplification of the model. Several other models, including linear and vertical undulations, along with horizontal and mosaic simplification models, were compared to the sinusoidal undulation model. In order to achieve this, numerical values are useful. The following tables provide the material and geometric properties used to calculate the properties. These particular values [7] were chosen as they were commonly used in unit cell models and will allow for comparison with other published results. These properties will be used in all the calculations unless otherwise noted.

**Table 1. Composite Yarn Properties**

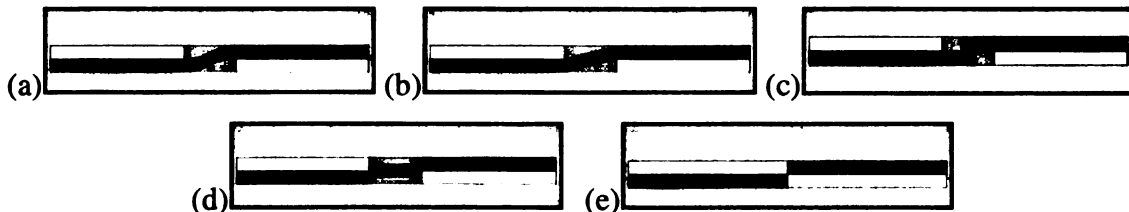
$E_{11}$ (GPa)	144.8
$E_{22}$ (GPa)	11.728
$E_{33}$ (GPa)	11.728
$G_{12}$ (GPa)	5.516
$G_{13}$ (GPa)	5.516
$G_{23}$ (GPa)	5.516
$\nu_{12}$	0.23
$\nu_{13}$	0.23
$\nu_{23}$	0.3
$\nu_f$	0.64

**Table 2. Matrix Material Properties**

$E_M$ (GPa)	3.448
$G_M$ (GPa)	1.276
$\nu_M$	0.35

**Table 3. Unit Cell Geometric Properties**

$a$ (mm)	10
$a_u$ (mm)	1.467
$h$ (mm)	0.989

**Figure 7. Side Views of (a) Sinusoidal Undulation, (b) Linear Undulation, (c) Vertical Undulation, (d) Horizontal Model, and (e) Mosaic Model**

The graphical versions of the five models are presented in Figure 7. The models (b)-(e) would all greatly simplify the calculation in the undulation region. The sinusoidal model is traditionally believed to be most like the actual, physical unit cell. Obviously, the horizontal model and the mosaic model could not physically occur. Only their use as

a mathematical model was analyzed. The thickness of the yarn in the vertical model is kept constant at  $h$ .

For the linear model, the undulation angle remains constant through the undulation. It is therefore determined from the following equation.

$$\theta = \tan^{-1}\left(\frac{h}{a_u}\right) \quad (22)$$

The equation is derived from inspection of Figure 8.

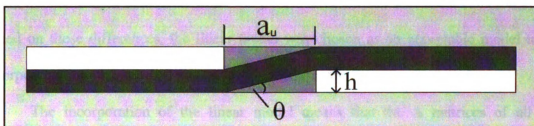


**Figure 8.** Undulation Angle of Linear Model

The vertical, horizontal, and mosaic models were calculated the same as the subregions with stacked yarns and Classical Laminate Theory was used for the calculation.

The results of the different undulation models are shown in Table 4. Due to the balance of the unit cell in the  $x$  and  $y$  directions, properties such as  $E_x$  and  $E_y$  are equivalent.

**Table 4.** Comparison of Undulation Models for 2D Plain Weave

	<b>Sinusoidal</b>	<b>Linear</b>	<b>Vertical</b>	<b>Horizontal</b>	<b>Mosaic</b>
$E_x$ (GPa)	62.23	61.41	66.46	67.49	78.81
$E_y$ (GPa)	62.23	61.41	66.46	67.49	78.81
$E_z$ (GPa)	12.83	12.25	35.11	11.31	12.62
$G_{xy}$ (GPa)	4.894	4.89	5.49	4.89	5.52
$G_{xz}$ (GPa)	6.204	6.44	5.49	4.89	5.52
$G_{yz}$ (GPa)	6.204	6.44	5.49	4.89	5.52
$\nu_{xy}$	0.0313	0.0284	0.0524	0.0362	0.0345
$\nu_{xz}$	0.3321	0.3613	0.1052	0.2942	0.2925
$\nu_{yz}$	0.3321	0.3613	0.1052	0.2942	0.2925
<b>Angle (<math>\theta</math>)</b>	19.31	33.99	90	0	0

As seen in Table 4, the values of the sinusoidal and linear models are very similar. The vertical model has greater in-plane properties and much greater out-of-plane properties. This is due to the yarns aligned vertically. The horizontal model has increased in-plane properties and decreased out-of-plane properties, compared to the sinusoidal model. The mosaic model has significantly larger in-plane properties as there are no pure matrix zones and the yarns are ideally aligned horizontally. The major reasons for the differences in the models can be concluded to be the pure matrix content and the undulation angle. Based on these differences, the linear model was chosen as an acceptable model to be incorporated into the unit cell model. This greatly simplified the calculations.

The incorporation of the linear model means that the **A** matrices of all the subregions remain constant for each constituent and no longer vary with position. Therefore, the integration becomes algebra and simplifies the equations. The subregion calculations reduce significantly and are shown in the following equations.

#### Region 1 – Subregion 1

$$A_{mk_1} = (\bar{C}_{mk})_{0^\circ} \cdot h + (\bar{C}_{mk})_{\phi^\circ} \cdot h \quad (23)$$

#### Region 1 – Subregion 2

$$A_{mk_2} = (\bar{C}_{mk})_{\phi^\circ, undulated} \cdot h + (\bar{C}_{mk})_{Matrix} \cdot h \quad (24)$$

#### Region 1 – Subregion 3

$$A_{mk_3} = (\bar{C}_{mk})_{0^\circ, undulated} \cdot h + (\bar{C}_{mk})_{Matrix} \cdot h \quad (25)$$

### Region 1 – Subregion 4

$$A_{mk_4} = (\bar{C}_{mk})_{Matrix} \cdot 2h \quad (26)$$

These four subregions are summed to give the integrated A matrix of Region 1. The *sine* term from the integration is a result of the change in volume associated with the weaving angle.

### Region 1

$$\tilde{A}_{mk} = A_{mk_1} \left( \frac{a_0^2}{4} \sin(\phi) \right) + A_{mk_2} \left( \frac{a_u a_o}{4} \sin(\phi) \right) + A_{mk_3} \left( \frac{a_u a_o}{4} \sin(\phi) \right) + A_{mk_4} \left( \frac{a_u^2}{4} \sin(\phi) \right) \quad (27)$$

The other three regions have identical constituents that are arranged in different locations. Their calculation is carried out in the same manner.

#### 2.1.3 Subregion Integration

Thus far, in this thesis and in published models, during the summation of the regions and subregions, the constituents have been assumed to be in a parallel or series (Parallel/Series) arrangement. This is shown in Figure 9. That is true for all the flat regions, but the undulation portions are a special case. They are neither arranged in parallel or series. For small undulation angles an assumption could be made that the series or parallel arrangements would be a good approximation. For relatively large undulation angles, this requires separate analysis involving both series and parallel arrangements.

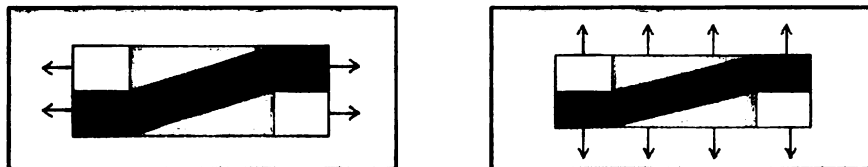


**Figure 9.** Subregion Alignment of (a) Parallel and (b) Series

The undulation region was divided into many slices allowing both series and parallel (Series-Parallel) arguments to be used. By analyzing the slices in series first, the addition could be carried out as before. Therefore, the slices would be either arranged vertically or horizontally depending on the direction of summation. Figure 10 shows both of these alignments. The red portions represent the composite portions of the slices while the gray portions are pure matrix. As the number of slices increases, the slices cause the regions to become more like the linear undulation and greater accuracy of the model is achieved. As the number of slices increases, the geometry will tend to match that of the linear model. Enough slices were used so that the numbers would converge on a value. The horizontal alignment required approximately one-thousand slices for the number to converge, as seen in Table 5.

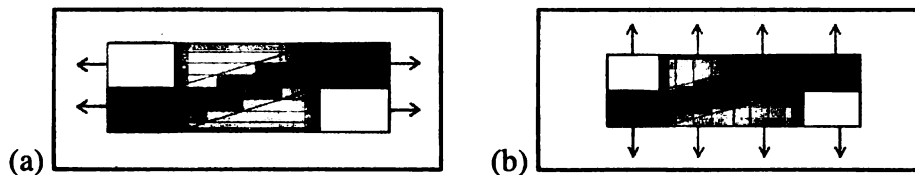


**Figure 10.** Series-Parallel Undulation Alignments with (a) Horizontal Slices and (b) Vertical Slices

The slices allow the undulation regions to have the same alignment as the flat regions. However, the size of the slices must be determined. For the horizontal slices, the equation of the linear lines that bound them was used, as each slice does not have the same length. From these equations, the length of the yarn (red) portion of each slice can be found. For the vertical case, each of the slices has the same dimensions. Simple trigonometry was used to determine their heights. Finding the A matrix of the slices permits them to be treated as subregions with constant properties. They can then be

integrated through the thickness and then over the area, as done with the other subregions. This allows the previous summation to be conducted.

Horizontal slices are used for finding in-plane properties. The vertical slices are used for finding out-of-plane properties. When summing in the  $x$  direction, the warp yarns are already aligned in parallel and do not need to be divided into slices. The same holds true for the fill yarns when summing in the  $y$  direction.

The division of the undulation region into slices was incorporated into the original model and compared using the same properties as before. The comparison of the two undulation models is shown below in Table 5, based on one-thousand slices.

**Table 5. Comparison of the Subregion Alignments**

	<b>Parallel/Series Alignment</b>	<b>Series-Parallel Alignment</b>
$E_x$ (GPa)	61.41	62.77
$E_y$ (GPa)	61.41	62.77
$E_z$ (GPa)	12.25	12.33
$G_{xy}$ (GPa)	4.89	4.89
$G_{xz}$ (GPa)	6.44	6.45
$G_{yz}$ (GPa)	6.44	6.45
$\nu_{xy}$	0.0284	0.0279
$\nu_{xz}$	0.3613	0.3595
$\nu_{yz}$	0.3613	0.3595

The change in the model is found to have an impact on the Young's moduli and the Poisson's ratios. The shear moduli remain largely unaffected by the modification to the model. Depending on the geometric properties, the series-parallel arrangement can cause the properties to either increase or decrease. The differences in the effective properties were found to be fairly small. This study helps to justify the use of the Parallel/Series alignment for small undulation angles. For this study, the undulation angle was  $34^\circ$ .

#### 2.1.4 Computer Code

A computer code based on the commercial package *Mathematica* was written to complete all the calculations. The input to the code is the material properties of the yarn fibers and matrix as well as the geometric properties of the unit cell. The output is the mechanical properties of the corresponding unit cell. This allows the properties to be quickly found for varying inputs. Also, it allowed trends to be found by varying any of the inputs and plotting the changes of the output. The flow chart that covers the process of calculation in the code is shown in Figure 11. The computer codes for all weaving patterns analyzed are shown in Appendix B.

The geometrical models were generated using *Unigraphics*. This allowed visualization of the unit cells and corresponding dimensions. A clear visual comparison of the weaving patterns could also be achieved.

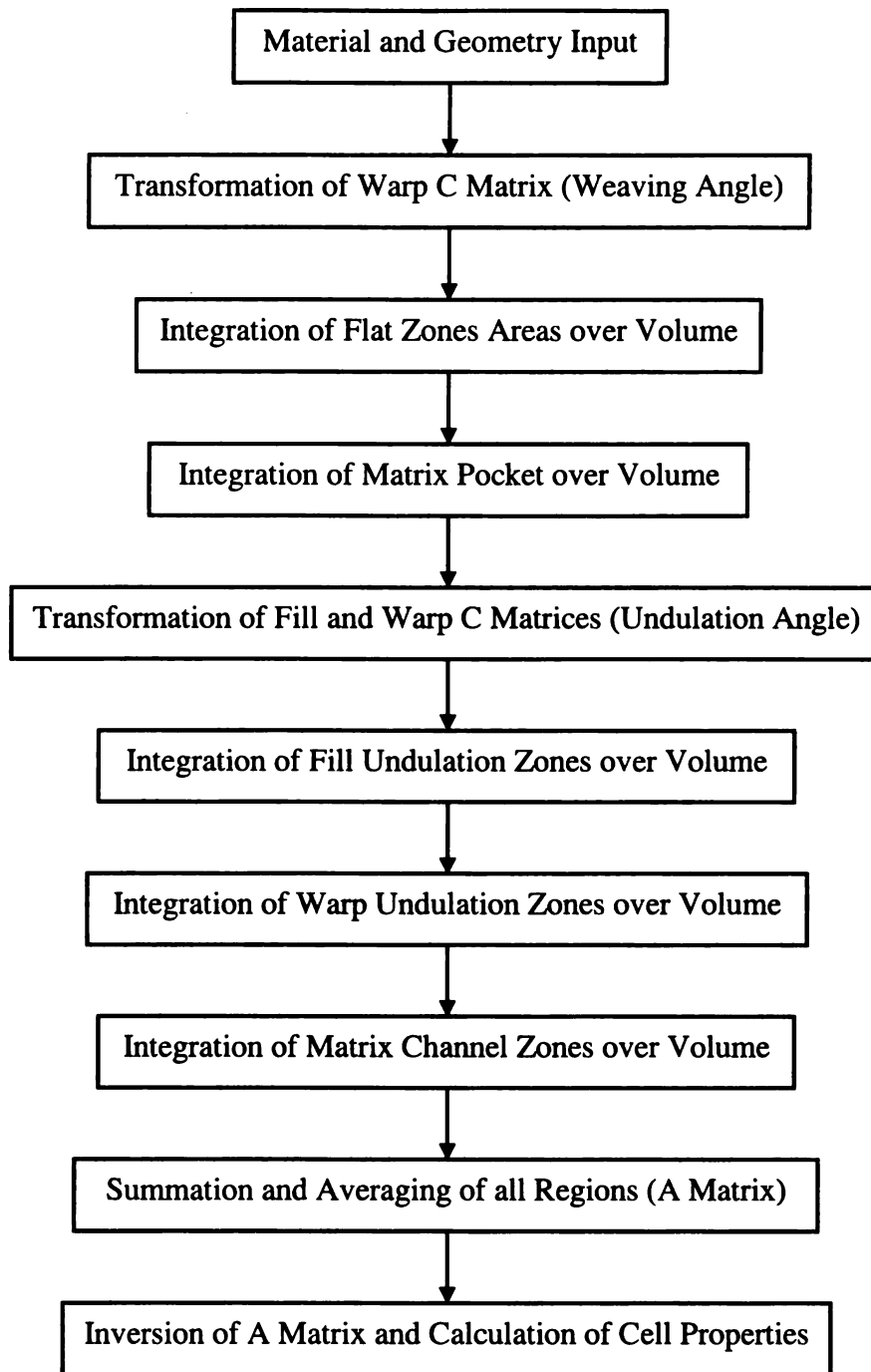


**Figure 11.** Flow Chart for Unit Cell Computer Code

## 2.2 Comparison with Published Articles

Upon completion of the model, it is necessary to determine the validity by comparing with other results. The model was compared with four other models that analyzed 2D Plain Weave unit cells that have been published in journals. For this purpose, the model was derived using the Plain Weave.

The current model was found to be in very good agreement with the other published models. The comparison is shown in Table 6. This comparison gives confidence into the validity and accuracy of the current model.

**Table 6.** Comparison with Published Articles

	<b>Current Model</b>	<b>Nalk [7]</b>	<b>Hur et al [10]</b>	<b>Foye [13]</b>	<b>Raju [6]</b>
$E_x$ (GPa)	62.77	64.38	64.41	63.78	60.61
$E_y$ (GPa)	62.77	64.38	64.41	63.78	60.61
$E_z$ (GPa)	12.33	11.49	11.73	-	-
$G_{xy}$ (GPa)	4.89	4.87	5.05	4.827	4.894
$G_{xz}$ (GPa)	6.45	5.64	5.77	-	-
$G_{yz}$ (GPa)	6.45	5.64	5.77	-	-
$\nu_{xy}$	0.0279	0.027	0.0312	0.03	0.041
$\nu_{xz}$	0.3595	0.396	0.4033	-	-
$\nu_{yz}$	0.3595	0.396	0.4033	-	-

Table 7 displays the differences in using a 2D and 3D analysis in the current model. Besides the fact that none of the out-of-plane properties are known, most of the in-plane properties increase. This is a result of inverting a 3x3 matrix as opposed to the 6x6 matrix in the calculation of the constants. The difference in the properties is not very significant, but depending on the material and geometric constraints the difference could increase.

**Table 7.** Comparison of 3D and 2D Models

	<b>3D Analysis</b>	<b>2D Analysis</b>
$E_x$ (GPa)	62.77	64.11
$E_y$ (GPa)	62.77	64.11
$E_z$ (GPa)	12.33	-
$G_{xy}$ (GPa)	4.89	4.89
$G_{xz}$ (GPa)	6.45	-
$G_{yz}$ (GPa)	6.45	-
$\nu_{xy}$	0.0279	0.0549
$\nu_{xz}$	0.3595	-
$\nu_{yz}$	0.3595	-

Completion of the analytical model will now allow an in-depth study into the material and geometric parameters of the unit cell and how they affect the properties. Other weaving patterns, such as the Q3D Weave, may also be analyzed.

### **2.3 Summary**

A model based on Classical Laminate Theory was derived to calculate the effective properties of composite unit cells. The model used three dimensional analysis. It was found that the undulation regions could accurately be modeled as linear to reduce the complexity of the calculations. The subregion integration was found to affect the in-plane Young's moduli of the cell. The undulation regions were forced to have a series and parallel alignment by the addition of multiple slices acting as subregions. This would give higher accuracy in the model. The values from the example unit cell were compared with published articles and found to have good consistency. The next step involves multiple case studies on the unit cell parameters.

## **CHAPTER 3 – STUDY OF MICROSTRUCTURE GEOMETRY**

There are many variations of composite weaving that can be used. The fibers may be placed in different orientations, constrained by different geometries, resulting in many different material properties. In this chapter, several case studies of the 2D Plain Weave pattern will be analyzed. This will involve different material and geometric variations that can be placed on the weave. The geometric constraints will be changed over a domain to see the effect on the overall properties and to find trends. The Young's and shear moduli will be displayed on graphs for each case study. The Poisson's ratios of these trends will be shown in Appendix A. In all of the cases, the geometric and material properties of Chapter 2 are used, unless otherwise noted. Also, for the case studies involving the changing of a parameter, only that parameter is varied and the others are considered constant. The unit cell parameters may be divided into those that deal with the yarns, the cell, and layers.

### **3.1 Yarn Parameters**

#### **3.1.1 Fiber Volume Fraction**

One very important parameter is the fiber volume fraction of the cell. This is the percentage of the volume that is occupied by the fibers. This parameter is affected by the manufacturing of the composite and will affect the properties of the composite. The fibers give the composite its stiffness and strength, so it is expected that an increase in the fiber volume fraction would also increase the effective cell properties. By increasing the volume fraction, the individual fill and warp yarn properties increase. As a result, this

was found to have a significant effect on the cell properties. The composite moduli for this case study have the following dependency, where  $E^C$  represents the cell properties.

$$E^C = f(a(A_{eff}(\tilde{A}(A(v_f, E_{constituent})))))) \quad (28)$$

As seen in Figure 12, the cell moduli increase in a linear fashion with the volume fraction. The Young's modulus in the z direction is not as dependent on the fiber volume fraction as the other moduli. The domain of the fiber volume fraction in the graph covers most practical applications. The in-plane Young's moduli and the shear moduli have a difference of 50% over the domain. The Young's modulus in the z-direction varies 33%.

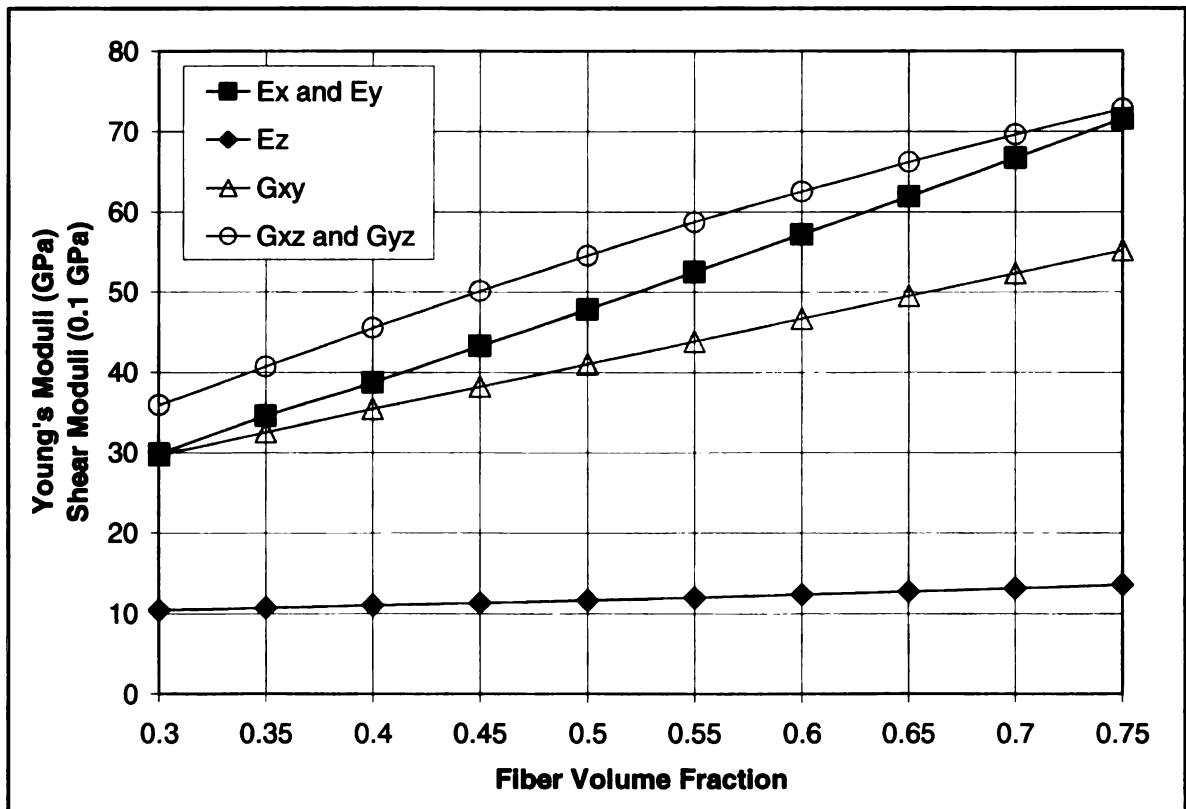


**Figure 12.** Effective Moduli for Varying Yarn Fiber Volume Fraction

One form of composite manufacturing is the use of prepreg tape. These are sheets of fibers that have matrix already in the sheet. The sheets are cut and woven or stacked to create the desired microstructure. Then the woven or stacked material must be cured

and shaped. During the curing process, the matrix may become liquid and leave the mold, resulting in the decrease of the yarns. This will increase the fiber volume fraction of the yarns. Based on the original fiber volume fraction and the thickness of the final composite, the fiber volume fraction as a function of the yarn thickness may be found. This is displayed in Figure 13. The volume fraction increases significantly as the thickness of the yarns are decreased. This graph is based on an initial fiber volume fraction of 0.64.

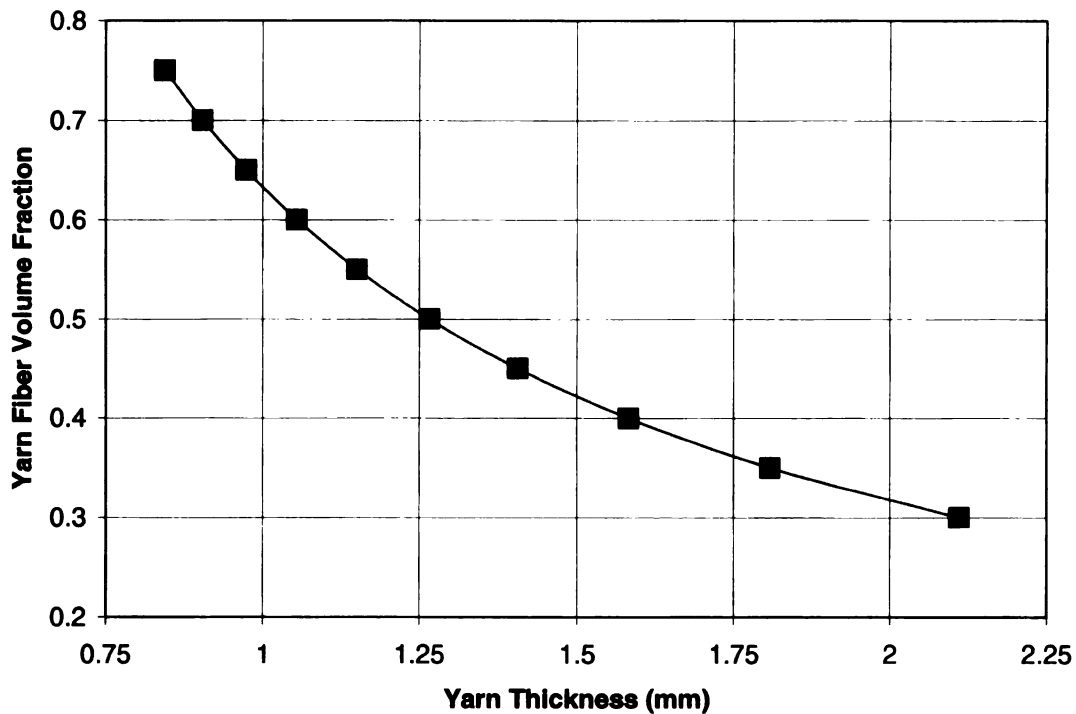


**Figure 13.** Yarn Fiber Volume Fraction for Varying Yarn Thickness

### 3.1.2 Yarn Thickness

Besides fiber volume fraction, there are many other geometric parameters that can affect the unit cell properties. These include undulation length ( $a_u$ ), non-undulated length ( $a_0$ ), cell size ( $a$ ), yarn thickness ( $h$ ), weaving angle ( $\varphi$ ), matrix layers, and number of

layers. Figure 14 displays four of these parameters. Variation of these parameters will be seen in the following case studies.

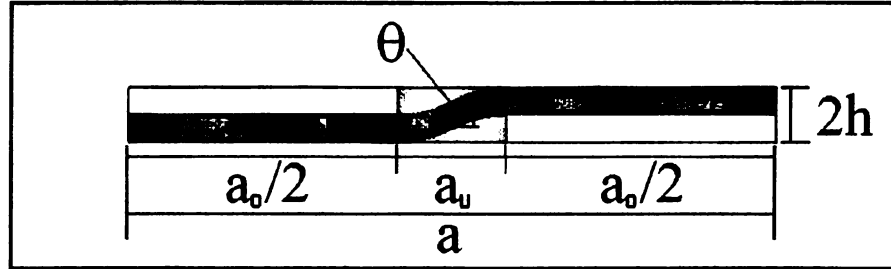


**Figure 14.** 2D Plain Weave Side View

The thickness of the yarns is one geometric parameter that affects the cell properties. For isotropic materials, the thickness will have no effect on the properties. However, increasing the height of the cell will increase the undulation angle if the undulation length,  $a_u$ , is fixed. This case study assumes that the volume fraction of the yarns is held constant for the changing thickness. Therefore, the following parameters affect this case study.

$$E^c = f(a(A_{eff}(\tilde{A}(a_u, a, h)))) \quad (29)$$

Figure 15 shows the effect of the yarn thickness on the cell moduli. For ease of visualization the height ratio,  $h/a$ , is introduced. The domain was chosen so that convergence of the properties was achieved.

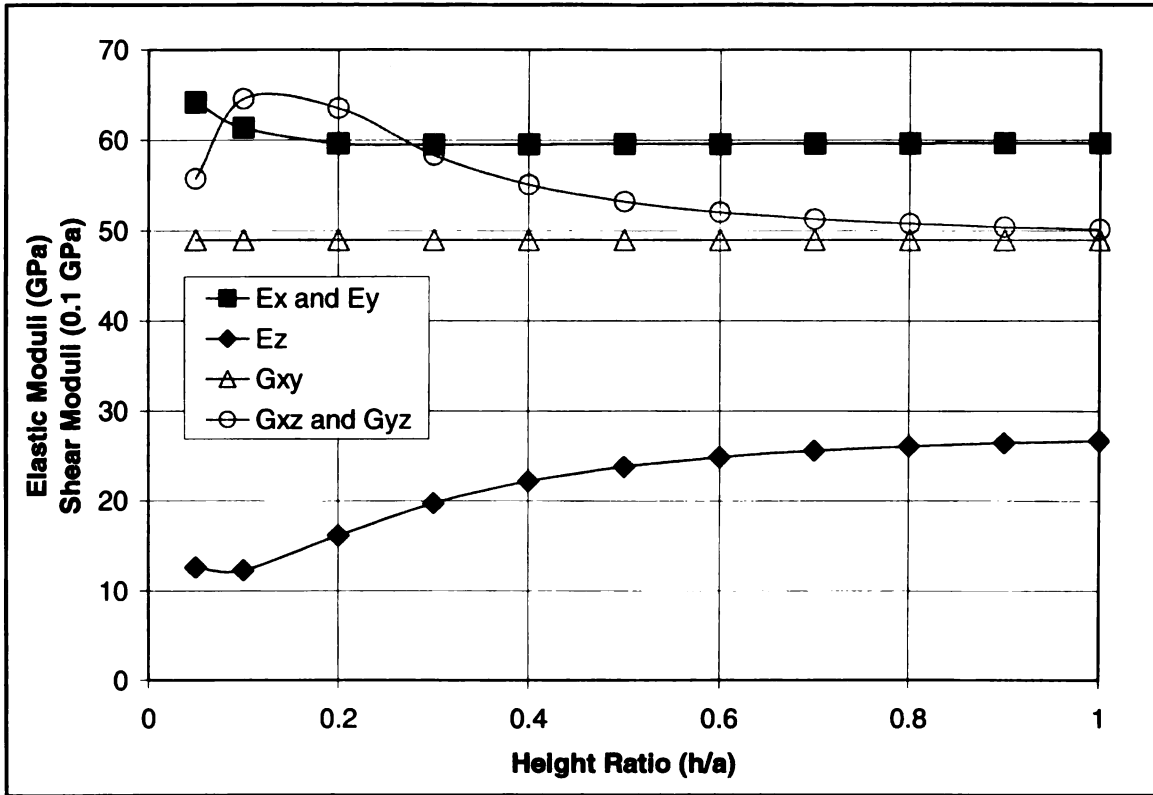


**Figure 15.** Effective Moduli for Varying Yarn Thickness

The in-plane Young's moduli decreases slightly with increasing height ratio and then converges. Only for very small height ratios does a change in the ratio affect those properties. The Young's modulus in the z-direction is significantly affected. This is because the undulation length remains the same and thickness is increased, resulting in a large undulation angle. Therefore, the volume of the fibers aligning in the vertical direction increases as the undulation angle is increased.  $E_z$  increases over 100% over the domain. The out-of-plane shear moduli decrease with the height ratio and then converge toward the same value as the in-plane shear moduli, which are unaffected. The out-of plane shear moduli decrease 30% over the domain.

## 3.2 Cell Parameters

### 3.2.1 Undulation Length

A major geometric variation is the undulation distance,  $a_u$ . This is the horizontal distance of the fiber undulation due to the weaving pattern. It is also the undulation distance of weaving between adjacent fibers. If this distance is varied, it will cause the undulation angle to change. It will also change the volume of the matrix channels and pocket that fill the voids left by the fibers. These two changes have a dramatic effect on the properties of the unit cell.

In order to view the effect of the undulation distance on the unit cell, the undulation ratio,  $a_u/a$ , is defined. This is the fraction of the unit cell length that is undulated. The case study dependency is shown in Equation (30).

$$E^c = f\left(a\left(A_{eff}\left(\tilde{A}(a_u, a, h)\right)\right)\right) \quad (30)$$

Figure 16 shows the cell moduli plotted versus the change in the undulation ratio. The domain varies from  $a_u = h$  ( $a_u/a \approx 0.05$ ) to  $a_u = a$ , which are the lower and upper bounds of the unit cell, respectively. The lower bound is such as the length of the undulation may not be any shorter than the thickness of the yarns. The upper bound is such as the length of the non-undulation may vanish. Linear undulation was used as described in Chapter 2.

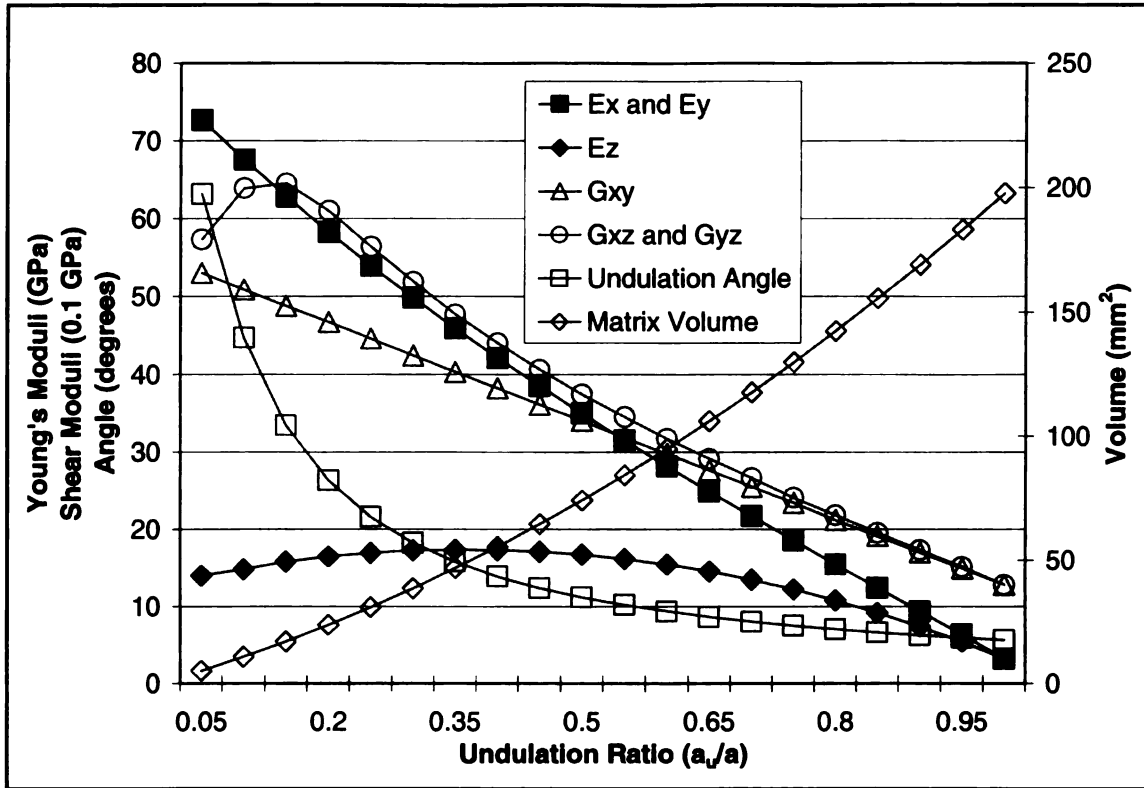


**Figure 16.** Effective Moduli for Varying Undulation Length

The graph shows the Young's moduli in the in-plane directions to be the most sensitive to the changes. There is a decrease of over 90% over the domain of that property. As the undulation length gets longer, there are fewer fibers aligned completely in the  $x$ - $y$  plane. Even though the undulation angle is increased as the undulation length decreases, the in-plane properties will increase. The decrease in size of matrix regions is the major reason for the increase in moduli. The Young's modulus in the through-thickness direction is not nearly as sensitive to the change. It increases about 20% and then decreases after a particular ratio value. There is an optimal point of the fiber alignment and volume of the matrix regions for this property.

The shear moduli tend to decrease with increasing undulation length, as well. The in-plane shear modulus decreases linearly at a much smaller rate than the in-plane Young's moduli. The out-of-plane shear moduli increase initially and then decrease at a

larger rate than the in-plane moduli. There appears to be an optimal point for the out-of-plane shear moduli that balances the undulation length and angle. All the shear moduli decrease approximately 75% over the domain.

### 3.2.2 Weaving Angle

The geometric change that affects the largest number of cell properties is the weaving angle. Figure 17 displays the weave angle between the fill and warp yarns. Changing the direction of the warp (white) yarns significantly affects almost all of the cell properties.

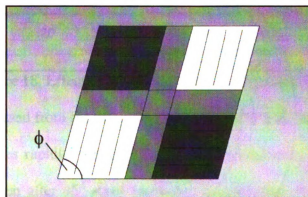


Figure 17. Top View of the Weaving Angle

The use of small differences of weaving angles between successive layers, such as 15°, has been shown to improve delamination resistance [3]. It is therefore important to know how this parameter affects the cell properties. The parameters that effect this case study are shown in Equation (31).

$$E^C = f\left(a\left(A_{eff}\left(\tilde{A}\left(A\left(E_{warp}^C(\phi)\right)\right)\right)\right)\right) \quad (31)$$

The trends associated with the elastic and shear moduli are displayed in Figure 18. The graph domain varies from 0° to 90°, as that is the orthogonal position of the fibers. Due to the lack of symmetry for this parameter, none of the properties will be identical.

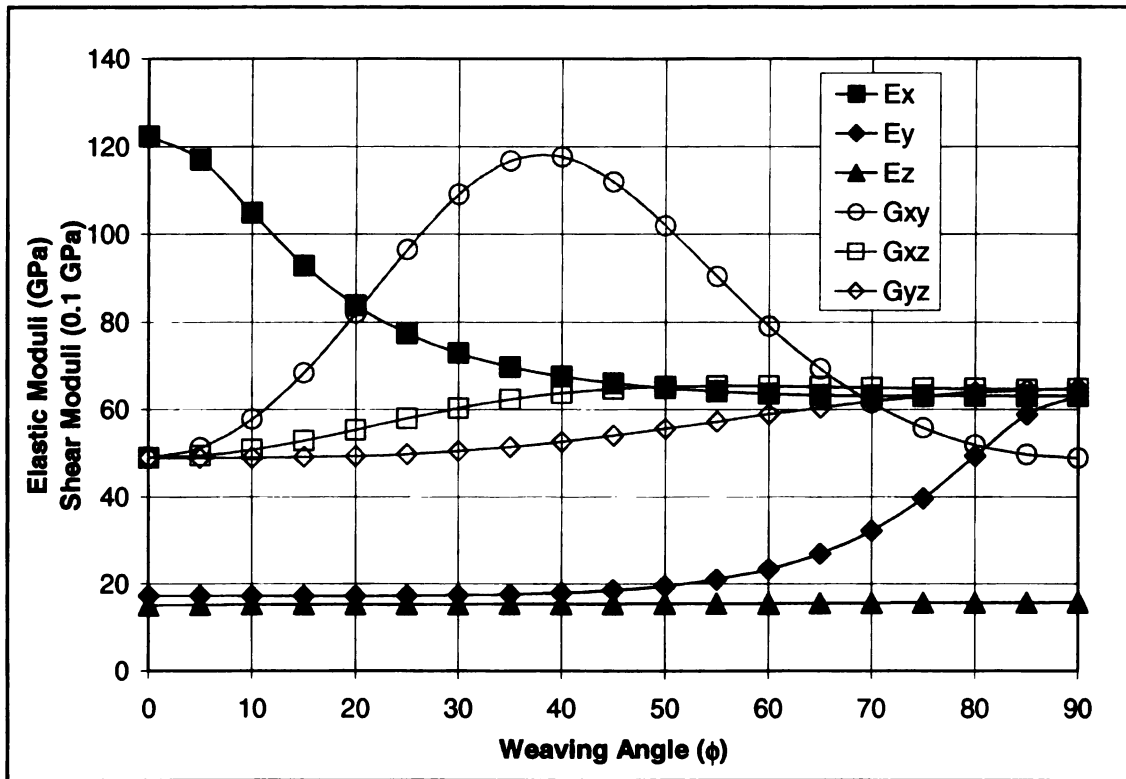


Figure 18. Effective Moduli for Varying Weaving Angle

As the angle is decreased from the orthogonal alignment ( $90^\circ$ ),  $E_x$  stays fairly steady until  $45^\circ$  and then increases rapidly, almost 100%, with the decreasing angle.  $E_y$  decreases rapidly, 75%, and then after  $45^\circ$  stays constant. It approaches the value of  $E_z$ , which changes very little with the angle.

The in-plane shear modulus has a parabolic shape. It increases 140% as the weaving angle decreases. The maximum value is between  $35^\circ$  and  $40^\circ$ . This is due to the lack of perfect symmetry between the warp and fill fibers. Otherwise the peak value would be at  $45^\circ$ . Both of the out-of-plane shear moduli decrease about 25% as the angle is decreased. They take somewhat different paths, however, with the changing values. All three of the shear moduli converge upon the same value when the weave angle approaches  $0^\circ$ .

### 3.2.3 Cell Size

Another geometric change is the size of the cell. In this study, a square area,  $a^* \times a^*$ , was defined and filled by a varying number of unit cells,  $n \times n$ . For example, the area could be filled by one square cell at length  $a^*$ , four cells at length  $a^*/2$ , 9 cells at length  $a^*/3$ , and so forth. This is shown in Figure 19. The height of the cells was kept constant so that only the effect of the cell length was analyzed. The domain is defined in terms of the ratio  $a/a^*$ .

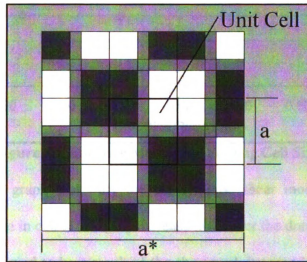
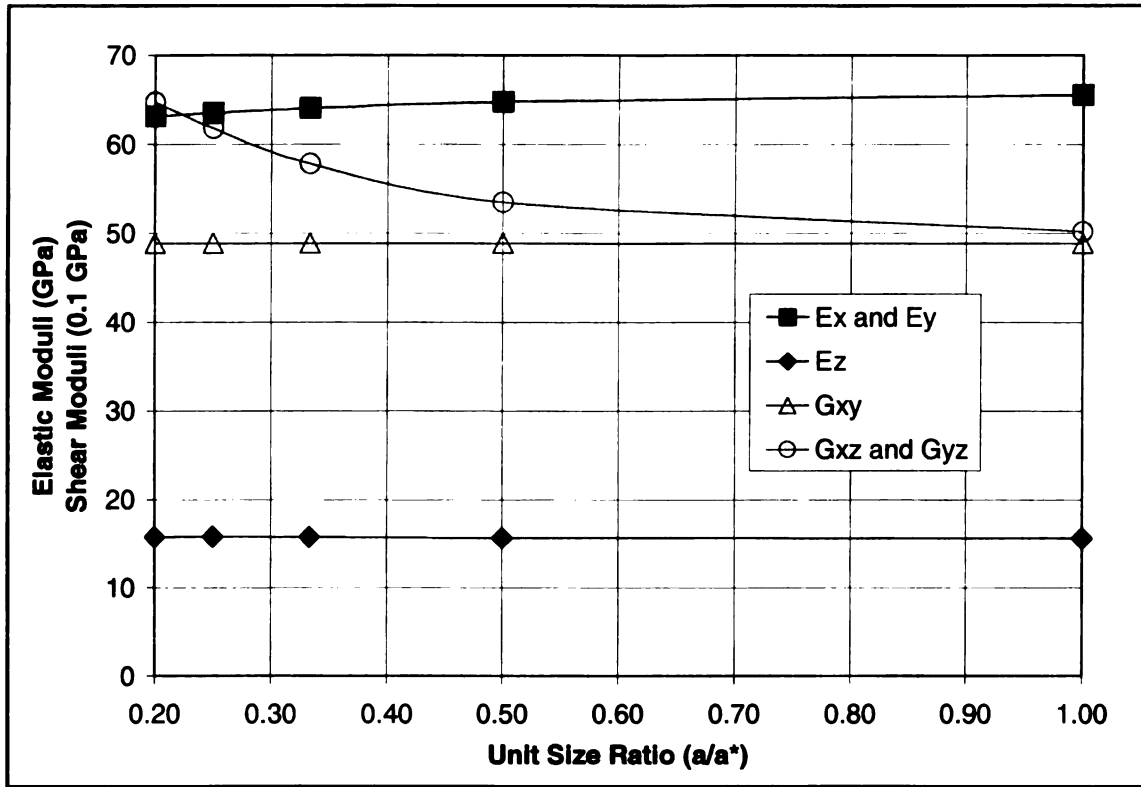


Figure 19. Top View of Unit Cell Size

As the number of cells increased, all the dimensions of the cell except the thickness were scaled down. The lower bound of the domain is when the undulation length,  $a_u$ , is equal to the yarn thickness,  $h$ . This occurred at 5 cells per length. Therefore, the undulation angle would increase slightly with the number of cells. Equation (32) shows the affected parameters.

$$E^c = f\left(a\left(A_{eff}\left(\bar{A}\left(a, a^*, a_u, h\right)\right)\right)\right) \quad (32)$$

Figure 20 shows the changes of the cell moduli as the number of cells in the specified area is changed.



**Figure 20.** Effective Moduli for Varying Cell Size

It is seen in graph that only the out-of-plane shear moduli are significantly affected by the change in cell size. They increase 30% over the domain as the cell size is reduced. This is believed to be a result of the shortened distance between yarns aligned in the vertical direction (undulation regions). The other moduli change very little or not at all. The in-plane Young's moduli decrease only slightly as the cell size is reduced. There is much less change in comparison to the undulation length case study as the change in the undulation ratio,  $a_w/a$ , is much less. This is due to the increase of the undulation angle as all the dimensions, except height, as scaled accordingly.

### 3.2.4 Undulation Angle Effects

From many of the previous case studies, it has been observed that several of the parameters indirectly affect the cell properties by changing the undulation angle. Table 8 shows the parameters that affect the undulation angle and their bounds. The angle  $5.65^\circ$  refers to a unit cell composed entirely of undulation.

**Table 8.** Undulation Angle Parameters

Parameter	Lower Bound		Upper Bound	
	Bound	Angle	Bound	Angle
$a_u$	$h$	$90^\circ$	$a$	$5.65^\circ$
$h$	Fiber Diameter	$0^\circ$	Infinity	$90^\circ$
$a^*$	$3h$	$90^\circ$	$a$	$5.65^\circ$

It was determined that a detailed study was needed covering the effects of the undulation angle on all important parameters. Through this study, the thickness of the yarns,  $h$ , is assumed to be constant except in the undulation area. Therefore, any changes in the undulation angle come from a change in the undulation length. This will change the volume of the pure matrix regions in the unit cell. Figure 21 shows the parameters involved. The distance  $d$  is thickness of the yarns in the undulation area, which decreases as the undulation angle increases.

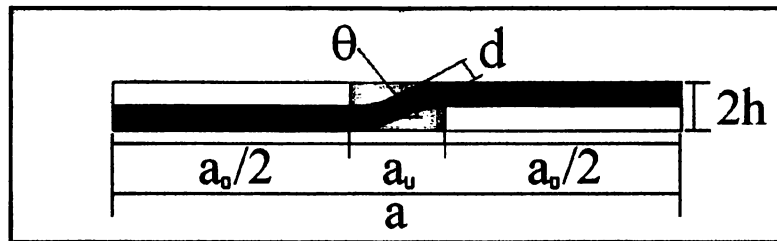


**Figure 21.** Parameters Affected by the Undulation Angle

The overall fiber volume fraction of the cell is assumed to stay constant. Therefore, the volume of fiber and matrix in the cell does not change. Only the positioning of the constituents is varied. Therefore, the average yarn fiber volume

fraction will change. All of the geometric changes as a result of the undulation are shown in Figure 22.

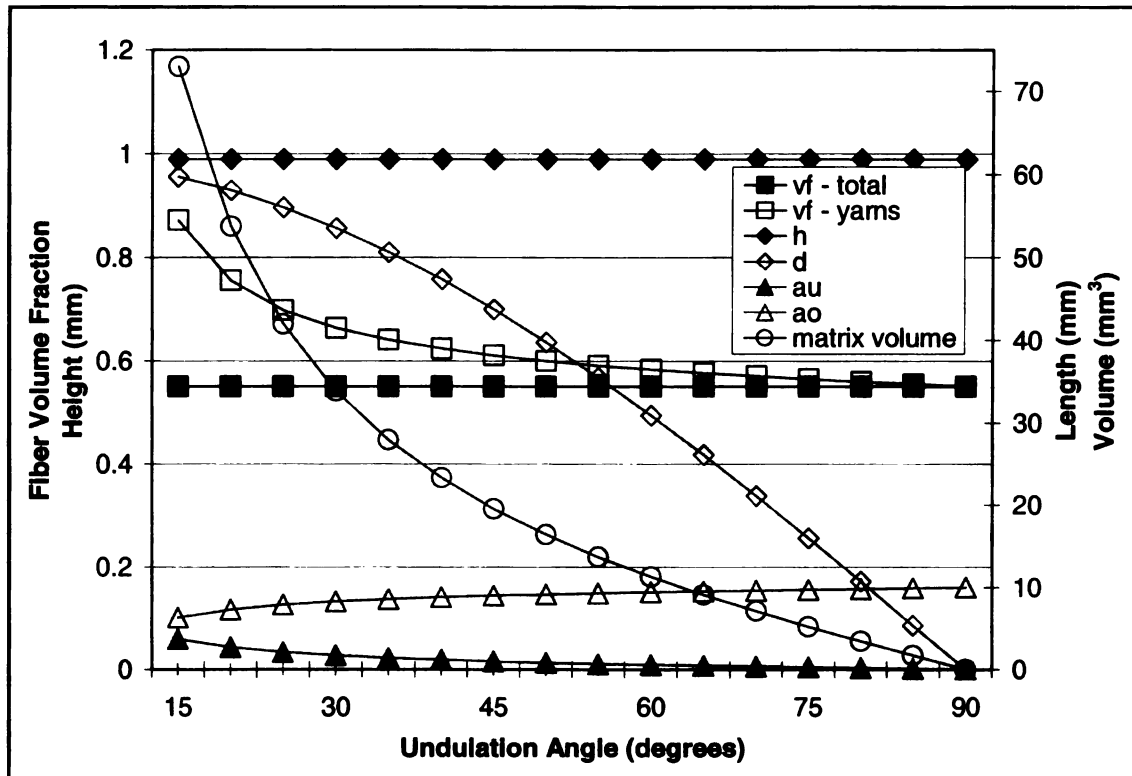


Figure 22. Geometric Changes for Varying Undulation Angles

The minimum angle of the unit cell for this geometry is approximately 15°. This is because angles lower than this value require the yarn fiber volume fraction to exceed the maximum geometric allowance of 90.7% for the fibers packed as close as possible. From the graph, it is seen that the overall fiber volume fraction of the unit cell is kept constant. The yarn fiber volume fraction decreases as the undulation angle is increased. This is a direct result of the volume of the pure matrix regions. With a low undulation angle, the regions of pure matrix have a large volume. However, they are decreased as the undulation angle increases. The matrix is forced into the yarns, thus reducing the yarn fiber volume fraction. As expected, when the matrix volume is zero at 90°, the

overall and yarn fiber volume fractions are equal. Also shown in the graph are the corresponding lengths,  $a_u$  and  $a_0$ . All of these parameters are shown in the case study parameter equation.

$$E^c = f\left(a\left(A_{eff}\left(\tilde{A}\left(a_u, a, h, A\left(v_f\right)\right)\right)\right)\right) \quad (33)$$

For each undulation angle, the corresponding geometry from Figure 22 was programmed into the computer code. This allowed the determination of the effective cell moduli. The trends are displayed in Figure 23.

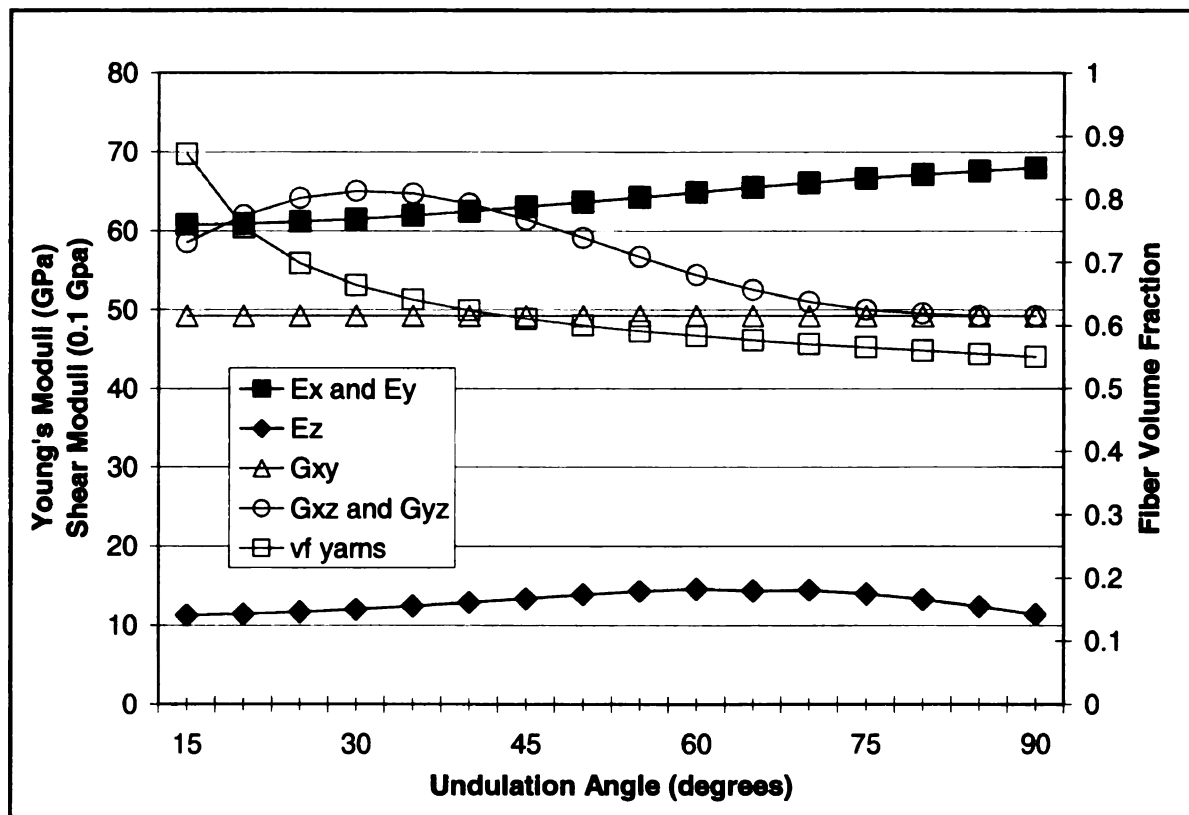


Figure 23. Effective Cell Moduli for Varying Undulation Angles

As seen in the graph, the in-plane Young's moduli increase with the undulation angle. However, they do not increase nearly as rapidly as in the previous undulation length case study. The decrease in the yarn fiber volume fraction causes the properties to not be as sensitive. The out-of-plane Young's modulus increases slightly to an optimal

point and then comes back toward the initial value. The change is not very large. The geometric changes work against each other to prevent any significant change. The in-plane shear moduli are unaffected by any of the changes that come from the increase in the undulation angle. The out-of-plane shear moduli increase initially to an optimal point and the decrease toward the in-plane value.

However, it is seen that the Young's moduli and out-of-plane shear moduli can be increased 10% or greater by simply varying the orientation of the constituents while keeping their volume constant. This study also showed that the parameters are all linked and that the changing of one parameter affects many other parameters.

### 3.3 Layer Parameters

#### 3.3.1 Matrix Layer Thickness

During manufacture of composites, it is possible that a matrix layer would be present in between the layers of fiber. This is shown graphically in Figure 24. The thickness of the matrix layer is represented by  $t_m$ .

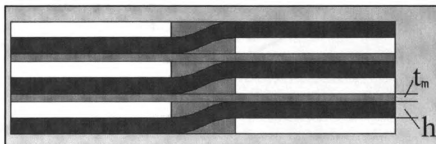


Figure 24. Side View of Matrix Layers in 2D Plain Weave Structure

The introduction of matrix layers would have a tendency to lower the effective properties. This is the case as it would decrease the overall fiber volume fraction of the composite. The case study is a function of the parameters shown in Equation (34).

$$E^c = f\left(a\left(A_{eff}\left(\tilde{A}\left(A\left(t_m, h, n\right)\right)\right)\right)\right) \quad (34)$$

Figure 25 shows the effects of the resin layer on the cell properties. The layer thickness is presented as a ratio of the ply height,  $t_m/h$ . The graph was generated using a three layer composite with, therefore, two layers of matrix as seen in the above picture. The domain of the matrix layer varies from no matrix layer to half the thickness of the yarns.

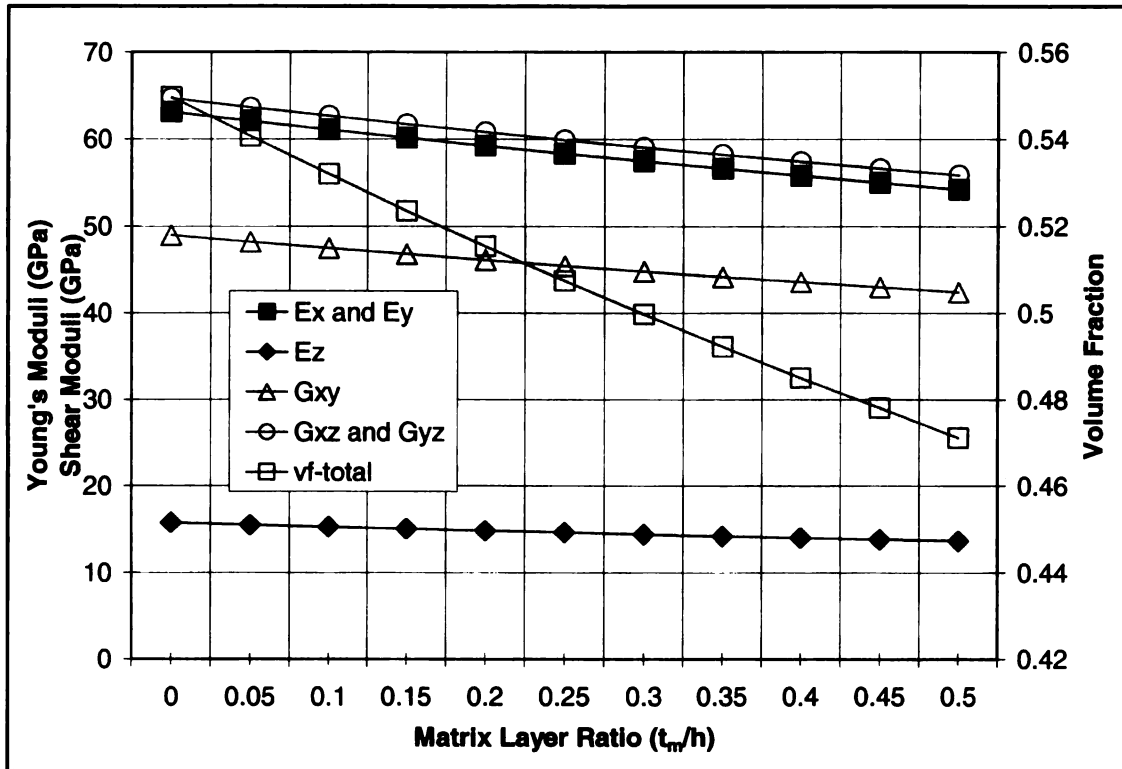
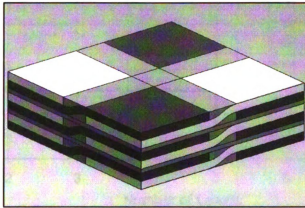


Figure 25. Effective Moduli for Varying Matrix Layer Thickness

As shown in the graph, all of the properties decrease linearly by 15% over the domain. The same trend holds true for the shear moduli. This is due to the decrease in overall fiber volume fraction of the cell, as seen in the graph.

### 3.3.2 Number of Layers (2D)

In most composite structures, multiple layers will be used. It is important to know how this will affect the properties. The addition of a matrix layer would cause the properties to vary as the number of layers,  $n$ , changes. Figure 26 displays the unit cells with matrix layers.



**Figure 26.** Projected View of Multiple 2D Unit Cells with Matrix Layers

The case study was performed with a matrix layer ratio,  $t_m/h$ , of 0.1. The case study is dependent on the following parameters.

$$E^C = f\left(\alpha\left(A_{eff}\left(\tilde{A}\left(A(n,h)\right)\right)\right)\right) \quad (35)$$

Figure 27 shows the trends in the moduli as the number of layers is increased. The solid lines indicate the presence of the matrix layers. The dashed lines indicate the properties without the presence of any matrix layers. These dashed lines are horizontal and do not vary.

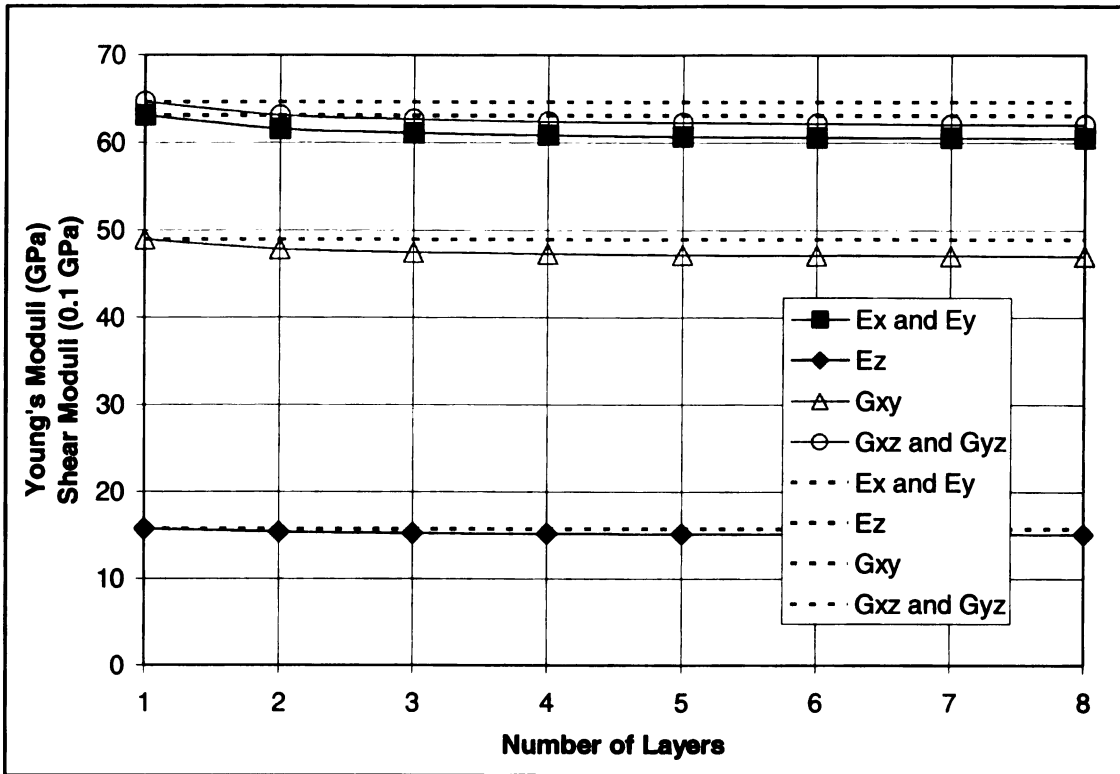


**Figure 27.** Effective Moduli for Varying Number of Layers

All of the moduli decrease slightly, 4%, and then converge upon a value after approximately 5 layers. The dashed lines show that the decrease in the moduli is not very significant as the layer number is increased. Also, the properties do not change with the number of layers without matrix layers present. It is therefore concluded that the 2D Plain Weave has very similar properties regardless of the number of layers.

### 3.3.3 Number of Layers (Q3D)

The number of layers,  $n$ , case study was also performed on the Q3D Weave. The details of analyzing the Q3D weave will be explained in detail in the next chapter. Figure 28 shows the Q3D Weave with 5 layers. With the Q3D weave, each layer is woven into layers above and below.

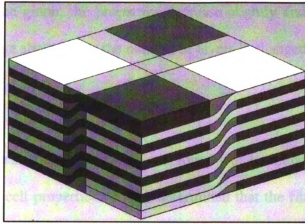


**Figure 28.** Projected View of Q3D Unit Cell with 5 Layers

The lack of symmetry in the z direction will cause the properties to change as the number of layers is changed. Equation (36) shows the varied parameters.

$$E^C = f\left(a\left(A_{eff}\left(\tilde{A}\left(A(n, h)\right)\right)\right)\right) \quad (36)$$

Figure 29 shows the changes in the cell moduli for several different layer numbers. The minimum number of layers for the Q3D Weave is three.

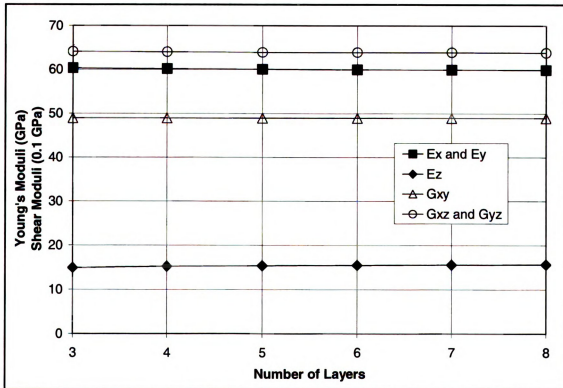


**Figure 29.** Effective Moduli for Varying Number of Q3D Layers

As seen in the graph, the properties decrease slightly and then converge. The properties only change about 1% as the number of layers is changed.

### **3.4 Summary**

From the case studies conducted, it was found which unit cell parameters have the largest effect on the cell properties. It was determined that the fiber volume fraction of the yarns is very important. Small changes in this parameter have a strong effect on the cell properties. It is also discovered that the location of the matrix in the cell can cause deviation in the cell properties.

Many of the geometric parameters were found to affect the cell properties by altering the undulation angle. The undulation regions are the most important geometric parameters that change the cell properties. Variations in this area control the amount of pure matrix regions and the orientations of many of the fibers. These two changes cause many of the variations in the cell properties.

The addition of multiple layers for the 2D and Q3D Weaves did not cause the cell properties to change significantly. Even with the addition of a small resin layer the differences were very small. Therefore, it gives confidence to the ability to use a single layer unit cell to predict the properties of a structure.

All of the above case studies aid in the understanding of composite properties. Optimization of the cell and composite properties may take place with this knowledge of the cell parameters. The composite design may be altered to best fit expected loadings.

## CHAPTER 4 – COMPARISON OF WEAVING PATTERNS

### 4.1 Weave Patterns

The previous analysis on the 2D Plain Weave allowed for the derivation of the analytical model and for various case studies to be conducted. Two other composite structures to be analyzed are the 0/90 Laminate and the Quasi-3D (Q3D) Weave.

#### 4.1.1 Laminate

The Laminate composite is two plies of unidirectional yarns stacked on each other. One layer consists of two plies. Figure 29 shows the unit cell and side view of a three layer 0/90 Laminate,  $L[0/90]_3$ .

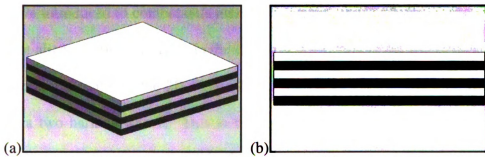


**Figure 30.** 0/90 Laminate Unit Cell (a) Projected View and (b) Side View

The green plies have fibers running parallel to the page. The white plies have fibers running into the page. This microstructure will give the highest possible in-plane properties as the fibers are perfectly aligned in the in-plane directions. There are no undulation areas or pure matrix zones. For designs that require only in-plane loading, this is a very good design. However, this microstructure is very susceptible to delamination. The plies are only held together by the weak matrix material in the yarns. Therefore, bending, impact, and fatigue loadings have a strong tendency to lead to delamination. This will result in weakened properties or even failure of the structure.

The properties of this microstructure were calculated using Classical Laminate Theory without any required modifications or averaging.

For loadings that can lead to delamination, this design must be modified. The shortcomings of stitching and z-pinning were discussed in Chapter 1. The 2D Plain Weave was one possible weave pattern that was introduced. It is effective in preventing delamination in each individual layer. However, the layers are only held together by the matrix material and have a tendency to delaminate. For structures requiring more than one layer, delamination will be an issue. Therefore, the weave must be further modified.

#### 4.1.2 Quasi-3D Weave

A weave introduced to combat delamination is the Quasi-3D (Q3D) Weave. The weave does not align any fibers directly in the thickness direction but the weave creates a solid, 3D structure. Similar to the 2D Plain Weave, the fill and warp fibers are woven together with a two harness weave. This is simply the frequency that the warp yarns overlap the fill yarns. However, as explained in Chapter 1, each ply is woven into the plies above and below. Therefore, there is not a stacking of layers, but an integration of the layers. This does not allow the plies to easily peel apart when the matrix holding them together fails. This design has been shown experimentally [15] to have higher structural integrity and greater delamination resistance than the 2D Plain Weave. The projected and side views of the Q3D unit cell are shown in Figure 31.

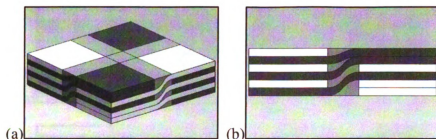


**Figure 31.** Quasi3D Weave Unit Cell (a) Projected View and (b) Side View

Analysis conducted on this weave was done using the same method as outlined in Chapter 2. As before, there were four regions that all had four subregions. The number of plies in the subregions was greater. There are two different undulation types in the Q3D weave. As seen in Figure 31(b), some of the yarns at the top and bottom of the cell do not have as large of an undulation as the other yarns. This is because these yarns at the top and bottom extremes are unable to be woven with yarns in the layers above or below as there are none.

The weaving pattern of the Q3D Weave is similar in style to that of the 2D Plain Weave. The improvement to the delamination resistance makes this weave an attractive design. However, it is important to know how much the additional weaving reduces effective properties of the weave.

## 4.2 Comparisons

### 4.2.1 Moduli

As mentioned, the composite microstructures of the Laminate, 2D Plain Weave, and Q3D Weave were all analyzed. Figure 32 shows the edge replication of the weaves that have been created with prepreg tape.

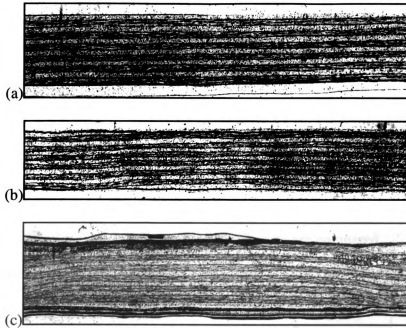


**Figure 32.** Edge Replication of the (a) Laminate, (b) 2D Plain Weave, and (c) Q3D Weave

The same material properties and geometric constraints were used in the calculation of all the weaves. These are displayed in Tables 9-11. Obviously, the undulation length ( $a_u$ ) is not applicable to the Laminate.

**Table 9.** Composite Yarn Properties

$E_{11}$ (GPa)	144.8
$E_{22}$ (GPa)	11.728
$E_{33}$ (GPa)	11.728
$G_{12}$ (GPa)	5.516
$G_{13}$ (GPa)	5.516
$G_{23}$ (GPa)	5.516
$\nu_{12}$	0.23
$\nu_{13}$	0.23
$\nu_{23}$	0.3
$\nu_f$	0.64

**Table 10.** Matrix Material Properties

$E_M$ (GPa)	3.448
$G_M$ (GPa)	1.276
$\nu_M$	0.35

**Table 11. Unit Cell Geometric Properties**

a (mm)	10
a <sub>u</sub> (mm)	1.467
h (mm)	0.989

Linear undulations with Series-Parallel alignments were used in the calculations. Table 12 shows the properties of these weaves. Along with the Young's moduli, shear moduli, and Poisson's ratios the Lekhnitskii and Chentsov coefficients are tabulated, for completeness. Therefore, all 21 independent coefficients are compared.

**Table 12. Comparison of the Properties for Different Weaving Patterns**

	<b>Laminate</b>	<b>2D</b>	<b>Q3D</b>
E <sub>x</sub> (GPa)	78.81	62.77	60.33
E <sub>y</sub> (GPa)	78.81	62.77	60.33
E <sub>z</sub> (GPa)	12.62	12.33	14.91
G <sub>xy</sub> (GPa)	5.516	4.89	4.894
G <sub>xz</sub> (GPa)	5.516	6.45	6.41
G <sub>yz</sub> (GPa)	5.516	6.45	6.41
ν <sub>xy</sub>	0.0345	0.0279	0.0341
ν <sub>xz</sub>	0.2925	0.3595	0.2968
ν <sub>yz</sub>	0.2925	0.3595	0.2968
η <sub>11,23</sub>	0	-5.33E-18	-8.07E-19
η <sub>11,31</sub>	0	-2.24E-17	-1.41E-18
η <sub>11,12</sub>	0	1.53E-36	-1.67E-36
η <sub>22,23</sub>	0	2.24E-17	1.41E-18
η <sub>22,31</sub>	0	5.33E-18	8.07E-19
η <sub>22,12</sub>	0	1.53E-36	-1.67E-36
η <sub>33,23</sub>	0	2.67E-16	3.78E-17
η <sub>33,31</sub>	0	-2.67E-16	-3.78E-17
η <sub>33,12</sub>	0	4.78E-35	-2.11E-34
μ <sub>23,31</sub>	0	-7.40E-17	-2.57E-17
μ <sub>23,12</sub>	0	5.56E-34	-2.00E-33
μ <sub>31,12</sub>	0	-5.56E-34	2.00E-33

As expected, there is a significant difference in the properties when switching from laminate plies to woven fabrics. The in-plane Young's moduli reduce by 20%

between the Laminate and the 2D Plain Weave. There is little difference in the out-of-plane Young's modulus as the increased undulation angle and the introduction of the matrix regions offset each other. The in-plane shear moduli decrease and the out-of-plane moduli increase more than 15%. This is also due to the undulation of the woven yarns as opposed to the unidirectionality of the laminate. The Poisson Ratios follow the same trends as the shear moduli. On the average, the in-plane properties decrease 20% and the out-of-plane properties increase 20% when switching from laminates to woven fabrics. The exception is the Young's modulus in the  $z$ -direction as it does not change significantly.

The table shows that the differences between the 2D Plain Weave and the Q3D Weave are not very large. The differences in the in-plane Young's moduli are less than 5%. The out-of-plane Young's modulus increases by 20%. The shear moduli have no significant change between the weaving patterns. The Poisson's ratio differences are 20% or less. The in-plane ratios increase while the out-of-plane ratios decrease. The only significant property change between the two patterns is the increase of  $E_z$ .

The Lekhnitskii and Chentsov coefficients are either zero or extremely small for all the microstructures. These are the relations between normal stress/strain to shear strain/stress and the relation between shear stress and strain in different plains, respectively.

For better visual aid in the differences in the properties between weaves, Figures 33-35 show the comparison for varying weave angles.

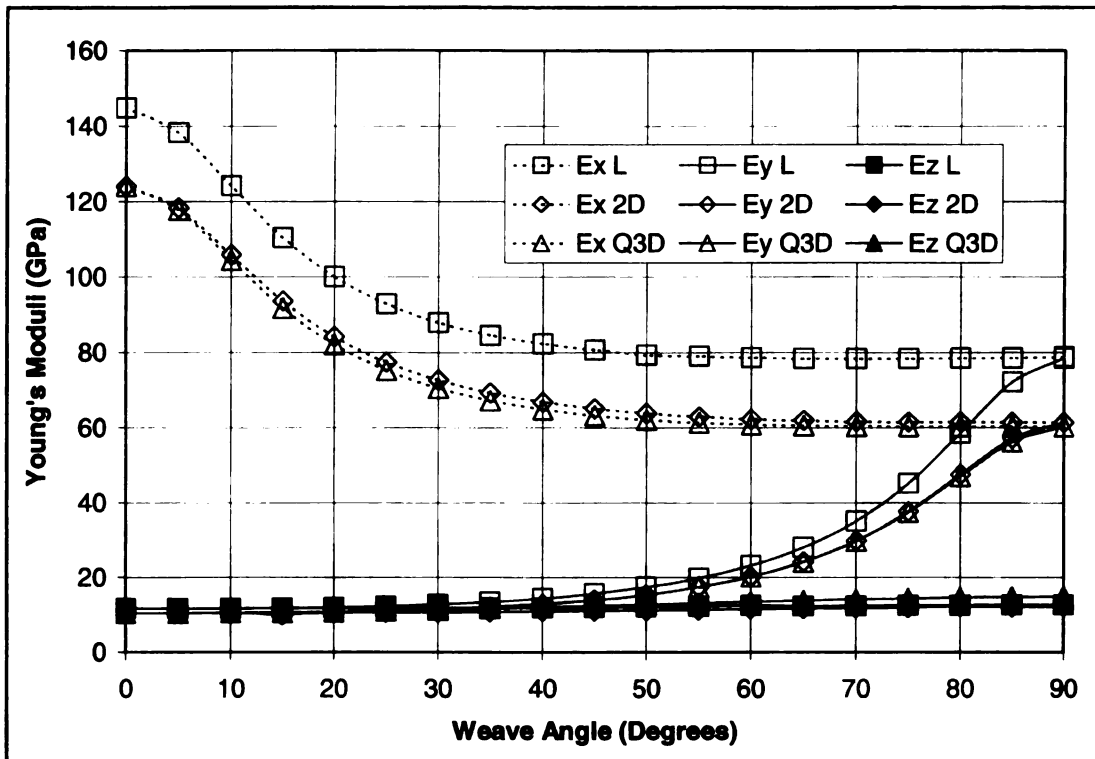


Figure 33. Comparison of Weave Pattern Young's Moduli for Varying Weaving Angle

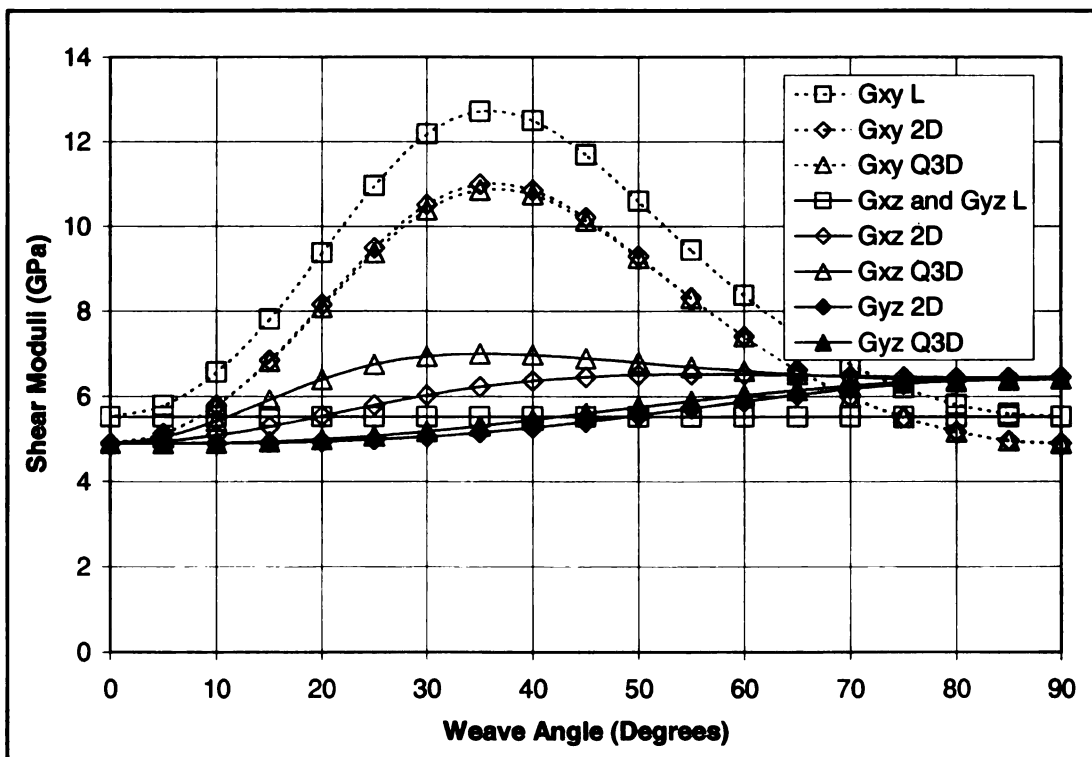


Figure 34. Comparison of Weave Pattern Shear Moduli for Varying Weaving Angle

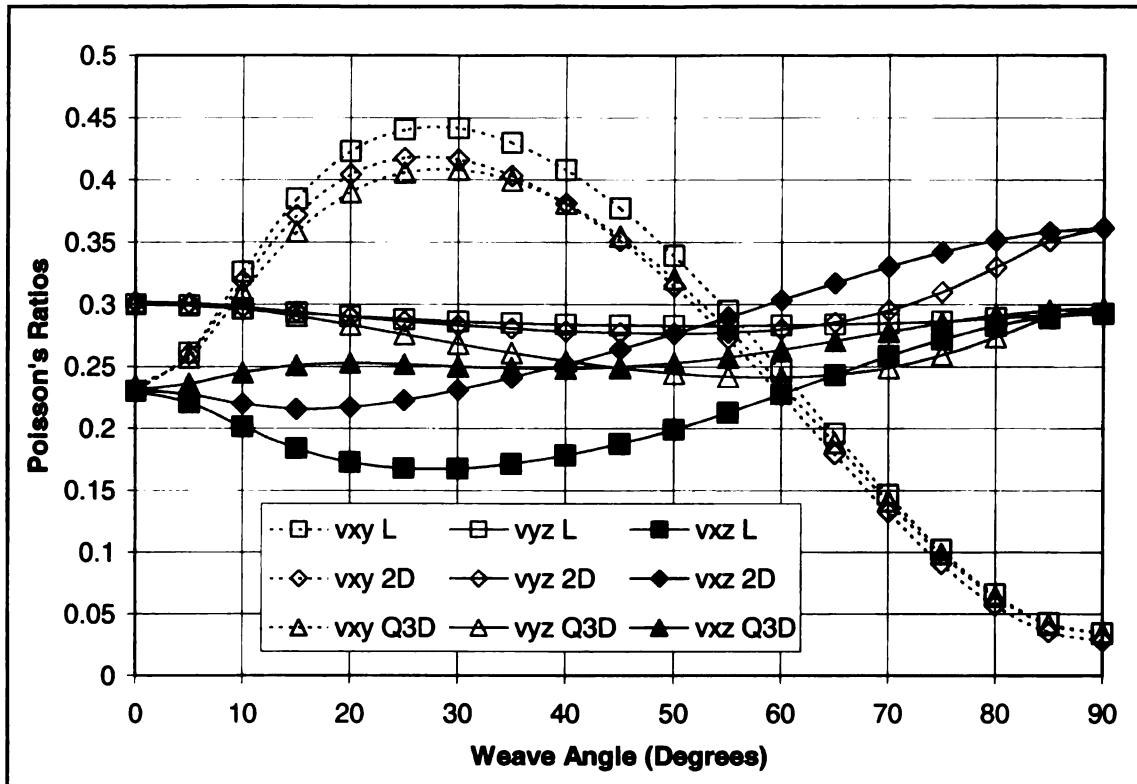


Figure 35. Comparison of Weave Pattern Poisson's Ratios for Varying Weaving Angle

The graphs show the gap between the properties of the laminated composites and woven fabrics. However, the difference in properties between the 2D Plain Weave and the Q3D Weave is very small.

#### 4.2.2 Bending Stiffness

The different orientations of the warp and fill fibers cause a bending mismatch. The difference in the resistance to bending in the yarns will cause them to delaminate if the bending moment is great enough. If the warp fibers have a different resistance to bending than the fill fibers, there will be a stress concentration at the interface that will lead to delamination. The resistance to bending is governed by the **D** matrix. The **D** matrix is calculated by the following equation.

$$A_{mk} = \sum_{j=1}^n \bar{C}_{mk} \cdot \Delta z^3 \quad (37)$$

Figure 36 shows the bending resistance coefficients of a woven fabric for different weaving angles. The graph displays the difference in the bending resistance between the fill and the warp yarns. The smaller the difference between yarns, the greater the delamination resistance.

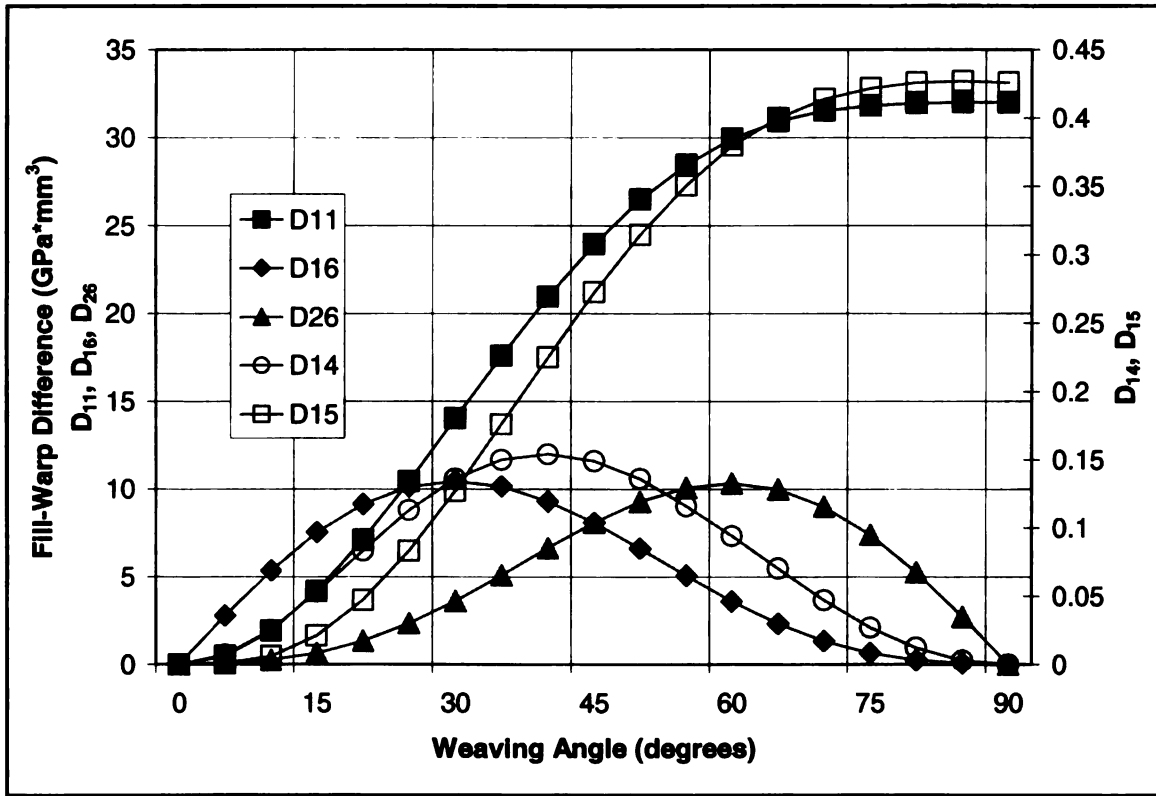


Figure 36. Bending Stiffness for Varying Weave Angle

The coefficients in the graph represent the relation between bending along the  $x$ -axis and curvature in various planes. These represent delamination from the three possible modes. As seen in the graph, the resistance for all of the coefficients is very small for small weaving angles. Therefore, the probability of delamination can be greatly reduced by employing small weaving angles. This could be especially effective for the

bottom layers of a structure as this is a very common location of delamination from impact and bending loadings.

### **4.3 Summary**

This chapter shows the property differences between laminated composites and woven fabrics. The in-plane moduli of the laminated composites are much higher than that of the woven fabrics. However, the possibility of delamination makes the laminated microstructures a poor choice in many applications. The 2D Plain Weave greatly improves the delamination resistance for one layer designs. The major tradeoff in this weave is the sacrificing of 20% of the maximum (laminated) in-plane Young's moduli. The other properties all have smaller changes that are very acceptable for the improved delamination resistance. The increase in the structural integrity of a composite with only one layer, while still achieving 80% of the maximum stiffness, is not a great tradeoff.

The Q3D weave protects against delamination for weaves with a higher number of layers. As seen in the above tables and graphs, it has very similar properties to the 2D Plain Weave. Therefore, it also achieves approximately 75% of the maximum stiffness while allowing multiple layers that are integrated together. This is a much more acceptable tradeoff.

## CHAPTER 5 – CONCLUSIONS AND RECOMMENDATIONS

### 5.1 Conclusions

1. A model for calculating the properties of composite weaving patterns from unit cell analysis, based on Classical Laminate Theory, was derived. It is a 3D model that considers linear undulation and employs series-parallel subregion integration.
2. The area found to have the most critical effect on the unit cell properties is the undulation zone. Many of the unit cell parameters that were discussed changed the properties because of their effect on the undulation angle. These include the undulation length ( $a_u$ ), yarn thickness ( $h$ ), and cell size ( $a^*$ ). This zone controls the orientation of a significant portion of the yarn fibers, as well as the amount of pure matrix regions in the unit cell. A 1% increase in the undulation length caused a 1.2% decrease in the in-plane properties. This translates into a 0.5 mm increase causing a 14 GPa decrease in the modulus for the given example.
3. The addition of multiple layers beyond the minimum number of layers does not significantly affect the composite properties. Therefore, the minimum layer unit cell will give a very good representation of the entire structure properties. The minimum layer unit cell is one layer for the 0/90 Laminate and the 2D Plain Weave. For the Q3D Weave it is three layers because of the weave design. It was seen in the case studies involving layer numbers that the properties changed less than 1% as the number of layers increased for any of the weaves.
4. There is a loss of in-plane stiffness of 20-25% when switching to 2D or Q3D weaves from laminated composites. The woven fabrics are used to combat

delamination. Laminated composites are held together by only matrix bonding. The 2D Plain Weave improves delamination resistance over the Laminate for only one layer and sacrifices 20% of the Laminate's in-plane stiffness. The interlocking of the yarns in the 2D Plain Weave helps to prevent delamination in a single layer. However, successive layers are held together by only matrix bonding, as with the Laminate. However, the Q3D Weave improves delamination resistance for multiple layers and sacrifices 25% of the Laminate's in-plane stiffness. This weave interlocks the yarns for all layers and thus giving delamination resistance through the thickness. Therefore, the Q3D weave seems to be a much more practical and useful design.

5. Based on the geometric case studies of Chapter 3, the following recommendations will cause the properties of woven fabrics to approach those of laminated composites:

- a) Thin Yarns
- b) Longer Cell Length (Higher Harness)
- c) Small Undulation Length

## **5.2 Recommendations**

1. Unit cell analysis of the Q3D Weave with the three and five harness tows would be useful. The harness is the frequency of undulation. This would mean that the length of the non-undulated portions of the fibers would be longer for these harnesses. Also, the increased complexity of this weave causes the much of the pure matrix zones to be filled with yarns. It is therefore expected that the in-plane

properties of those weaves to increase compared to the basic two harness Q3D weave.

2. The effective properties of the composite weave could be substituted into a finite element code. This would allow for analysis of a complete composite structure without concern for the weaving pattern. There would be a significant savings in time and data if the composite structures were treated as an anisotropic material with constant properties instead of modeling the entire weave.

## APPENDICES

### Appendix A – Poisson Ratios of Case Studies

#### A.1 Fiber Volume Fraction

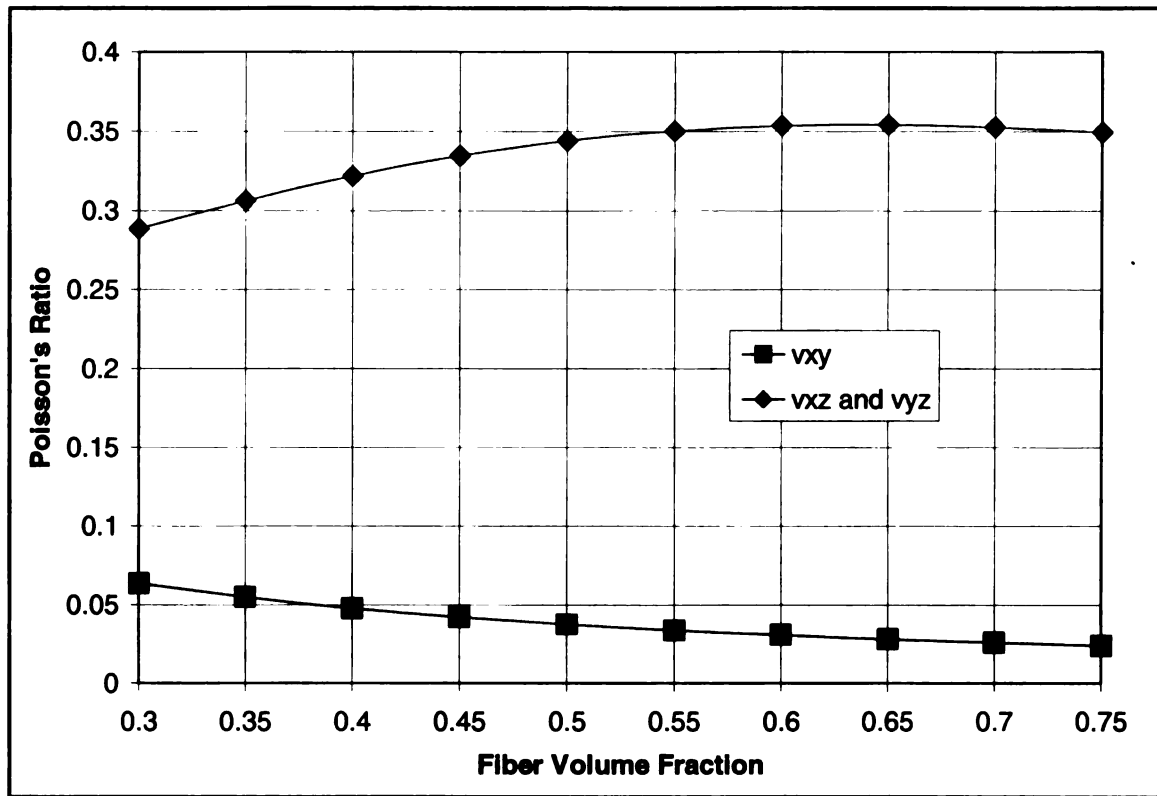


Figure 37. Poisson's Ratios for Varying Yarn Fiber Volume Fraction

### A.2 Yarn Thickness

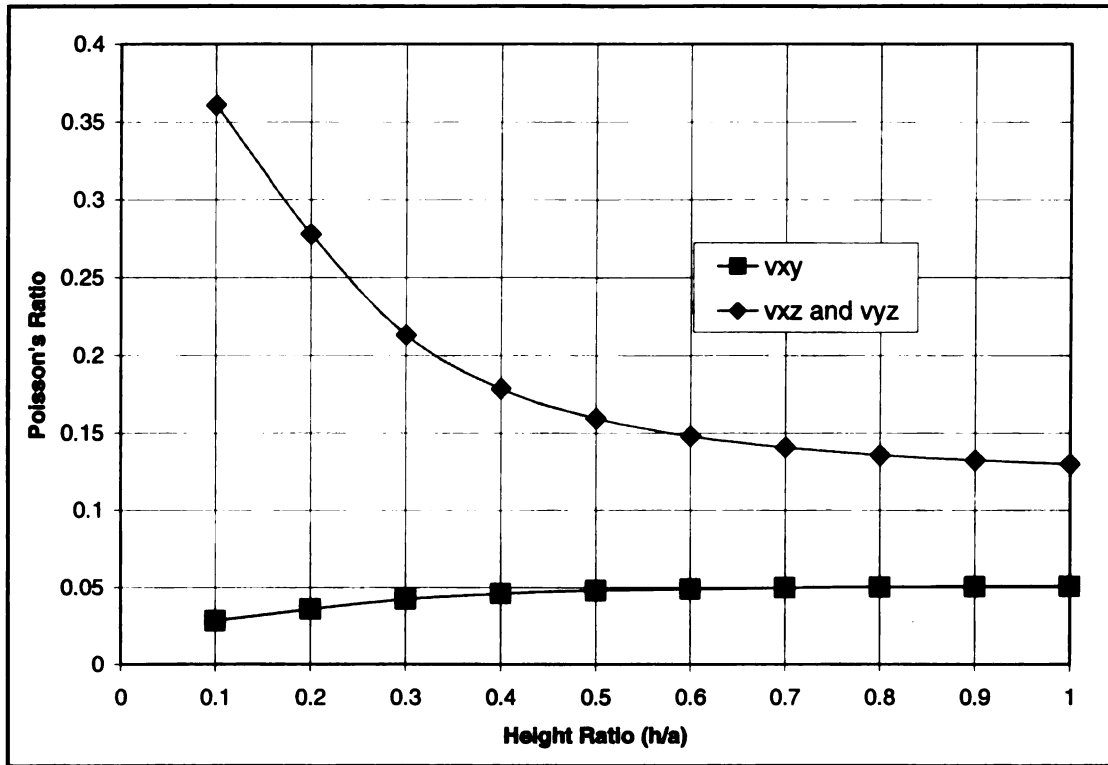


Figure 38. Poisson's Ratios for Varying Yarn Thickness

### A.3 Undulation Length

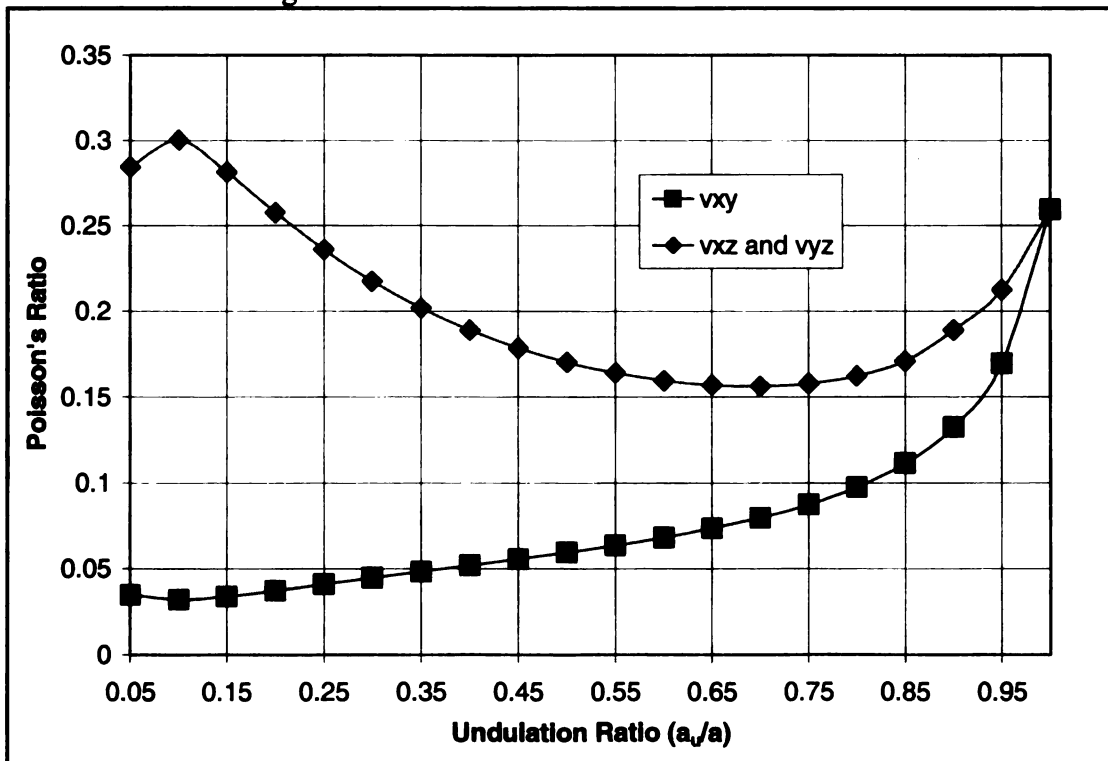


Figure 39. Poisson's Ratios for Varying Undulation Length

#### A.4 Weaving Angle

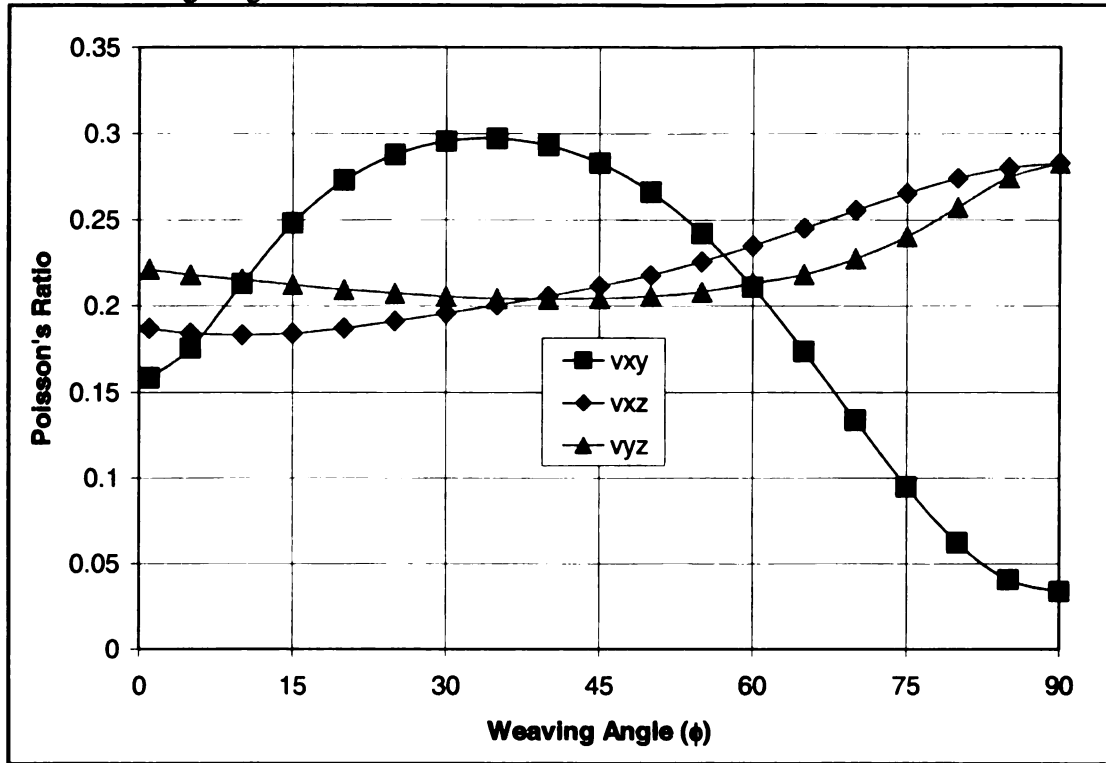


Figure 40. Poisson's Ratios for Varying Weaving Angle

#### A.5 Cell Size

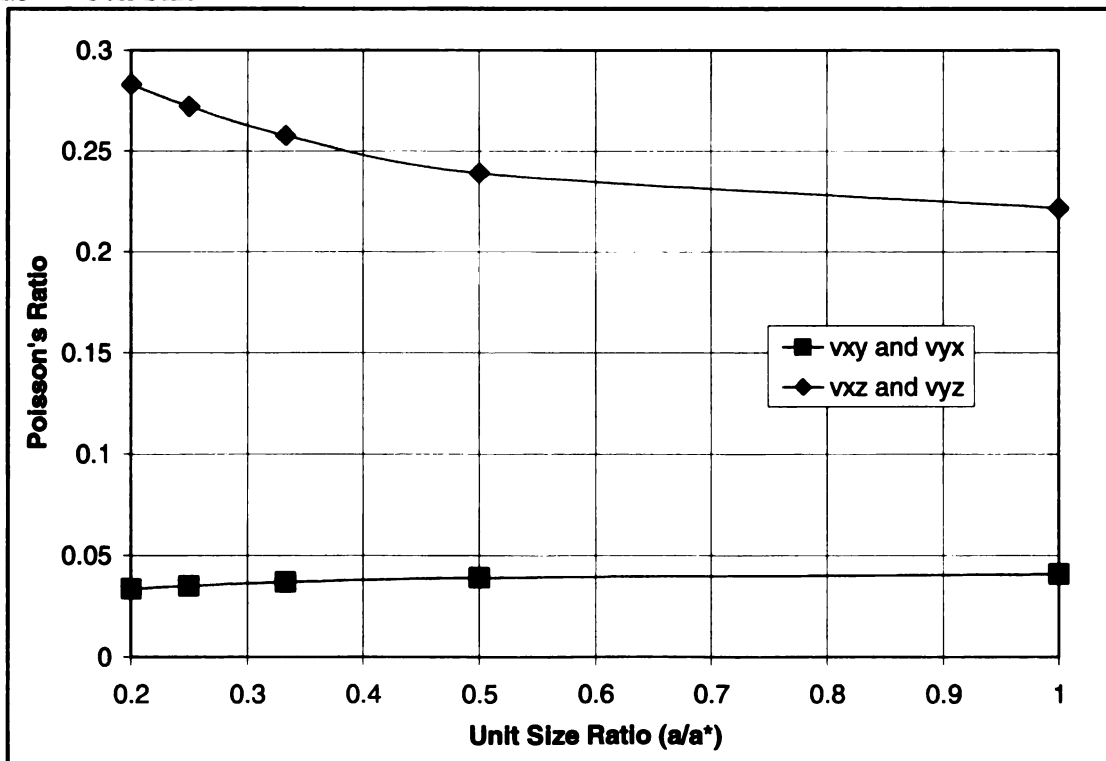


Figure 41. Poisson's Ratios for Varying Cell Size

### A.6 Undulation Angle Effects

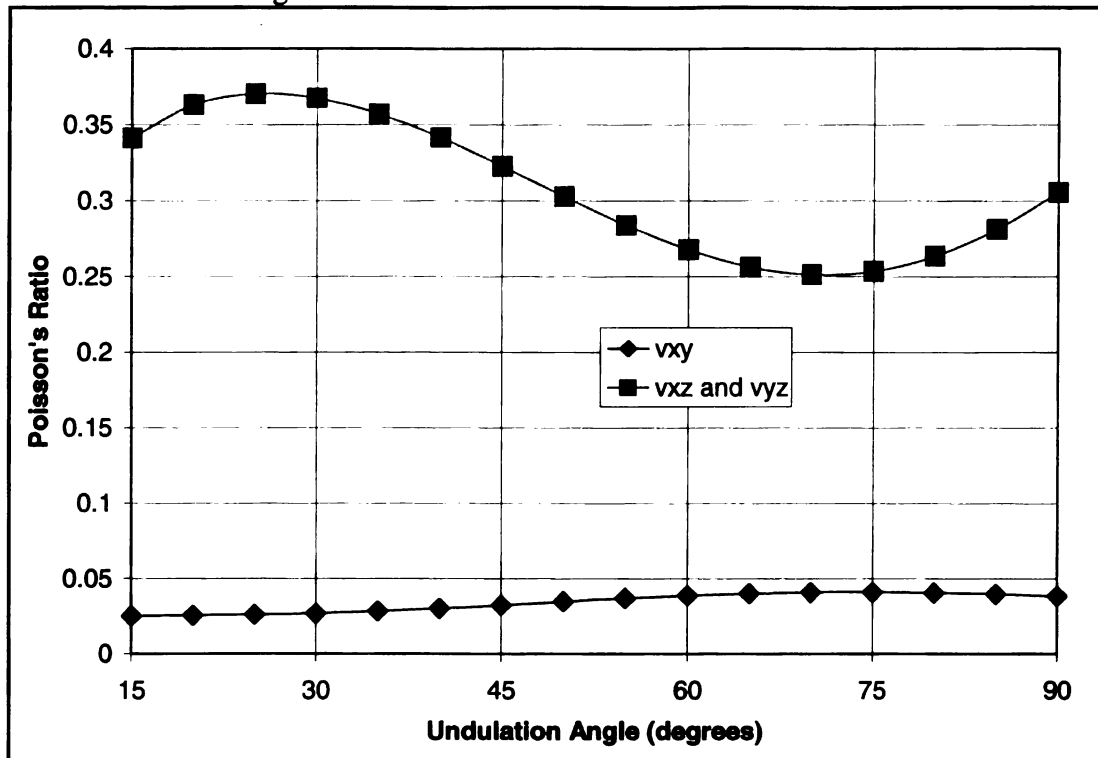


Figure 42. Poisson's Ratios for Varying Undulation Angles

### A.7 Matrix Layer Thickness

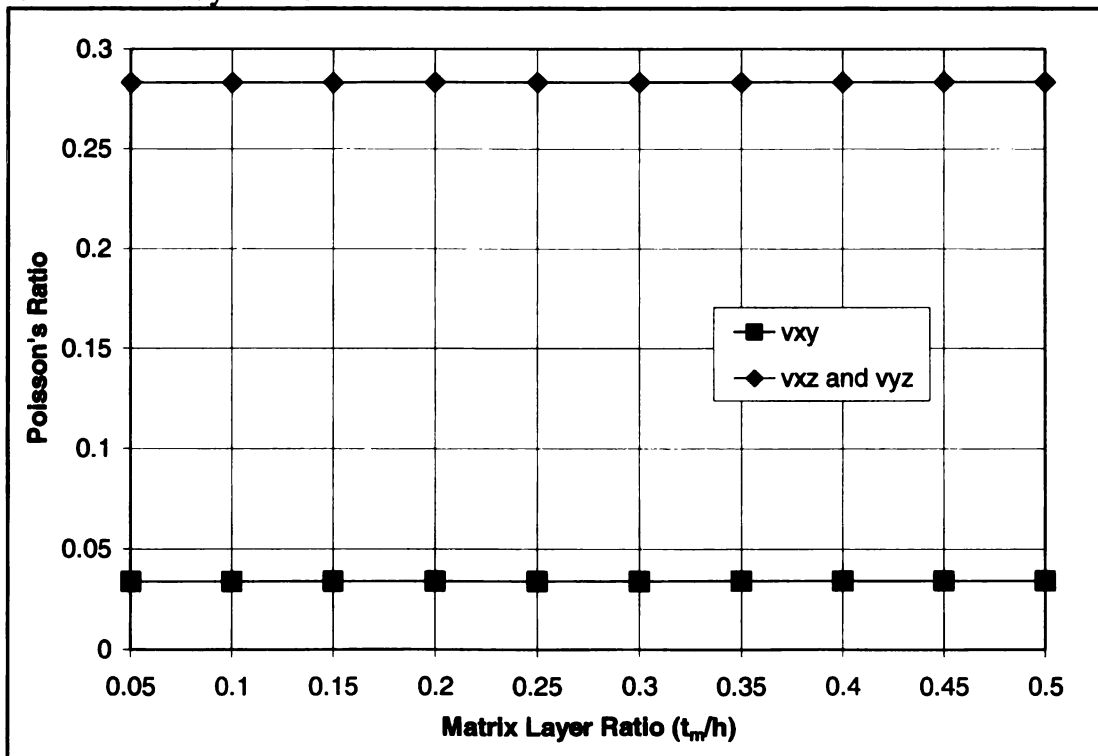


Figure 43. Poisson's Ratios for Varying Matrix Layer Thickness

A.8 Number of Layers

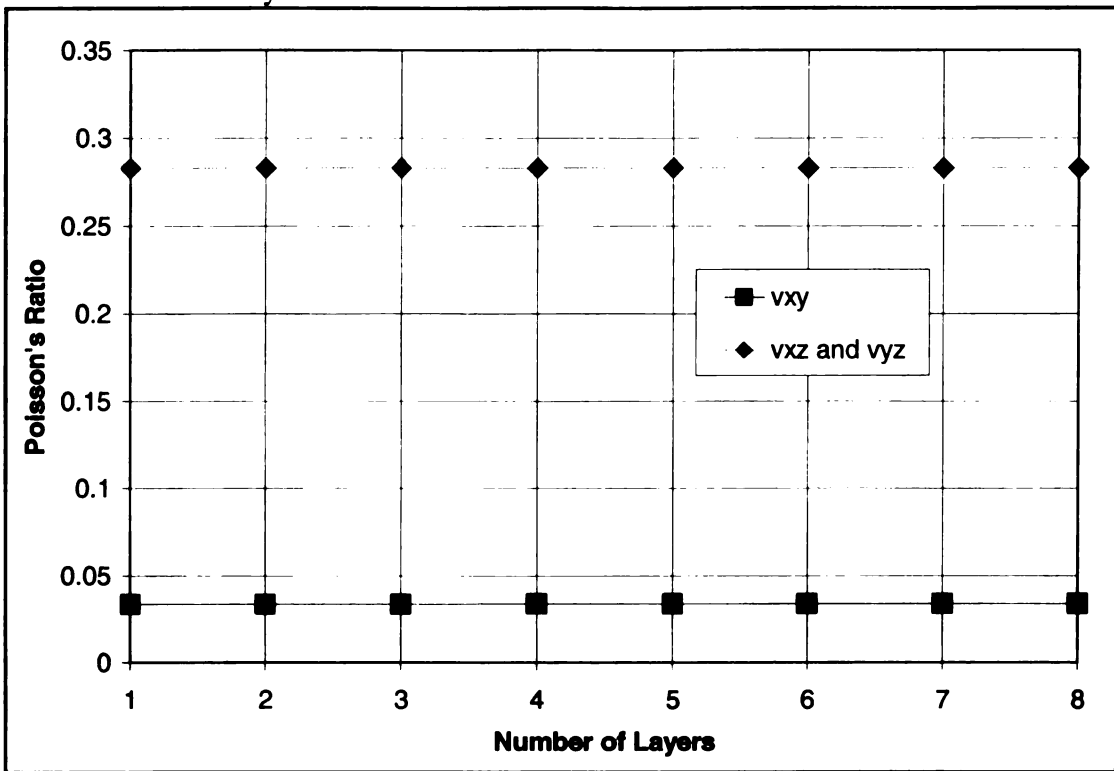


Figure 44. Poisson's Ratios for Varying Number of Layers

A.9 Q3D Number of Layers

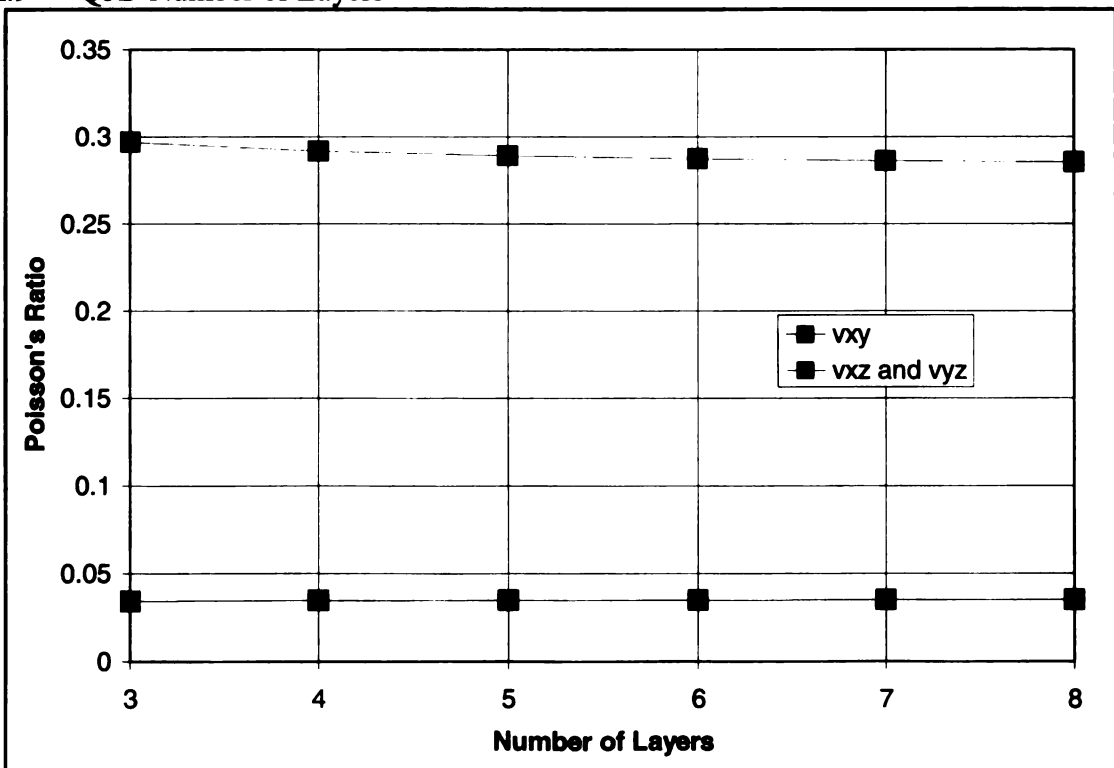


Figure 45. Poisson's Ratios for Varying Number of Q3D Layers

## Appendix B – Mathematica Code

### B.1 Laminate

**ClearAll[]**

$$\mathbf{B} = \begin{pmatrix} \frac{1}{E_x} & \frac{-\nu_{yx}}{E_y} & \frac{-\nu_{zx}}{E_z} & 0 & 0 & 0 \\ \frac{-\nu_{xy}}{E_x} & \frac{1}{E_y} & \frac{-\nu_{zy}}{E_z} & 0 & 0 & 0 \\ \frac{-\nu_{xz}}{E_x} & \frac{-\nu_{yz}}{E_y} & \frac{1}{E_z} & 0 & 0 & 0 \\ 0 & 0 & 0 & \frac{1}{G_{yz}} & 0 & 0 \\ 0 & 0 & 0 & 0 & \frac{1}{G_{xz}} & 0 \\ 0 & 0 & 0 & 0 & 0 & \frac{1}{G_{xy}} \end{pmatrix};$$

**(\*Inverting Stress–Strain\*)**

**Q = Simplify[Inverse[B]]; (\*Q Matrix for Fibers\*)**

**E<sub>x</sub> = 144.8 \* 10<sup>9</sup>; (\*Material Properties\*)**

**E<sub>y</sub> = 11.728 \* 10<sup>9</sup>;**

**E<sub>z</sub> = 11.728 \* 10<sup>9</sup>;**

**G<sub>xy</sub> = 5.516 \* 10<sup>9</sup>;**

**G<sub>xz</sub> = 5.516 \* 10<sup>9</sup>;**

**G<sub>yz</sub> = 5.516 \* 10<sup>9</sup>;**

**E<sub>M</sub> = 3.448 \* 10<sup>9</sup>;**

**ν<sub>xy</sub> = 0.23;**

**ν<sub>xz</sub> = 0.23;**

**ν<sub>yz</sub> = 0.3;**

**ν<sub>M</sub> = 0.35;**

**G<sub>M</sub> = 1.276 \* 10<sup>9</sup>;**

**n = 1; (\*Number of Layers\*)**

**a = (10 \* 10<sup>-3</sup>); (\*Geometric Properties\*)**

**h = 0.989 \* 10<sup>-3</sup>;**

**h<sub>t</sub> = h;**

**a<sub>0</sub> = a - a<sub>u</sub>;**

**φ = 90 \* π / 180;**

**t = 2 \* h \* n;**

$$v_{yx} = \frac{E_y}{E_x} * v_{xy}; \quad (*\text{Poisson Definition}*)$$

$$v_{zx} = \frac{E_z}{E_x} * v_{xz};$$

$$v_{zy} = \frac{E_z}{E_y} * v_{yz};$$

$$l = \begin{pmatrix} \cos[\phi] & \cos[\phi + \frac{\pi}{2}] & 0 \\ \cos[\phi - \frac{\pi}{2}] & \cos[\phi] & 0 \\ 0 & 0 & 1 \end{pmatrix};$$

(\*Fiber Direction Transformation\*)

L =

$$\begin{pmatrix} \text{Part}[l, 1, 1]^2 & \text{Part}[l, 2, 1]^2 & \text{Part}[l, 3, 1]^2 \\ \text{Part}[l, 1, 2]^2 & \text{Part}[l, 2, 2]^2 & \text{Part}[l, 3, 2]^2 \\ \text{Part}[l, 1, 3]^2 & \text{Part}[l, 2, 3]^2 & \text{Part}[l, 3, 3]^2 \\ \text{Part}[l, 1, 2] * \text{Part}[l, 1, 3] & \text{Part}[l, 2, 2] * \text{Part}[l, 2, 3] & \text{Part}[l, 3, 2] * \text{Part}[l, 3, 3] \\ \text{Part}[l, 1, 1] * \text{Part}[l, 1, 3] & \text{Part}[l, 2, 1] * \text{Part}[l, 2, 3] & \text{Part}[l, 3, 1] * \text{Part}[l, 3, 3] \\ \text{Part}[l, 1, 1] * \text{Part}[l, 1, 2] & \text{Part}[l, 2, 1] * \text{Part}[l, 2, 2] & \text{Part}[l, 3, 1] * \text{Part}[l, 3, 2] \end{pmatrix};$$

P = L.Q.Transpose[L];

P;

FLAT = Table[0, {i, 1, 6}, {j, 1, 6}];

(\*Flat Fiber Region\*)

Part[FLAT, 1, 1] = Part[P, 1, 1] \* n \* h + Part[Q, 1, 1] \* n \* h;

Part[FLAT, 1, 2] = Part[P, 1, 2] \* n \* h + Part[Q, 1, 2] \* n \* h;

Part[FLAT, 2, 1] = Part[P, 1, 2] \* n \* h + Part[Q, 1, 2] \* n \* h;

Part[FLAT, 2, 2] = Part[P, 2, 2] \* n \* h + Part[Q, 2, 2] \* n \* h;

Part[FLAT, 1, 3] = Part[P, 1, 3] \* n \* h + Part[Q, 1, 3] \* n \* h;

Part[FLAT, 3, 1] = Part[P, 3, 1] \* n \* h + Part[Q, 3, 1] \* n \* h;

Part[FLAT, 2, 3] = Part[P, 2, 3] \* n \* h + Part[Q, 2, 3] \* n \* h;

Part[FLAT, 3, 2] = Part[P, 3, 2] \* n \* h + Part[Q, 3, 2] \* n \* h;

Part[FLAT, 3, 3] = Part[P, 3, 3] \* n \* h + Part[Q, 3, 3] \* n \* h;

**Part[FLAT, 1, 4] = Part[P, 1, 4] \* n \* h + Part[Q, 1, 4] \* n \* h;**  
**Part[FLAT, 4, 1] = Part[P, 4, 1] \* n \* h + Part[Q, 4, 1] \* n \* h;**  
**Part[FLAT, 1, 5] = Part[P, 1, 5] \* n \* h + Part[Q, 1, 5] \* n \* h;**  
**Part[FLAT, 5, 1] = Part[P, 5, 1] \* n \* h + Part[Q, 5, 1] \* n \* h;**  
**Part[FLAT, 1, 6] = Part[P, 1, 6] \* n \* h + Part[Q, 1, 6] \* n \* h;**  
**Part[FLAT, 6, 1] = Part[P, 6, 1] \* n \* h + Part[Q, 6, 1] \* n \* h;**  
**Part[FLAT, 2, 4] = Part[P, 2, 4] \* n \* h + Part[Q, 2, 4] \* n \* h;**  
**Part[FLAT, 4, 2] = Part[P, 4, 2] \* n \* h + Part[Q, 4, 2] \* n \* h;**  
**Part[FLAT, 2, 5] = Part[P, 2, 5] \* n \* h + Part[Q, 2, 5] \* n \* h;**  
**Part[FLAT, 5, 2] = Part[P, 5, 2] \* n \* h + Part[Q, 5, 2] \* n \* h;**  
**Part[FLAT, 2, 6] = Part[P, 2, 6] \* n \* h + Part[Q, 2, 6] \* n \* h;**  
**Part[FLAT, 6, 2] = Part[P, 6, 2] \* n \* h + Part[Q, 6, 2] \* n \* h;**  
**Part[FLAT, 3, 4] = Part[P, 3, 4] \* n \* h + Part[Q, 3, 4] \* n \* h;**  
**Part[FLAT, 4, 3] = Part[P, 4, 3] \* n \* h + Part[Q, 4, 3] \* n \* h;**  
**Part[FLAT, 3, 5] = Part[P, 3, 5] \* n \* h + Part[Q, 3, 5] \* n \* h;**  
**Part[FLAT, 5, 3] = Part[P, 5, 3] \* n \* h + Part[Q, 5, 3] \* n \* h;**  
**Part[FLAT, 3, 6] = Part[P, 3, 6] \* n \* h + Part[Q, 3, 6] \* n \* h;**  
**Part[FLAT, 6, 3] = Part[P, 6, 3] \* n \* h + Part[Q, 6, 3] \* n \* h;**  
**Part[FLAT, 4, 4] = Part[P, 4, 4] \* n \* h + Part[Q, 4, 4] \* n \* h;**  
**Part[FLAT, 4, 5] = Part[P, 4, 5] \* n \* h + Part[Q, 4, 5] \* n \* h;**  
**Part[FLAT, 5, 4] = Part[P, 5, 4] \* n \* h + Part[Q, 5, 4] \* n \* h;**  
**Part[FLAT, 4, 6] = Part[P, 4, 6] \* n \* h + Part[Q, 4, 6] \* n \* h;**  
**Part[FLAT, 6, 4] = Part[P, 6, 4] \* n \* h + Part[Q, 6, 4] \* n \* h;**  
**Part[FLAT, 5, 5] = Part[P, 5, 5] \* n \* h + Part[Q, 5, 5] \* n \* h;**  
**Part[FLAT, 5, 6] = Part[P, 5, 6] \* n \* h + Part[Q, 5, 6] \* n \* h;**  
**Part[FLAT, 6, 5] = Part[P, 6, 5] \* n \* h + Part[Q, 6, 5] \* n \* h;**  
**Part[FLAT, 6, 6] = Part[P, 6, 6] \* n \* h + Part[Q, 6, 6] \* n \* h;**  
**FLAT;**  
**FLATAREA = FLAT \* (a)<sup>2</sup> \* Sin[φ];**  
**FLATTOTAL = FLATAREA;**

$$\text{TOTAL} = \text{FLATTOTAL};$$

$$\text{AVERAGE} = \frac{\text{TOTAL}}{(a)^2 * \text{Sin}[\phi]};$$

$$\alpha = \text{Inverse}[\text{AVERAGE}];$$

$$\text{Print}["E_x="]$$

$$\frac{1}{\text{Part}[\alpha, 1, 1]} * t$$

$$\text{Print}["E_y="]$$

$$\frac{1}{\text{Part}[\alpha, 2, 2]} * t$$

$$\text{Print}["E_z="]$$

$$\frac{1}{\text{Part}[\alpha, 3, 3]} * t$$

$$\text{Print}["G_{xy}="]$$

$$\frac{1}{\text{Part}[\alpha, 6, 6]} * t$$

$$\text{Print}["G_{xz}="]$$

$$\frac{1}{\text{Part}[\alpha, 5, 5]} * t$$

$$\text{Print}["G_{yz}="]$$

$$\frac{1}{\text{Part}[\alpha, 4, 4]} * t$$

$$\text{Print}["\nu_{xy}="]$$

$$\frac{\text{Part}[\alpha, 2, 1]}{\text{Part}[\alpha, 1, 1]}$$

$$\text{Print}["\nu_{yx}="]$$

$$\frac{\text{Part}[\alpha, 1, 2]}{\text{Part}[\alpha, 2, 2]}$$

```
Print[" $\gamma_{xz}$ ="]  
Part[ $\alpha$ , 1, 3]  
-----  
Part[ $\alpha$ , 1, 1]
```

```
Print[" $\gamma_{zx}$ ="]  
Part[ $\alpha$ , 1, 3]  
-----  
Part[ $\alpha$ , 3, 3]
```

```
Print[" $\gamma_{yz}$ ="]  
Part[ $\alpha$ , 2, 3]  
-----  
Part[ $\alpha$ , 2, 2]
```

```
Print[" $\gamma_{zy}$ ="]  
Part[ $\alpha$ , 2, 3]  
-----  
Part[ $\alpha$ , 3, 3]
```

## B.2 2D Plain Weave

**ClearAll[]**

$$\mathbf{B} = \begin{pmatrix} \frac{1}{E_x} & \frac{-\nu_{yx}}{E_y} & \frac{-\nu_{zx}}{E_z} & 0 & 0 & 0 \\ \frac{-\nu_{xy}}{E_x} & \frac{1}{E_y} & \frac{-\nu_{zy}}{E_z} & 0 & 0 & 0 \\ \frac{-\nu_{xz}}{E_x} & \frac{-\nu_{yz}}{E_y} & \frac{1}{E_z} & 0 & 0 & 0 \\ 0 & 0 & 0 & \frac{1}{G_{yz}} & 0 & 0 \\ 0 & 0 & 0 & 0 & \frac{1}{G_{xz}} & 0 \\ 0 & 0 & 0 & 0 & 0 & \frac{1}{G_{xy}} \end{pmatrix};$$

**(\*Inverting Stress-Strain\*)**

**Q = Simplify[Inverse[B]]; (\*Q Matrix for Fibers\*)**

**E<sub>x</sub> = 144.8 \* 10<sup>9</sup>; (\*Material Properties\*)**

**E<sub>y</sub> = 11.728 \* 10<sup>9</sup>;**

**E<sub>z</sub> = 11.728 \* 10<sup>9</sup>;**

**G<sub>xy</sub> = 5.516 \* 10<sup>9</sup>;**

**G<sub>xz</sub> = 5.516 \* 10<sup>9</sup>;**

**G<sub>yz</sub> = 5.516 \* 10<sup>9</sup>;**

**E<sub>M</sub> = 3.448 \* 10<sup>9</sup>;**

**ν<sub>xy</sub> = 0.23;**

**ν<sub>xz</sub> = 0.23;**

**ν<sub>yz</sub> = 0.3;**

**ν<sub>M</sub> = 0.35;**

**G<sub>M</sub> = 1.276 \* 10<sup>9</sup>;**

**n = 1; (\*Number of Unit Cells\*)**

**m = 100000; (\*Number of Elements\*)**

**b = m/2 - 1;**

**(\*Number of Elements in half undulation\*)**

**τ = 2 \* h / m; (\*Thickness of elements\*)**

**area = a<sub>u</sub> \* τ; (\*Area of elements\*)**

$$\kappa = \frac{a_u}{m};$$

$$a_u = (1.467 * 10^{-3}) / n;$$

(\*Geometric Properties\*)

$$a = (10 * 10^{-3}) / n;$$

$$h = 0.989 * 10^{-3};$$

$$h_t = h;$$

$$a_0 = a - a_u;$$

$$\phi = 90 * \pi / 180;$$

$$\theta = \text{ArcTan}\left[\frac{h}{a_u} * \text{Cos}\left[\phi - \frac{\pi}{2}\right]\right];$$

$$t = 2 * h;$$

$$v_{yx} = \frac{E_y}{E_x} * v_{xy}; \quad (*\text{Poisson Definition}*)$$

$$v_{zx} = \frac{E_z}{E_x} * v_{xz};$$

$$v_{zy} = \frac{E_z}{E_y} * v_{yz};$$

$$l = \begin{pmatrix} \text{Cos}[\phi] & \text{Cos}\left[\phi + \frac{\pi}{2}\right] & 0 \\ \text{Cos}\left[\phi - \frac{\pi}{2}\right] & \text{Cos}[\phi] & 0 \\ 0 & 0 & 1 \end{pmatrix};$$

(\*Fiber Direction Transformation\*)

L =

$$\begin{pmatrix} \text{Part}[l, 1, 1]^2 & \text{Part}[l, 2, 1]^2 & \text{Par} \\ \text{Part}[l, 1, 2]^2 & \text{Part}[l, 2, 2]^2 & \text{Par} \\ \text{Part}[l, 1, 3]^2 & \text{Part}[l, 2, 3]^2 & \text{Par} \\ \text{Part}[l, 1, 2] * \text{Part}[l, 1, 3] & \text{Part}[l, 2, 2] * \text{Part}[l, 2, 3] & \text{Part}[l, 3, \\ \text{Part}[l, 1, 1] * \text{Part}[l, 1, 3] & \text{Part}[l, 2, 1] * \text{Part}[l, 2, 3] & \text{Part}[l, 3, \\ \text{Part}[l, 1, 1] * \text{Part}[l, 1, 2] & \text{Part}[l, 2, 1] * \text{Part}[l, 2, 2] & \text{Part}[l, 3, \end{pmatrix};$$

$$P = \text{L.Q.Transpose}[L];$$

P;

$$R = \begin{pmatrix} \frac{E_M}{1-\nu_M^2} & \frac{\nu_M \cdot E_M}{1-\nu_M^2} & \frac{\nu_M \cdot E_M}{1-\nu_M^2} & 0 & 0 & 0 \\ \frac{\nu_M \cdot E_M}{1-\nu_M^2} & \frac{E_M}{1-\nu_M^2} & \frac{\nu_M \cdot E_M}{1-\nu_M^2} & 0 & 0 & 0 \\ \frac{\nu_M \cdot E_M}{1-\nu_M^2} & \frac{\nu_M \cdot E_M}{1-\nu_M^2} & \frac{E_M}{1-\nu_M^2} & 0 & 0 & 0 \\ 0 & 0 & 0 & G_M & 0 & 0 \\ 0 & 0 & 0 & 0 & G_M & 0 \\ 0 & 0 & 0 & 0 & 0 & G_M \end{pmatrix};$$

(\*Q Matrix for Resin\*)

FLAT = Table[0, {i, 1, 6}, {j, 1, 6}];

(\*Flat Fiber Region\*)

Part[FLAT, 1, 1] = Part[P, 1, 1] \* h + Part[Q, 1, 1] \* h;  
Part[FLAT, 1, 2] = Part[P, 1, 2] \* h + Part[Q, 1, 2] \* h;  
Part[FLAT, 2, 1] = Part[P, 1, 2] \* h + Part[Q, 1, 2] \* h;  
Part[FLAT, 2, 2] = Part[P, 2, 2] \* h + Part[Q, 2, 2] \* h;  
Part[FLAT, 1, 3] = Part[P, 1, 3] \* h + Part[Q, 1, 3] \* h;  
Part[FLAT, 3, 1] = Part[P, 3, 1] \* h + Part[Q, 3, 1] \* h;  
Part[FLAT, 2, 3] = Part[P, 2, 3] \* h + Part[Q, 2, 3] \* h;  
Part[FLAT, 3, 2] = Part[P, 3, 2] \* h + Part[Q, 3, 2] \* h;  
Part[FLAT, 3, 3] = Part[P, 3, 3] \* h + Part[Q, 3, 3] \* h;  
Part[FLAT, 1, 4] = Part[P, 1, 4] \* h + Part[Q, 1, 4] \* h;  
Part[FLAT, 4, 1] = Part[P, 4, 1] \* h + Part[Q, 4, 1] \* h;  
Part[FLAT, 1, 5] = Part[P, 1, 5] \* h + Part[Q, 1, 5] \* h;  
Part[FLAT, 5, 1] = Part[P, 5, 1] \* h + Part[Q, 5, 1] \* h;  
Part[FLAT, 1, 6] = Part[P, 1, 6] \* h + Part[Q, 1, 6] \* h;  
Part[FLAT, 6, 1] = Part[P, 6, 1] \* h + Part[Q, 6, 1] \* h;  
Part[FLAT, 2, 4] = Part[P, 2, 4] \* h + Part[Q, 2, 4] \* h;  
Part[FLAT, 4, 2] = Part[P, 4, 2] \* h + Part[Q, 4, 2] \* h;  
Part[FLAT, 2, 5] = Part[P, 2, 5] \* h + Part[Q, 2, 5] \* h;  
Part[FLAT, 5, 2] = Part[P, 5, 2] \* h + Part[Q, 5, 2] \* h;  
Part[FLAT, 2, 6] = Part[P, 2, 6] \* h + Part[Q, 2, 6] \* h;  
Part[FLAT, 6, 2] = Part[P, 6, 2] \* h + Part[Q, 6, 2] \* h;  
Part[FLAT, 3, 4] = Part[P, 3, 4] \* h + Part[Q, 3, 4] \* h;  
Part[FLAT, 4, 3] = Part[P, 4, 3] \* h + Part[Q, 4, 3] \* h;  
Part[FLAT, 3, 5] = Part[P, 3, 5] \* h + Part[Q, 3, 5] \* h;  
Part[FLAT, 5, 3] = Part[P, 5, 3] \* h + Part[Q, 5, 3] \* h;

**Part[FLAT, 3, 6] = Part[P, 3, 6] \* h + Part[Q, 3, 6] \* h;**  
**Part[FLAT, 6, 3] = Part[P, 6, 3] \* h + Part[Q, 6, 3] \* h;**  
**Part[FLAT, 4, 4] = Part[P, 4, 4] \* h + Part[Q, 4, 4] \* h;**  
**Part[FLAT, 4, 5] = Part[P, 4, 5] \* h + Part[Q, 4, 5] \* h;**  
**Part[FLAT, 5, 4] = Part[P, 5, 4] \* h + Part[Q, 5, 4] \* h;**  
**Part[FLAT, 4, 6] = Part[P, 4, 6] \* h + Part[Q, 4, 6] \* h;**  
**Part[FLAT, 6, 4] = Part[P, 6, 4] \* h + Part[Q, 6, 4] \* h;**  
**Part[FLAT, 5, 5] = Part[P, 5, 5] \* h + Part[Q, 5, 5] \* h;**  
**Part[FLAT, 5, 6] = Part[P, 5, 6] \* h + Part[Q, 5, 6] \* h;**  
**Part[FLAT, 6, 5] = Part[P, 6, 5] \* h + Part[Q, 6, 5] \* h;**  
**Part[FLAT, 6, 6] = Part[P, 6, 6] \* h + Part[Q, 6, 6] \* h;**  
**FLAT;**

$$\text{FLATAREA} = \text{FLAT} * \left(\frac{a_0}{2}\right)^2 * \text{Sin}[\phi];$$

$$\text{FLATTOTAL} = \text{FLATAREA} * 4;$$

**MATRIX = Table[0, {i, 1, 6}, {j, 1, 6}];**

**(\*Matrix Pocket Region\*)**

**Part[MATRIX, 1, 1] = Part[R, 1, 1] \* 2 \* h;**  
**Part[MATRIX, 1, 2] = Part[R, 1, 2] \* 2 \* h;**  
**Part[MATRIX, 2, 1] = Part[R, 1, 2] \* 2 \* h;**  
**Part[MATRIX, 2, 2] = Part[R, 2, 2] \* 2 \* h;**  
**Part[MATRIX, 1, 3] = Part[R, 1, 3] \* 2 \* h;**  
**Part[MATRIX, 3, 1] = Part[R, 1, 3] \* 2 \* h;**  
**Part[MATRIX, 2, 3] = Part[R, 2, 3] \* 2 \* h;**  
**Part[MATRIX, 3, 2] = Part[R, 2, 3] \* 2 \* h;**  
**Part[MATRIX, 3, 3] = Part[R, 3, 3] \* 2 \* h;**  
**Part[MATRIX, 1, 4] = Part[R, 1, 4] \* 2 \* h;**  
**Part[MATRIX, 4, 1] = Part[R, 4, 1] \* 2 \* h;**  
**Part[MATRIX, 1, 5] = Part[R, 1, 5] \* 2 \* h;**  
**Part[MATRIX, 5, 1] = Part[R, 5, 1] \* 2 \* h;**  
**Part[MATRIX, 1, 6] = Part[R, 1, 6] \* 2 \* h;**  
**Part[MATRIX, 6, 1] = Part[R, 6, 1] \* 2 \* h;**  
**Part[MATRIX, 2, 4] = Part[R, 2, 4] \* 2 \* h;**  
**Part[MATRIX, 4, 2] = Part[R, 4, 2] \* 2 \* h;**  
**Part[MATRIX, 2, 5] = Part[R, 2, 5] \* 2 \* h;**  
**Part[MATRIX, 5, 2] = Part[R, 5, 2] \* 2 \* h;**  
**Part[MATRIX, 2, 6] = Part[R, 2, 6] \* 2 \* h;**  
**Part[MATRIX, 6, 2] = Part[R, 6, 2] \* 2 \* h;**



```

FILL = Table[0, {i, 1, 6}, {j, 1, 6}];
(*Fill Undulation Region*)
Part[FILL, 1, 1] = Part[Y, 1, 1] * h;
Part[FILL, 1, 2] = Part[Y, 1, 2] * h;
Part[FILL, 2, 1] = Part[Y, 2, 1] * h;
Part[FILL, 2, 2] = Part[Y, 2, 2] * h;
Part[FILL, 1, 3] = Part[Y, 1, 3] * h;
Part[FILL, 3, 1] = Part[Y, 3, 1] * h;
Part[FILL, 2, 3] = Part[Y, 2, 3] * h;
Part[FILL, 3, 2] = Part[Y, 3, 2] * h;
Part[FILL, 3, 3] = Part[Y, 3, 3] * h;
Part[FILL, 1, 4] = Part[Y, 1, 4] * h;
Part[FILL, 4, 1] = Part[Y, 4, 1] * h;
Part[FILL, 1, 5] = Part[Y, 1, 5] * h;
Part[FILL, 5, 1] = Part[Y, 5, 1] * h;
Part[FILL, 1, 6] = Part[Y, 1, 6] * h;
Part[FILL, 6, 1] = Part[Y, 6, 1] * h;
Part[FILL, 2, 4] = Part[Y, 2, 4] * h;
Part[FILL, 4, 2] = Part[Y, 4, 2] * h;
Part[FILL, 2, 5] = Part[Y, 2, 5] * h;
Part[FILL, 5, 2] = Part[Y, 5, 2] * h;
Part[FILL, 2, 6] = Part[Y, 2, 6] * h;
Part[FILL, 6, 2] = Part[Y, 6, 2] * h;
Part[FILL, 3, 4] = Part[Y, 3, 4] * h;
Part[FILL, 4, 3] = Part[Y, 4, 3] * h;
Part[FILL, 3, 5] = Part[Y, 3, 5] * h;
Part[FILL, 5, 3] = Part[Y, 5, 3] * h;
Part[FILL, 3, 6] = Part[Y, 3, 6] * h;
Part[FILL, 6, 3] = Part[Y, 6, 3] * h;
Part[FILL, 4, 4] = Part[Y, 4, 4] * h;
Part[FILL, 4, 5] = Part[Y, 4, 5] * h;
Part[FILL, 5, 4] = Part[Y, 5, 4] * h;
Part[FILL, 4, 6] = Part[Y, 4, 6] * h;
Part[FILL, 6, 4] = Part[Y, 6, 4] * h;
Part[FILL, 5, 5] = Part[Y, 5, 5] * h;
Part[FILL, 5, 6] = Part[Y, 5, 6] * h;
Part[FILL, 6, 5] = Part[Y, 6, 5] * h;
Part[FILL, 6, 6] = Part[Y, 6, 6] * h;
FILL;

```

$$\text{FILLAREA} = \text{FILL} * \frac{a_0}{2} * \frac{a_U}{2} * \text{Sin}[\phi];$$

**AA = Table[0, {i, 1, b}];**

**BB = Table[0, {i, 1, b}];**

**CC = Table[0, {i, 1, b}];**

**FF = Table[0, {i, 1, b}];**

**MM = Table[0, {i, 1, b}];**

**Qs = Table[0, {i, 1, b}];**

**As = Table[0, {i, 1, b}];**

**Do[Part[AA, i] =  $\tau * i$ , {i, 1, b}]**

**Do[Part[BB, i] = Part[AA, i] \*  $\frac{a_U}{h} * \tau$ , {i, 1, b}]**

**Do[Part[CC, i] = area - Part[BB, i], {i, 1, b}]**

**Do[Part[FF, i] = Part[BB, i] / area, {i, 1, b}]**

**Do[Part[MM, i] = Part[CC, i] / area, {i, 1, b}]**

**Do[Part[Qs, i] =  $\frac{1}{\frac{\text{Part[FF,i]}}{\text{Part[Y,1,1]}} + \frac{\text{Part[MM,i]}}{\text{Part[R,1,1]}}}$ , {i, 1, b}]**

**Do[Part[As, i] = Part[Qs, i] \*  $a_U * \tau * a_0$ , {i, 1, b}]**

**Ts = 0;**

**Do[Ts = Ts + Part[As, i], {i, 1, b}]**

**Part[FILLAREA, 1, 1] = Ts \* 2 \* Sin[ $\phi$ ];**

$$\lambda = \frac{h}{\text{Cos}[\theta * \frac{\pi}{180}]} - \frac{\kappa}{\text{Tan}[\theta * \frac{\pi}{180}]};$$

**ar = 2 \* h \*  $\kappa$ ;**

**fiber =  $\lambda * \kappa$ ;**

**matrix = (2 \* h -  $\lambda$ ) \*  $\kappa$ ;**

**fibrat = fiber / ar;**

**matrat = matrix / ar;**

$$\text{QUs} = \frac{1}{\frac{1}{\text{Part[Y,3,3]}} + \frac{1}{\text{Part[R,3,3]}}};$$

**AUs = (QUs \* 2 \* h \*  $\kappa * a_0$ ) \* m;**

**Part[FILLAREA, 3, 3] = AUs \* Sin[ $\phi$ ];**

**FILLTOTAL = FILLAREA \* 4;**

**WARP = Table[0, {i, 1, 6}, {j, 1, 6}];**  
**Part[WARP, 1, 1] = Part[X, 1, 1] \* h;**  
**Part[WARP, 1, 2] = Part[X, 1, 2] \* h;**  
**Part[WARP, 2, 1] = Part[X, 2, 1] \* h;**  
**Part[WARP, 2, 2] = Part[X, 2, 2] \* h;**  
**Part[WARP, 1, 3] = Part[X, 1, 3] \* h;**  
**Part[WARP, 3, 1] = Part[X, 3, 1] \* h;**  
**Part[WARP, 2, 3] = Part[X, 2, 3] \* h;**  
**Part[WARP, 3, 2] = Part[X, 3, 2] \* h;**  
**Part[WARP, 3, 3] = Part[X, 3, 3] \* h;**  
**Part[WARP, 1, 4] = Part[X, 1, 4] \* h;**  
**Part[WARP, 4, 1] = Part[X, 4, 1] \* h;**  
**Part[WARP, 1, 5] = Part[X, 1, 5] \* h;**  
**Part[WARP, 5, 1] = Part[X, 5, 1] \* h;**  
**Part[WARP, 1, 6] = Part[X, 1, 6] \* h;**  
**Part[WARP, 6, 1] = Part[X, 6, 1] \* h;**  
**Part[WARP, 2, 4] = Part[X, 2, 4] \* h;**  
**Part[WARP, 4, 2] = Part[X, 4, 2] \* h;**  
**Part[WARP, 2, 5] = Part[X, 2, 5] \* h;**  
**Part[WARP, 5, 2] = Part[X, 5, 2] \* h;**  
**Part[WARP, 2, 6] = Part[X, 2, 6] \* h;**  
**Part[WARP, 6, 2] = Part[X, 6, 2] \* h;**  
**Part[WARP, 3, 4] = Part[X, 3, 4] \* h;**  
**Part[WARP, 4, 3] = Part[X, 4, 3] \* h;**  
**Part[WARP, 3, 5] = Part[X, 3, 5] \* h;**  
**Part[WARP, 5, 3] = Part[X, 5, 3] \* h;**  
**Part[WARP, 3, 6] = Part[X, 3, 6] \* h;**  
**Part[WARP, 6, 3] = Part[X, 6, 3] \* h;**  
**Part[WARP, 4, 4] = Part[X, 4, 4] \* h;**  
**Part[WARP, 4, 5] = Part[X, 4, 5] \* h;**  
**Part[WARP, 5, 4] = Part[X, 5, 4] \* h;**  
**Part[WARP, 4, 6] = Part[X, 4, 6] \* h;**  
**Part[WARP, 6, 4] = Part[X, 6, 4] \* h;**  
**Part[WARP, 5, 5] = Part[X, 5, 5] \* h;**  
**Part[WARP, 5, 6] = Part[X, 5, 6] \* h;**  
**Part[WARP, 6, 5] = Part[X, 6, 5] \* h;**  
**Part[WARP, 6, 6] = Part[X, 6, 6] \* h;**  
**WARP;**

$$\text{WARPAREA} = \text{WARP} * \frac{a_0}{2} * \frac{a_u}{2} * \text{Sin}[\phi];$$

$$\text{Part}[\text{WARPAREA}, 2, 2] = 2 * \text{Ts} * \text{Sin}[\phi];$$

$$\text{Part}[\text{WARPAREA}, 3, 3] = \text{AUs} * \text{Sin}[\phi];$$

$$\text{WARPTOTAL} = \text{WARPAREA} * 4;$$

$$\text{RESIN} = \text{Table}[0, \{i, 1, 6\}, \{j, 1, 6\}];$$

$$\text{Part}[\text{RESIN}, 1, 1] = \text{Part}[\text{R}, 1, 1] * h;$$

$$\text{Part}[\text{RESIN}, 1, 2] = \text{Part}[\text{R}, 1, 2] * h;$$

$$\text{Part}[\text{RESIN}, 2, 1] = \text{Part}[\text{R}, 2, 1] * h;$$

$$\text{Part}[\text{RESIN}, 2, 2] = \text{Part}[\text{R}, 2, 2] * h;$$

$$\text{Part}[\text{RESIN}, 1, 3] = \text{Part}[\text{R}, 1, 3] * h;$$

$$\text{Part}[\text{RESIN}, 3, 1] = \text{Part}[\text{R}, 3, 1] * h;$$

$$\text{Part}[\text{RESIN}, 2, 3] = \text{Part}[\text{R}, 2, 3] * h;$$

$$\text{Part}[\text{RESIN}, 3, 2] = \text{Part}[\text{R}, 3, 2] * h;$$

$$\text{Part}[\text{RESIN}, 3, 3] = \text{Part}[\text{R}, 3, 3] * h;$$

$$\text{Part}[\text{RESIN}, 1, 4] = \text{Part}[\text{R}, 1, 4] * h;$$

$$\text{Part}[\text{RESIN}, 4, 1] = \text{Part}[\text{R}, 4, 1] * h;$$

$$\text{Part}[\text{RESIN}, 1, 5] = \text{Part}[\text{R}, 1, 5] * h;$$

$$\text{Part}[\text{RESIN}, 5, 1] = \text{Part}[\text{R}, 5, 1] * h;$$

$$\text{Part}[\text{RESIN}, 1, 6] = \text{Part}[\text{R}, 1, 6] * h;$$

$$\text{Part}[\text{RESIN}, 6, 1] = \text{Part}[\text{R}, 6, 1] * h;$$

$$\text{Part}[\text{RESIN}, 2, 4] = \text{Part}[\text{R}, 2, 4] * h;$$

$$\text{Part}[\text{RESIN}, 4, 2] = \text{Part}[\text{R}, 4, 2] * h;$$

$$\text{Part}[\text{RESIN}, 2, 5] = \text{Part}[\text{R}, 2, 5] * h;$$

$$\text{Part}[\text{RESIN}, 5, 2] = \text{Part}[\text{R}, 5, 2] * h;$$

$$\text{Part}[\text{RESIN}, 2, 6] = \text{Part}[\text{R}, 2, 6] * h;$$

$$\text{Part}[\text{RESIN}, 6, 2] = \text{Part}[\text{R}, 6, 2] * h;$$

$$\text{Part}[\text{RESIN}, 3, 4] = \text{Part}[\text{R}, 3, 4] * h;$$

$$\text{Part}[\text{RESIN}, 4, 3] = \text{Part}[\text{R}, 4, 3] * h;$$

$$\text{Part}[\text{RESIN}, 3, 5] = \text{Part}[\text{R}, 3, 5] * h;$$

$$\text{Part}[\text{RESIN}, 5, 3] = \text{Part}[\text{R}, 5, 3] * h;$$

$$\text{Part}[\text{RESIN}, 3, 6] = \text{Part}[\text{R}, 3, 6] * h;$$

$$\text{Part}[\text{RESIN}, 6, 3] = \text{Part}[\text{R}, 6, 3] * h;$$

$$\text{Part}[\text{RESIN}, 4, 4] = \text{Part}[\text{R}, 4, 4] * h;$$

$$\text{Part}[\text{RESIN}, 4, 5] = \text{Part}[\text{R}, 4, 5] * h;$$

$$\text{Part}[\text{RESIN}, 5, 4] = \text{Part}[\text{R}, 5, 4] * h;$$

$$\text{Part}[\text{RESIN}, 4, 6] = \text{Part}[\text{R}, 4, 6] * h;$$

$$\text{Part}[\text{RESIN}, 6, 4] = \text{Part}[\text{R}, 6, 4] * h;$$

**Part[RESIN, 5, 5] = Part[R, 5, 5] \* h;**

**Part[RESIN, 5, 6] = Part[R, 5, 6] \* h;**

**Part[RESIN, 6, 5] = Part[R, 6, 5] \* h;**

**Part[RESIN, 6, 6] = Part[R, 6, 6] \* h;**

**RESIN;**

**RESINAREA = RESIN \*  $\left(\frac{a_u}{2}\right) * \left(\frac{a_0}{2}\right) * \text{Sin}[\phi];$**

**RESINTOTAL = RESINAREA \* 8;**

**TOTAL = FLATTOTAL + MATRIXTOTAL + FILLTOTAL +  
WARPTOTAL + RESINTOTAL;**

**AVERAGE =  $\frac{n^2 * \text{TOTAL}}{(n * a)^2 * \text{Sin}[\phi]}$ ;**

**$\alpha = \text{Inverse}[\text{AVERAGE}];$**

**Print["E<sub>x</sub>="]  
1  
-----  
Part[ $\alpha$ , 1, 1] \* t**

**Print["E<sub>y</sub>="]  
1  
-----  
Part[ $\alpha$ , 2, 2] \* t**

**Print["E<sub>z</sub>="]  
1  
-----  
Part[ $\alpha$ , 3, 3] \* t**

**Print["G<sub>xy</sub>="]  
1  
-----  
Part[ $\alpha$ , 6, 6] \* t**

**Print["G<sub>xz</sub>="]  
1  
-----  
Part[ $\alpha$ , 5, 5] \* t**

**Print["G<sub>yz</sub>="]  
1  
-----  
Part[ $\alpha$ , 4, 4] \* t**

**Print[" $\nu_{xy}$ ="]  
Part[ $\alpha$ , 2, 1]  
-----  
Part[ $\alpha$ , 1, 1]**

$$\frac{\text{Print}["\nu_{yx}="] \text{Part}[\alpha, 1, 2]}{\text{Part}[\alpha, 2, 2]}$$

$$\frac{\text{Print}["\nu_{xz}="] \text{Part}[\alpha, 1, 3]}{\text{Part}[\alpha, 1, 1]}$$

$$\frac{\text{Print}["\nu_{zx}="] \text{Part}[\alpha, 1, 3]}{\text{Part}[\alpha, 3, 3]}$$

$$\frac{\text{Print}["\nu_{yz}="] \text{Part}[\alpha, 2, 3]}{\text{Part}[\alpha, 2, 2]}$$

$$\frac{\text{Print}["\nu_{zy}="] \text{Part}[\alpha, 2, 3]}{\text{Part}[\alpha, 3, 3]}$$

### B.3 Q3D Weave

**ClearAll[]**

$$\mathbf{B} = \begin{pmatrix} \frac{1}{E_x} & \frac{-\nu_{yx}}{E_y} & \frac{-\nu_{zx}}{E_z} & 0 & 0 & 0 \\ \frac{-\nu_{xy}}{E_x} & \frac{1}{E_y} & \frac{-\nu_{zy}}{E_z} & 0 & 0 & 0 \\ \frac{-\nu_{xz}}{E_x} & \frac{-\nu_{yz}}{E_y} & \frac{1}{E_z} & 0 & 0 & 0 \\ 0 & 0 & 0 & \frac{1}{G_{yz}} & 0 & 0 \\ 0 & 0 & 0 & 0 & \frac{1}{G_{xz}} & 0 \\ 0 & 0 & 0 & 0 & 0 & \frac{1}{G_{xy}} \end{pmatrix};$$

**(\*Inverting Stress-Strain\*)**

**Q = Simplify[Inverse[B]]; (\*Q Matrix for Fibers\*)**

**E<sub>x</sub> = 144.8 \* 10<sup>9</sup>; (\*Material Properties\*)**

**E<sub>y</sub> = 11.728 \* 10<sup>9</sup>;**

**E<sub>z</sub> = 11.728 \* 10<sup>9</sup>;**

**G<sub>xy</sub> = 5.516 \* 10<sup>9</sup>;**

**G<sub>xz</sub> = 5.516 \* 10<sup>9</sup>;**

**G<sub>yz</sub> = 5.516 \* 10<sup>9</sup>;**

**E<sub>M</sub> = 3.448 \* 10<sup>9</sup>;**

**ν<sub>xy</sub> = 0.23;**

**ν<sub>xz</sub> = 0.23;**

**ν<sub>yz</sub> = 0.3;**

**ν<sub>M</sub> = 0.35;**

**G<sub>M</sub> = 1.276 \* 10<sup>9</sup>;**

**n = 1; (\*Number of Unit Cells\*)**

**a<sub>U</sub> = (1.467 \* 10<sup>-3</sup>) / n; (\*Geometric Properties\*)**

**a = (10 \* 10<sup>-3</sup>) / n;**

**h = 0.989 \* 10<sup>-3</sup>;**

**h<sub>t</sub> = h;**

**a<sub>0</sub> = a - a<sub>U</sub>;**

**φ = 90 \* π / 180;**

**p = 3; (\*Number of Layers\*)**

**q = p - 2;**

$$\theta = \text{ArcTan}\left[\frac{h}{a_u} * \text{Cos}\left[\phi - \frac{\pi}{2}\right]\right];$$

$$\beta = \text{ArcTan}\left[\frac{2 * h}{a_u} * \text{Cos}\left[\phi - \frac{\pi}{2}\right]\right];$$

$$t = 2 * h;$$

$$v_{yx} = \frac{E_y}{E_x} * v_{xy}; \quad (*\text{Poisson Definition}*)$$

$$v_{zx} = \frac{E_z}{E_x} * v_{xz};$$

$$v_{zy} = \frac{E_z}{E_y} * v_{yz};$$

$$I = \begin{pmatrix} \text{Cos}[\phi] & \text{Cos}\left[\phi + \frac{\pi}{2}\right] & 0 \\ \text{Cos}\left[\phi - \frac{\pi}{2}\right] & \text{Cos}[\phi] & 0 \\ 0 & 0 & 1 \end{pmatrix};$$

(\*Fiber Direction Transformation\*)

L =

$$\begin{pmatrix} \text{Part}[I, 1, 1]^2 & \text{Part}[I, 2, 1]^2 & \text{Part}[I, 3, 1]^2 \\ \text{Part}[I, 1, 2]^2 & \text{Part}[I, 2, 2]^2 & \text{Part}[I, 3, 2]^2 \\ \text{Part}[I, 1, 3]^2 & \text{Part}[I, 2, 3]^2 & \text{Part}[I, 3, 3]^2 \\ \text{Part}[I, 1, 2] * \text{Part}[I, 1, 3] & \text{Part}[I, 2, 2] * \text{Part}[I, 2, 3] & \text{Part}[I, 3, 2] * \text{Part}[I, 3, 3] \\ \text{Part}[I, 1, 1] * \text{Part}[I, 1, 3] & \text{Part}[I, 2, 1] * \text{Part}[I, 2, 3] & \text{Part}[I, 3, 1] * \text{Part}[I, 3, 3] \\ \text{Part}[I, 1, 1] * \text{Part}[I, 1, 2] & \text{Part}[I, 2, 1] * \text{Part}[I, 2, 2] & \text{Part}[I, 3, 1] * \text{Part}[I, 3, 2] \end{pmatrix};$$

P = L.Q.Transpose[L];

P;

$$R = \begin{pmatrix} \frac{E_M}{1-v_M^2} & \frac{v_M * E_M}{1-v_M^2} & \frac{v_M * E_M}{1-v_M^2} & 0 & 0 & 0 \\ \frac{v_M * E_M}{1-v_M^2} & \frac{E_M}{1-v_M^2} & \frac{v_M * E_M}{1-v_M^2} & 0 & 0 & 0 \\ \frac{v_M * E_M}{1-v_M^2} & \frac{v_M * E_M}{1-v_M^2} & \frac{E_M}{1-v_M^2} & 0 & 0 & 0 \\ 0 & 0 & 0 & G_M & 0 & 0 \\ 0 & 0 & 0 & 0 & G_M & 0 \\ 0 & 0 & 0 & 0 & 0 & G_M \end{pmatrix};$$

(\*Q Matrix for Resin\*)

**FLAT = Table[0, {i, 1, 6}, {j, 1, 6}];**

**(\*Flat Fiber Region\*)**

**Part[FLAT, 1, 1] = Part[P, 1, 1] \* h + Part[Q, 1, 1] \* h;**

**Part[FLAT, 1, 2] = Part[P, 1, 2] \* h + Part[Q, 1, 2] \* h;**

**Part[FLAT, 2, 1] = Part[P, 1, 2] \* h + Part[Q, 1, 2] \* h;**

**Part[FLAT, 2, 2] = Part[P, 2, 2] \* h + Part[Q, 2, 2] \* h;**

**Part[FLAT, 1, 3] = Part[P, 1, 3] \* h + Part[Q, 1, 3] \* h;**

**Part[FLAT, 3, 1] = Part[P, 3, 1] \* h + Part[Q, 3, 1] \* h;**

**Part[FLAT, 2, 3] = Part[P, 2, 3] \* h + Part[Q, 2, 3] \* h;**

**Part[FLAT, 3, 2] = Part[P, 3, 2] \* h + Part[Q, 3, 2] \* h;**

**Part[FLAT, 3, 3] = Part[P, 3, 3] \* h + Part[Q, 3, 3] \* h;**

**Part[FLAT, 1, 4] = Part[P, 1, 4] \* h + Part[Q, 1, 4] \* h;**

**Part[FLAT, 4, 1] = Part[P, 4, 1] \* h + Part[Q, 4, 1] \* h;**

**Part[FLAT, 1, 5] = Part[P, 1, 5] \* h + Part[Q, 1, 5] \* h;**

**Part[FLAT, 5, 1] = Part[P, 5, 1] \* h + Part[Q, 5, 1] \* h;**

**Part[FLAT, 1, 6] = Part[P, 1, 6] \* h + Part[Q, 1, 6] \* h;**

**Part[FLAT, 6, 1] = Part[P, 6, 1] \* h + Part[Q, 6, 1] \* h;**

**Part[FLAT, 2, 4] = Part[P, 2, 4] \* h + Part[Q, 2, 4] \* h;**

**Part[FLAT, 4, 2] = Part[P, 4, 2] \* h + Part[Q, 4, 2] \* h;**

**Part[FLAT, 2, 5] = Part[P, 2, 5] \* h + Part[Q, 2, 5] \* h;**

**Part[FLAT, 5, 2] = Part[P, 5, 2] \* h + Part[Q, 5, 2] \* h;**

**Part[FLAT, 2, 6] = Part[P, 2, 6] \* h + Part[Q, 2, 6] \* h;**

**Part[FLAT, 6, 2] = Part[P, 6, 2] \* h + Part[Q, 6, 2] \* h;**

**Part[FLAT, 3, 4] = Part[P, 3, 4] \* h + Part[Q, 3, 4] \* h;**

**Part[FLAT, 4, 3] = Part[P, 4, 3] \* h + Part[Q, 4, 3] \* h;**

**Part[FLAT, 3, 5] = Part[P, 3, 5] \* h + Part[Q, 3, 5] \* h;**

**Part[FLAT, 5, 3] = Part[P, 5, 3] \* h + Part[Q, 5, 3] \* h;**

**Part[FLAT, 3, 6] = Part[P, 3, 6] \* h + Part[Q, 3, 6] \* h;**

**Part[FLAT, 6, 3] = Part[P, 6, 3] \* h + Part[Q, 6, 3] \* h;**

**Part[FLAT, 4, 4] = Part[P, 4, 4] \* h + Part[Q, 4, 4] \* h;**

**Part[FLAT, 4, 5] = Part[P, 4, 5] \* h + Part[Q, 4, 5] \* h;**

**Part[FLAT, 5, 4] = Part[P, 5, 4] \* h + Part[Q, 5, 4] \* h;**

**Part[FLAT, 4, 6] = Part[P, 4, 6] \* h + Part[Q, 4, 6] \* h;**

**Part[FLAT, 6, 4] = Part[P, 6, 4] \* h + Part[Q, 6, 4] \* h;**

**Part[FLAT, 5, 5] = Part[P, 5, 5] \* h + Part[Q, 5, 5] \* h;**

**Part[FLAT, 5, 6] = Part[P, 5, 6] \* h + Part[Q, 5, 6] \* h;**

**Part[FLAT, 6, 5] = Part[P, 6, 5] \* h + Part[Q, 6, 5] \* h;**

**Part[FLAT, 6, 6] = Part[P, 6, 6] \* h + Part[Q, 6, 6] \* h;**

**FLAT;**

**FLATAREA = FLAT \*  $\left(\frac{a_0}{2}\right)^2 * \text{Sin}[\phi];$**

**FLATTOTAL = 4 \* (2 + q) \* FLATAREA;**

```

MATRIX = Table[0, {i, 1, 6}, {j, 1, 6}];
(*Matrix Pocket Region*)
Part[MATRIX, 1, 1] = Part[R, 1, 1] * 2 * p * h;
Part[MATRIX, 1, 2] = Part[R, 1, 2] * 2 * p * h;
Part[MATRIX, 2, 1] = Part[R, 1, 2] * 2 * p * h;
Part[MATRIX, 2, 2] = Part[R, 2, 2] * 2 * p * h;
Part[MATRIX, 1, 3] = Part[R, 1, 3] * 2 * p * h;
Part[MATRIX, 3, 1] = Part[R, 1, 3] * 2 * p * h;
Part[MATRIX, 2, 3] = Part[R, 2, 3] * 2 * p * h;
Part[MATRIX, 3, 2] = Part[R, 2, 3] * 2 * p * h;
Part[MATRIX, 3, 3] = Part[R, 3, 3] * 2 * p * h;
Part[MATRIX, 1, 4] = Part[R, 1, 4] * 2 * p * h;
Part[MATRIX, 4, 1] = Part[R, 4, 1] * 2 * p * h;
Part[MATRIX, 1, 5] = Part[R, 1, 5] * 2 * p * h;
Part[MATRIX, 5, 1] = Part[R, 5, 1] * 2 * p * h;
Part[MATRIX, 1, 6] = Part[R, 1, 6] * 2 * p * h;
Part[MATRIX, 6, 1] = Part[R, 6, 1] * 2 * p * h;
Part[MATRIX, 2, 4] = Part[R, 2, 4] * 2 * p * h;
Part[MATRIX, 4, 2] = Part[R, 4, 2] * 2 * p * h;
Part[MATRIX, 2, 5] = Part[R, 2, 5] * 2 * p * h;
Part[MATRIX, 5, 2] = Part[R, 5, 2] * 2 * p * h;
Part[MATRIX, 2, 6] = Part[R, 2, 6] * 2 * p * h;
Part[MATRIX, 6, 2] = Part[R, 6, 2] * 2 * p * h;
Part[MATRIX, 3, 4] = Part[R, 3, 4] * 2 * p * h;
Part[MATRIX, 4, 3] = Part[R, 4, 3] * 2 * p * h;
Part[MATRIX, 3, 5] = Part[R, 3, 5] * 2 * p * h;
Part[MATRIX, 5, 3] = Part[R, 5, 3] * 2 * p * h;
Part[MATRIX, 3, 6] = Part[R, 3, 6] * 2 * p * h;
Part[MATRIX, 6, 3] = Part[R, 6, 3] * 2 * p * h;
Part[MATRIX, 4, 4] = Part[R, 4, 4] * 2 * p * h;
Part[MATRIX, 4, 5] = Part[R, 4, 5] * 2 * p * h;
Part[MATRIX, 5, 4] = Part[R, 5, 4] * 2 * p * h;
Part[MATRIX, 4, 6] = Part[R, 4, 6] * 2 * p * h;
Part[MATRIX, 6, 4] = Part[R, 6, 4] * 2 * p * h;
Part[MATRIX, 5, 5] = Part[R, 5, 5] * 2 * p * h;
Part[MATRIX, 5, 6] = Part[R, 5, 6] * 2 * p * h;
Part[MATRIX, 6, 5] = Part[R, 6, 5] * 2 * p * h;
Part[MATRIX, 6, 6] = Part[R, 6, 6] * 2 * p * h;
MATRIX;
MATRIXAREA = MATRIX *  $\left(\frac{a_u}{2}\right)^2 * \text{Sin}[\phi];$ 
MATRIXTOTAL = MATRIXAREA * 4;

```

$$I = \begin{pmatrix} \cos[\theta] & 0 & \cos[\theta - \frac{\pi}{2}] \\ 0 & 1 & 0 \\ \cos[\theta + \frac{\pi}{2}] & 0 & \cos[\theta] \end{pmatrix};$$

(\*Undulation Transformation\*)

M =

$$\begin{pmatrix} \text{Part}[I, 1, 1]^2 & \text{Part}[I, 2, 1]^2 & \text{Part}[I, 3, 1]^2 \\ \text{Part}[I, 1, 2]^2 & \text{Part}[I, 2, 2]^2 & \text{Part}[I, 3, 2]^2 \\ \text{Part}[I, 1, 3]^2 & \text{Part}[I, 2, 3]^2 & \text{Part}[I, 3, 3]^2 \\ \text{Part}[I, 1, 2] * \text{Part}[I, 1, 3] & \text{Part}[I, 2, 2] * \text{Part}[I, 2, 3] & \text{Part}[I, 3, 2] * \text{Part}[I, 3, 3] \\ \text{Part}[I, 1, 1] * \text{Part}[I, 1, 3] & \text{Part}[I, 2, 1] * \text{Part}[I, 2, 3] & \text{Part}[I, 3, 1] * \text{Part}[I, 3, 3] \\ \text{Part}[I, 1, 1] * \text{Part}[I, 1, 2] & \text{Part}[I, 2, 1] * \text{Part}[I, 2, 2] & \text{Part}[I, 3, 1] * \text{Part}[I, 3, 2] \end{pmatrix};$$

Y = M.Q.Transpose[M]; (\*Small Undulation\*)

X = L.Y.Transpose[L];

$$I = \begin{pmatrix} \cos[\beta] & 0 & \cos[\beta - \frac{\pi}{2}] \\ 0 & 1 & 0 \\ \cos[\beta + \frac{\pi}{2}] & 0 & \cos[\beta] \end{pmatrix};$$

(\*Undulation Transformation\*)

M =

$$\begin{pmatrix} \text{Part}[I, 1, 1]^2 & \text{Part}[I, 2, 1]^2 & \text{Part}[I, 3, 1]^2 \\ \text{Part}[I, 1, 2]^2 & \text{Part}[I, 2, 2]^2 & \text{Part}[I, 3, 2]^2 \\ \text{Part}[I, 1, 3]^2 & \text{Part}[I, 2, 3]^2 & \text{Part}[I, 3, 3]^2 \\ \text{Part}[I, 1, 2] * \text{Part}[I, 1, 3] & \text{Part}[I, 2, 2] * \text{Part}[I, 2, 3] & \text{Part}[I, 3, 2] * \text{Part}[I, 3, 3] \\ \text{Part}[I, 1, 1] * \text{Part}[I, 1, 3] & \text{Part}[I, 2, 1] * \text{Part}[I, 2, 3] & \text{Part}[I, 3, 1] * \text{Part}[I, 3, 3] \\ \text{Part}[I, 1, 1] * \text{Part}[I, 1, 2] & \text{Part}[I, 2, 1] * \text{Part}[I, 2, 2] & \text{Part}[I, 3, 1] * \text{Part}[I, 3, 2] \end{pmatrix};$$

V = M.Q.Transpose[M]; (\*Large Undulation\*)

U = L.V.Transpose[L];

```

FILL = Table[0, {i, 1, 6}, {j, 1, 6}];
Part[FILL, 1, 1] = Part[Y, 1, 1] * h;
Part[FILL, 1, 2] = Part[Y, 1, 2] * h;
Part[FILL, 2, 1] = Part[Y, 2, 1] * h;
Part[FILL, 2, 2] = Part[Y, 2, 2] * h;
Part[FILL, 1, 3] = Part[Y, 1, 3] * h;
Part[FILL, 3, 1] = Part[Y, 3, 1] * h;
Part[FILL, 2, 3] = Part[Y, 2, 3] * h;
Part[FILL, 3, 2] = Part[Y, 3, 2] * h;
Part[FILL, 3, 3] = Part[Y, 3, 3] * h;
Part[FILL, 1, 4] = Part[Y, 1, 4] * h;
Part[FILL, 4, 1] = Part[Y, 4, 1] * h;
Part[FILL, 1, 5] = Part[Y, 1, 5] * h;
Part[FILL, 5, 1] = Part[Y, 5, 1] * h;
Part[FILL, 1, 6] = Part[Y, 1, 6] * h;
Part[FILL, 6, 1] = Part[Y, 6, 1] * h;
Part[FILL, 2, 4] = Part[Y, 2, 4] * h;
Part[FILL, 4, 2] = Part[Y, 4, 2] * h;
Part[FILL, 2, 5] = Part[Y, 2, 5] * h;
Part[FILL, 5, 2] = Part[Y, 5, 2] * h;
Part[FILL, 2, 6] = Part[Y, 2, 6] * h;
Part[FILL, 6, 2] = Part[Y, 6, 2] * h;
Part[FILL, 3, 4] = Part[Y, 3, 4] * h;
Part[FILL, 4, 3] = Part[Y, 4, 3] * h;
Part[FILL, 3, 5] = Part[Y, 3, 5] * h;
Part[FILL, 5, 3] = Part[Y, 5, 3] * h;
Part[FILL, 3, 6] = Part[Y, 3, 6] * h;
Part[FILL, 6, 3] = Part[Y, 6, 3] * h;
Part[FILL, 4, 4] = Part[Y, 4, 4] * h;
Part[FILL, 4, 5] = Part[Y, 4, 5] * h;
Part[FILL, 5, 4] = Part[Y, 5, 4] * h;
Part[FILL, 4, 6] = Part[Y, 4, 6] * h;
Part[FILL, 6, 4] = Part[Y, 6, 4] * h;
Part[FILL, 5, 5] = Part[Y, 5, 5] * h;
Part[FILL, 5, 6] = Part[Y, 5, 6] * h;
Part[FILL, 6, 5] = Part[Y, 6, 5] * h;
Part[FILL, 6, 6] = Part[Y, 6, 6] * h;
FILL;

```

(\*Fill Undulation Region\*)

$$\text{FILLAREA} = \text{FILL} * \frac{a_0}{2} * \frac{a_u}{2} * \text{Sin}[\phi];$$

$$\text{FILLTOTAL} = \text{FILLAREA} * 4;$$

```

FILLER = Table[0, {i, 1, 6}, {j, 1, 6}];
(*Fill Large Undulation Region*)
Part[FILLER, 1, 1] = Part[V, 1, 1] * h;
Part[FILLER, 1, 2] = Part[V, 1, 2] * h;
Part[FILLER, 2, 1] = Part[V, 2, 1] * h;
Part[FILLER, 2, 2] = Part[V, 2, 2] * h;
Part[FILLER, 1, 3] = Part[V, 1, 3] * h;
Part[FILLER, 3, 1] = Part[V, 3, 1] * h;
Part[FILLER, 2, 3] = Part[V, 2, 3] * h;
Part[FILLER, 3, 2] = Part[V, 3, 2] * h;
Part[FILLER, 3, 3] = Part[V, 3, 3] * h;
Part[FILLER, 1, 4] = Part[V, 1, 4] * h;
Part[FILLER, 4, 1] = Part[V, 4, 1] * h;
Part[FILLER, 1, 5] = Part[V, 1, 5] * h;
Part[FILLER, 5, 1] = Part[V, 5, 1] * h;
Part[FILLER, 1, 6] = Part[V, 1, 6] * h;
Part[FILLER, 6, 1] = Part[V, 6, 1] * h;
Part[FILLER, 2, 4] = Part[V, 2, 4] * h;
Part[FILLER, 4, 2] = Part[V, 4, 2] * h;
Part[FILLER, 2, 5] = Part[V, 2, 5] * h;
Part[FILLER, 5, 2] = Part[V, 5, 2] * h;
Part[FILLER, 2, 6] = Part[V, 2, 6] * h;
Part[FILLER, 6, 2] = Part[V, 6, 2] * h;
Part[FILLER, 3, 4] = Part[V, 3, 4] * h;
Part[FILLER, 4, 3] = Part[V, 4, 3] * h;
Part[FILLER, 3, 5] = Part[V, 3, 5] * h;
Part[FILLER, 5, 3] = Part[V, 5, 3] * h;
Part[FILLER, 3, 6] = Part[V, 3, 6] * h;
Part[FILLER, 6, 3] = Part[V, 6, 3] * h;
Part[FILLER, 4, 4] = Part[V, 4, 4] * h;
Part[FILLER, 4, 5] = Part[V, 4, 5] * h;
Part[FILLER, 5, 4] = Part[V, 5, 4] * h;
Part[FILLER, 4, 6] = Part[V, 4, 6] * h;
Part[FILLER, 6, 4] = Part[V, 6, 4] * h;
Part[FILLER, 5, 5] = Part[V, 5, 5] * h;
Part[FILLER, 5, 6] = Part[V, 5, 6] * h;
Part[FILLER, 6, 5] = Part[V, 6, 5] * h;
Part[FILLER, 6, 6] = Part[V, 6, 6] * h;
FILLER;
FILLERAREA = FILLER *  $\frac{a_0}{2}$  *  $\frac{a_u}{2}$  * Sin[ $\phi$ ];
FILLERTOTAL = FILLERAREA * (1 + q) * 4;

```

**WARP = Table[0, {i, 1, 6}, {j, 1, 6}];**  
**Part[WARP, 1, 1] = Part[X, 1, 1] \* h;**  
**Part[WARP, 1, 2] = Part[X, 1, 2] \* h;**  
**Part[WARP, 2, 1] = Part[X, 2, 1] \* h;**  
**Part[WARP, 2, 2] = Part[X, 2, 2] \* h;**  
**Part[WARP, 1, 3] = Part[X, 1, 3] \* h;**  
**Part[WARP, 3, 1] = Part[X, 3, 1] \* h;**  
**Part[WARP, 2, 3] = Part[X, 2, 3] \* h;**  
**Part[WARP, 3, 2] = Part[X, 3, 2] \* h;**  
**Part[WARP, 3, 3] = Part[X, 3, 3] \* h;**  
**Part[WARP, 1, 4] = Part[X, 1, 4] \* h;**  
**Part[WARP, 4, 1] = Part[X, 4, 1] \* h;**  
**Part[WARP, 1, 5] = Part[X, 1, 5] \* h;**  
**Part[WARP, 5, 1] = Part[X, 5, 1] \* h;**  
**Part[WARP, 1, 6] = Part[X, 1, 6] \* h;**  
**Part[WARP, 6, 1] = Part[X, 6, 1] \* h;**  
**Part[WARP, 2, 4] = Part[X, 2, 4] \* h;**  
**Part[WARP, 4, 2] = Part[X, 4, 2] \* h;**  
**Part[WARP, 2, 5] = Part[X, 2, 5] \* h;**  
**Part[WARP, 5, 2] = Part[X, 5, 2] \* h;**  
**Part[WARP, 2, 6] = Part[X, 2, 6] \* h;**  
**Part[WARP, 6, 2] = Part[X, 6, 2] \* h;**  
**Part[WARP, 3, 4] = Part[X, 3, 4] \* h;**  
**Part[WARP, 4, 3] = Part[X, 4, 3] \* h;**  
**Part[WARP, 3, 5] = Part[X, 3, 5] \* h;**  
**Part[WARP, 5, 3] = Part[X, 5, 3] \* h;**  
**Part[WARP, 3, 6] = Part[X, 3, 6] \* h;**  
**Part[WARP, 6, 3] = Part[X, 6, 3] \* h;**  
**Part[WARP, 4, 4] = Part[X, 4, 4] \* h;**  
**Part[WARP, 4, 5] = Part[X, 4, 5] \* h;**  
**Part[WARP, 5, 4] = Part[X, 5, 4] \* h;**  
**Part[WARP, 4, 6] = Part[X, 4, 6] \* h;**  
**Part[WARP, 6, 4] = Part[X, 6, 4] \* h;**  
**Part[WARP, 5, 5] = Part[X, 5, 5] \* h;**  
**Part[WARP, 5, 6] = Part[X, 5, 6] \* h;**  
**Part[WARP, 6, 5] = Part[X, 6, 5] \* h;**  
**Part[WARP, 6, 6] = Part[X, 6, 6] \* h;**  
**WARP;**  
**WARPAREA = WARP \*  $\frac{a_0}{2}$  \*  $\frac{a_u}{2}$  \* Sin[ $\phi$ ];**  
**WARPTOTAL = WARPAREA \* 4;**

**WARPER = Table[0, {i, 1, 6}, {j, 1, 6}];**  
**Part[WARPER, 1, 1] = Part[U, 1, 1] \* h;**  
**Part[WARPER, 1, 2] = Part[U, 1, 2] \* h;**  
**Part[WARPER, 2, 1] = Part[U, 2, 1] \* h;**  
**Part[WARPER, 2, 2] = Part[U, 2, 2] \* h;**  
**Part[WARPER, 1, 3] = Part[U, 1, 3] \* h;**  
**Part[WARPER, 3, 1] = Part[U, 3, 1] \* h;**  
**Part[WARPER, 2, 3] = Part[U, 2, 3] \* h;**  
**Part[WARPER, 3, 2] = Part[U, 3, 2] \* h;**  
**Part[WARPER, 3, 3] = Part[U, 3, 3] \* h;**  
**Part[WARPER, 1, 4] = Part[U, 1, 4] \* h;**  
**Part[WARPER, 4, 1] = Part[U, 4, 1] \* h;**  
**Part[WARPER, 1, 5] = Part[U, 1, 5] \* h;**  
**Part[WARPER, 5, 1] = Part[U, 5, 1] \* h;**  
**Part[WARPER, 1, 6] = Part[U, 1, 6] \* h;**  
**Part[WARPER, 6, 1] = Part[U, 6, 1] \* h;**  
**Part[WARPER, 2, 4] = Part[U, 2, 4] \* h;**  
**Part[WARPER, 4, 2] = Part[U, 4, 2] \* h;**  
**Part[WARPER, 2, 5] = Part[U, 2, 5] \* h;**  
**Part[WARPER, 5, 2] = Part[U, 5, 2] \* h;**  
**Part[WARPER, 2, 6] = Part[U, 2, 6] \* h;**  
**Part[WARPER, 6, 2] = Part[U, 6, 2] \* h;**  
**Part[WARPER, 3, 4] = Part[U, 3, 4] \* h;**  
**Part[WARPER, 4, 3] = Part[U, 4, 3] \* h;**  
**Part[WARPER, 3, 5] = Part[U, 3, 5] \* h;**  
**Part[WARPER, 5, 3] = Part[U, 5, 3] \* h;**  
**Part[WARPER, 3, 6] = Part[U, 3, 6] \* h;**  
**Part[WARPER, 6, 3] = Part[U, 6, 3] \* h;**  
**Part[WARPER, 4, 4] = Part[U, 4, 4] \* h;**  
**Part[WARPER, 4, 5] = Part[U, 4, 5] \* h;**  
**Part[WARPER, 5, 4] = Part[U, 5, 4] \* h;**  
**Part[WARPER, 4, 6] = Part[U, 4, 6] \* h;**  
**Part[WARPER, 6, 4] = Part[U, 6, 4] \* h;**  
**Part[WARPER, 5, 5] = Part[U, 5, 5] \* h;**  
**Part[WARPER, 5, 6] = Part[U, 5, 6] \* h;**  
**Part[WARPER, 6, 5] = Part[U, 6, 5] \* h;**  
**Part[WARPER, 6, 6] = Part[U, 6, 6] \* h;**  
**WARPER;**

$$\mathbf{WARPERAREA = WARPER * \frac{a_0}{2} * \frac{a_u}{2} * \sin[\phi];}$$

$$\mathbf{WARPRTOTAL = WARPERAREA * (1 + q) 4;}$$

**RESIN = Table[0, {i, 1, 6}, {j, 1, 6}];**  
**Part[RESIN, 1, 1] = Part[R, 1, 1] \* p \* h;**  
**Part[RESIN, 1, 2] = Part[R, 1, 2] \* p \* h;**  
**Part[RESIN, 2, 1] = Part[R, 2, 1] \* p \* h;**  
**Part[RESIN, 2, 2] = Part[R, 2, 2] \* p \* h;**  
**Part[RESIN, 1, 3] = Part[R, 1, 3] \* p \* h;**  
**Part[RESIN, 3, 1] = Part[R, 3, 1] \* p \* h;**  
**Part[RESIN, 2, 3] = Part[R, 2, 3] \* p \* h;**  
**Part[RESIN, 3, 2] = Part[R, 3, 2] \* p \* h;**  
**Part[RESIN, 3, 3] = Part[R, 3, 3] \* p \* h;**  
**Part[RESIN, 1, 4] = Part[R, 1, 4] \* p \* h;**  
**Part[RESIN, 4, 1] = Part[R, 4, 1] \* p \* h;**  
**Part[RESIN, 1, 5] = Part[R, 1, 5] \* p \* h;**  
**Part[RESIN, 5, 1] = Part[R, 5, 1] \* p \* h;**  
**Part[RESIN, 1, 6] = Part[R, 1, 6] \* p \* h;**  
**Part[RESIN, 6, 1] = Part[R, 6, 1] \* p \* h;**  
**Part[RESIN, 2, 4] = Part[R, 2, 4] \* p \* h;**  
**Part[RESIN, 4, 2] = Part[R, 4, 2] \* p \* h;**  
**Part[RESIN, 2, 5] = Part[R, 2, 5] \* p \* h;**  
**Part[RESIN, 5, 2] = Part[R, 5, 2] \* p \* h;**  
**Part[RESIN, 2, 6] = Part[R, 2, 6] \* p \* h;**  
**Part[RESIN, 6, 2] = Part[R, 6, 2] \* p \* h;**  
**Part[RESIN, 3, 4] = Part[R, 3, 4] \* p \* h;**  
**Part[RESIN, 4, 3] = Part[R, 4, 3] \* p \* h;**  
**Part[RESIN, 3, 5] = Part[R, 3, 5] \* p \* h;**  
**Part[RESIN, 5, 3] = Part[R, 5, 3] \* p \* h;**  
**Part[RESIN, 3, 6] = Part[R, 3, 6] \* p \* h;**  
**Part[RESIN, 6, 3] = Part[R, 6, 3] \* p \* h;**  
**Part[RESIN, 4, 4] = Part[R, 4, 4] \* p \* h;**  
**Part[RESIN, 4, 5] = Part[R, 4, 5] \* p \* h;**  
**Part[RESIN, 5, 4] = Part[R, 5, 4] \* p \* h;**  
**Part[RESIN, 4, 6] = Part[R, 4, 6] \* p \* h;**  
**Part[RESIN, 6, 4] = Part[R, 6, 4] \* p \* h;**  
**Part[RESIN, 5, 5] = Part[R, 5, 5] \* p \* h;**  
**Part[RESIN, 5, 6] = Part[R, 5, 6] \* p \* h;**  
**Part[RESIN, 6, 5] = Part[R, 6, 5] \* p \* h;**  
**Part[RESIN, 6, 6] = Part[R, 6, 6] \* p \* h;**  
**RESIN;**  
**RESINAREA = RESIN \*  $\left(\frac{a_u}{2}\right) * \left(\frac{a_0}{2}\right) * \sin[\phi];$**   
**RESINTOTAL = RESINAREA \* 8;**

**TOTAL = FLATTOTAL + MATRIXTOTAL + FILLTOTAL + FILLERTOTAL +  
WARPTOTAL + WARPERTOTAL + RESINTOTAL;**

$$\text{AVERAGE} = \frac{n^2 * \text{TOTAL}}{(n * a)^2 * \text{Sin}[\phi]};$$

**$\alpha$  = Inverse[AVERAGE];**

$$\frac{\text{Print["E}_x="]}{1} \\ \frac{\text{Part}[\alpha, 1, 1]}{\text{Part}[\alpha, 1, 1]} * p * t$$

$$\frac{\text{Print["E}_y="]}{1} \\ \frac{\text{Part}[\alpha, 2, 2]}{\text{Part}[\alpha, 2, 2]} * p * t$$

$$\frac{\text{Print["E}_z="]}{1} \\ \frac{\text{Part}[\alpha, 3, 3]}{\text{Part}[\alpha, 3, 3]} * p * t$$

$$\frac{\text{Print["G}_{xy}="]}{1} \\ \frac{\text{Part}[\alpha, 6, 6]}{\text{Part}[\alpha, 6, 6]} * p * t$$

$$\frac{\text{Print["G}_{xz}="]}{1} \\ \frac{\text{Part}[\alpha, 5, 5]}{\text{Part}[\alpha, 5, 5]} * p * t$$

$$\frac{\text{Print["G}_{yz}="]}{1} \\ \frac{\text{Part}[\alpha, 4, 4]}{\text{Part}[\alpha, 4, 4]} * p * t$$

$$\frac{\text{Print["}\nu_{xy}="]}{\text{Part}[\alpha, 2, 1]} \\ \frac{\text{Part}[\alpha, 2, 1]}{\text{Part}[\alpha, 1, 1]}$$

$$\frac{\text{Print["}\nu_{yx}="]}{\text{Part}[\alpha, 1, 2]} \\ \frac{\text{Part}[\alpha, 1, 2]}{\text{Part}[\alpha, 2, 2]}$$

$$\frac{\text{Print}["\nu_{xz}="] \text{Part}[\alpha, 1, 3]}{\text{Part}[\alpha, 1, 1]}$$

$$\frac{\text{Print}["\nu_{zx}="] \text{Part}[\alpha, 1, 3]}{\text{Part}[\alpha, 3, 3]}$$

$$\frac{\text{Print}["\nu_{yz}="] \text{Part}[\alpha, 2, 3]}{\text{Part}[\alpha, 2, 2]}$$

$$\frac{\text{Print}["\nu_{zy}="] \text{Part}[\alpha, 2, 3]}{\text{Part}[\alpha, 3, 3]}$$

## REFERENCES

- [1] Mouritz, A.P. "Review of Z-Pinned Composite Laminates," *Composites Part A*, 38, 2383-2397, 2007.
- [2] Kim, J. and M. Sham, "Impact and Delamination Failure of Woven-Fabric Composites," *Composites Science and Technology*, 60, 745-761, 2000.
- [3] Atas C. and D. Liu. "Impact Response of Woven Composites with Small Weaving Angles," *International Journal of Impact Engineering*, 35, 80-97, 2007.
- [4] <<http://www.3tex.com>>, 2007.
- [5] G. Coppen. "Effects of Three-Dimensional Geometry on Penetration and Perforation Resistance," Masters Thesis, Mechanical Engineering Dept., Michigan State Univ., East Lansing, MI, 2004.
- [6] Raju, I. S. and J.T. Wang. "Classical Laminate Theory Models for Woven Fabric Composites," *Journal of Composites Technology & Research*, 16(4), 289-303, Oct 1994.
- [7] R.A. Naik, "Analysis of Woven and Braided Fabric Reinforced Composites," *NASA Contract Report CR-194930*, 1994.
- [8] Naik, N.K. and V.K. Ganesh, "An Analytical Method for Plain Weave Fabric Composites", *Composites*, 26, 281-289, 1995.
- [9] Scida, D., Aboura, Z., Benzeggagh, M.L., and E. Bocherens, "A Micromechanics Model for 3D Elasticity and Failure of Woven-Fibre Composite Materials," *Composites Science and Technology*, 59, 505-517, 1999.
- [10] Hur, H., Johnson, E. R., and R. K. Kapania, "A Simple Homogenization of Degraded Micro-Cracked Plain Woven and Braided Textile Composites," *The 47<sup>th</sup> AIAA Structural Dynamics and Materials Conference*, May1-May4, 2006, Rhode Island, Newport, AIAA-2006-1692.
- [11] Hsieh, C. and W. Hsing. "Elastic and Thermal Expansion Behavior of Two-Phase Composites," *Materials Science and Engineering: A*, 425(1-2), 349-360, 2006.
- [12] J.D. Whitcomb, "Three-Dimensional Stress Analysis of Plain Weave Composites," *Composite Materials: Fatigue and Fracture*, 3, 417-438, 1991.
- [13] R.L. Foye, "Finite Element Analysis of the Stiffness of Fabric Reinforced Composites," *NASA Contract Report CR-189597*, 1992.

- [14] Baker, A., Dutton, S., and D. Kelly. "Structural Analysis," *Composite Materials for Aircraft Structures*, 2<sup>nd</sup> edition, Reston: AIAA, 2004. 171-211.
- [15] K. Rosario. "Harness and Quasi-3D Weaving Effects on Composite Material Impact and Compressive Properties," Masters Thesis, Mechanical Engineering Dept., Michigan State Univ., East Lansing, MI, 2008.

2

1

MICHIGAN STATE UNIVERSITY LIBRARIES



3 1293 02956 4840